Universitetet
i Stavanger

FACULTY OF SCIENCE AND TECHNOLOGY

MASTER'S THESIS

Study program/specialization: Petroleum Engineering - Drilling and Well Technology	Spring semester, 2009 Confidential
Author: André I. Røsbak	…………………………………………… (signature author)

Instructor: Erik Skaugen, The University of Stavanger

Supervisor(s): Jafar Abdollahi, StatoilHydro ASA

Title of Master's Thesis:

Calculation of Forces Acting on a Rotary Steerable Liner Drilling System

ECTS: 30

Subject headings: Liner drilling Casing drilling Steerable liner drilling Torque & Drag ECD	Pages: 93 + attachments/other: 33 Stavanger, 12.06.2009 Date/year

MPEMAS– Master Thesis
Petroleum Technology - Drilling & Well

Calculation of Forces Acting on a Rotary Steerable Liner Drilling System

Report

by:
André I. Røsbak [893886]

The University of Stavanger
June 15th, 2009

StatoilHydro

Universitetet i Stavanger

Preface

I would like to thank my instructor at the University of Stavanger, Erik Skaugen, for his guidance and feedback throughout the process of writing this thesis, along with his willingness to discuss different topics related to my thesis.

I would also like to thank my supervisor at StatoilHydro, Jafar Abdollahi, for allowing me to explore the topic of steerable liner drilling. His feedback, as well as our discussions, have been very valuable for me in order to focus my thesis in a given direction.

In addition, I would like to thank StatoilHydro, and especially the people in the SST DT ADV unit at Forus Øst who not only gave me a place to work from, but who also took the time to discuss the subject with me, and to help me with a reality check on what I was actually working on.

Furthermore, I would also like to thank Morten Eidem, Mohammad Jahangir, and Tore Weltzin of StatoilHydro for their valuable input and assistance.

Abstract

Torque and drag calculations performed on a new liner drilling design indicate that a very high grade drillpipe, up to S-135, is required in order to satisfy the requirements which both axial and torsional loading place upon the system. High torque connections for the drillpipe may also be required.

The torque values found both with simulations and manual calculations, indicate that the proposed standard VAM TOP liner connections may not be strong enough to be used in this well. It is therefore recommended that VAM HTF, or similar high torque liner connections, are used in order to meet torsional loading requirements.

The use of 6 5/8” drillpipe and 5 ½” drillpipe above the top of the liner is also considered. Based on the calculated recommended flow rates with regards to hole cleaning for the two systems, compared with the resulting ECD values, it is suggested that 6 5/8” drillpipe provides a better compromise between hole cleaning and ECD values. Simulations indicate that the drillpipe connections are strong enough, while manual calculations indicate that high-torque drillpipe connections should be considered.

The lifting force caused by the circulation of fluid is examined, but is not found to be of significant magnitude compared to the mechanical friction. It is important to examine this force, in order to determine whether or not the system will have problems related to buckling, although it does not appear to present a problem in this case.

A general approach which can be used in order to determine the fatigue loading and longevity of the liner connections is shown. However, since the actual data for the liner connections are kept confidential by the manufacturer, no specific recommendations are made.

It should be noted that the conclusions of this thesis are valid for the wellpath and well conditions presented in this thesis only, and that different wellpaths and well conditions may impose other limits, either more or less stringent, on the design and use of the steerable liner drilling system.

Table of Contents

List of Figures

List of Tables

1 Introduction

The main topic of this thesis is the 9 5/8” steerable liner drilling system which will be used in a pilot test on the Brage field operated by StatoilHydro on the Norwegian Continental Shelf. Initially, a brief historical introduction to casing and liner drilling is given, along with a more detailed introduction of this thesis. This is followed by a theory chapter which explains the theory related to drag and friction forces, torque, hydraulics, fatigue, and hole cleaning.

After introducing the relevant theory, a more thorough explanation and introduction to casing and liner drilling is given. In this chapter, different casing and liner drilling systems are discussed and described briefly. Case histories from different wells drilled with either casing or liner drilling are outlined, in order to put the steerable liner drilling system in this thesis into context. This chapter also introduces the smear effect, which is an often advertised, though not quite yet scientifically proven, benefit of casing and liner drilling. At the end of this chapter, the Brage well which will be used as the calculation basis for this thesis is also introduced.

The next chapter deals with the steerable liner drilling system which is the main topic of this thesis. It explains the background for developing it, based on StatoilHydro’s field portfolio. A brief overview of the different components of the system is also provided.

Torque, drag, and hydraulics calculations are performed on the system in order to see how these compare against those of conventional systems, in addition to using the steerable liner drilling system with a different drillpipe size. Fatigue and hole cleaning is also considered. The purpose of these calculations is to determine what loads the system will be exposed to, and the requirements it will have to face.

Finally, the results of the calculations will be discussed and a conclusion drawn, along with a glance at the future of the steerable liner drilling system, possibly combined with other systems.

2 General Theory - Torque, Drag and Fatigue

Two important design parameters for drilling systems are torque and drag. While there are several other factors, such as directional planning, mud weight program, mud rheology, well placement, and completion design which have to be taken into account, these two are very important in order to verify that the system will be able to operate safely with regards to the mechanic properties and loads on the system. Fatigue is important because the tubing which will be left in the hole after drilling has been completed needs to retain its integrity in order for the well to be useful.

2.1 Drag Forces

Drag forces are caused by the friction force between the drillstring and the drilling mud, and the friction between the drillstring and the wellbore, which may be either casing or formation. In a deviated well, contact friction will generally be larger than fluid friction. Usually, the torque and drag for a given drilling assembly and well path can be simulated using for instance a software package from Landmark EDM called WellPlan. This package, however, is currently not equipped to properly simulate the steerable liner drilling system. This is because the simulation software is not able to deal with a drillstring which rotates with two different speeds. According to Landmark representatives, it will be possible in future editions. In the meantime, manual calculations will have to be performed in order to have a reference point.

In order to properly calculate the friction forces in the well during drilling, the weight of the drillstring and bottom hole assembly (BHA) must first be known. This can be found by using the formula:

$$W = L \cdot w$$

where:

L = the length of the string section	[mMD]
w = the buoyed weight of the string section per unit length	[kg/m]

Since this formula only depends on the weight per unit length and the length of the string, it does not need to account for whether the string is being pulled through a build up section or other types of curved sections.

When moving on to the calculation of hook loads, however, the operation to be performed becomes relevant. Because of the friction experienced by the string when run into or pulled out of the hole, the formulas for finding the hoisting and lowering forces vary somewhat. Since the friction is what separates these two scenarios, it also becomes apparent that the hook load in vertical sections will not be affected, and thus remains the same as the weight in both cases.

To find the hook load during hoisting [1]:

In a straight inclined section:

$$F_2 = F_1 + w\Delta s[\cos\alpha + \mu\sin\alpha]$$

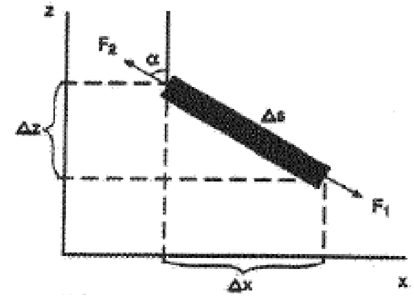

Figure 1: Forces in a straight inclined section [1]

In a drop-off section:

$$F_2 = F_1 e^{\mu(\alpha_2-\alpha_1)} + E$$

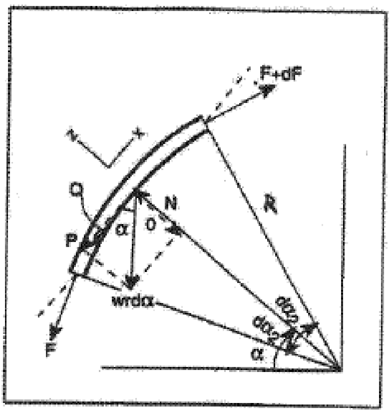

Figure 2: Forces in a Drop-off Bend

In a build-up section:

$$F_2 = F_1 e^{-\mu(\alpha_2-\alpha_1)} - G$$

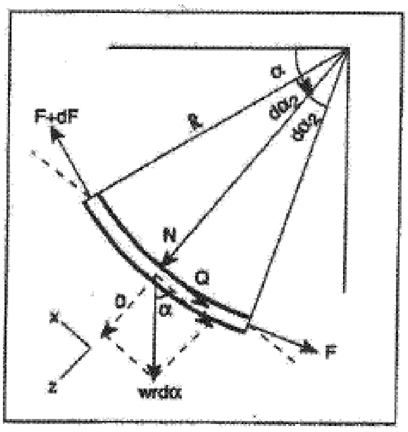

Figure 3: Forces in a Build-up Bend

In a bending section:

$$F_2 = \frac{1}{2}\left[He^{\mu(\phi_2-\phi_1)} - \frac{(wR)^2}{He^{\mu(\phi_2-\phi_1)}}\right]$$

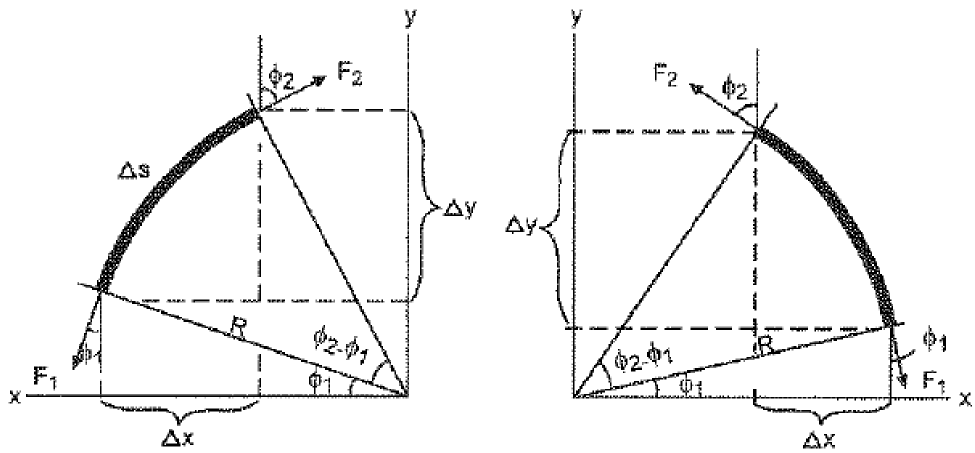

Figure 4: Forces in Left- and Right-side Bends

To find the hook load during lowering [1]:

In a straight inclined section:

$$F_2 = F_1 + w\Delta s[\cos\alpha - \mu\sin\alpha]$$

In a drop-off section:

$$F_2 = F_1 e^{-\mu(\alpha_2-\alpha_1)} + G$$

In a build-up section:

$$F_2 = F_1 e^{\mu(\alpha_2-\alpha_1)} - E$$

In a bending section:

$$F_2 = \frac{1}{2}\left[\frac{H}{e^{\mu(\phi_2-\phi_1)}} - \frac{(wR)^2}{H}e^{\mu(\phi_2-\phi_1)}\right]$$

Subscript 1 always denotes the deepest position in the well while subscript 2 always denotes the highest.

$$E = \frac{wR}{1+\mu^2}\left[\left(1-\mu^2\right)\left(\sin\alpha_2 - e^{\mu(\alpha_2-\alpha_1)}\sin\alpha_1\right) - 2\mu\left(\cos\alpha_2 - e^{\mu(\alpha_2-\alpha_1)}\cos\alpha_1\right)\right]$$

$$G = wR\left(\sin\alpha_2 - e^{-\mu(\alpha_2-\alpha_1)}\sin\alpha_1\right)$$

$$H = F_1 + \sqrt{F_1^{\,2} + (wR)^2}$$

μ = the coefficient of friction, dimensionless

F = force,	[kN]
T = torque	[kNm]
α = inclination	[degrees or radians]
ϕ = azimuth	[degrees or radians]

R = the wellpath radius of the bend in question [m]

In addition to the forces calculated above, there will be an upwards force acting on the bit, because of the high velocity mud jet from the bit nozzles, causing a reaction force. This force can be calculated once the fluid velocity and mass velocity of the mud is known.

The fluid velocity through the bit nozzles can be found by dividing the flow rate by the nozzle cross sectional area.

$$v = \frac{Q}{A_n}$$

where:
v = fluid velocity through the nozzles [m/s]
Q = flow rate [m^3/s]
A_n = nozzle cross sectional area [m^2]

The mass velocity is then found using the following formula.

$$\dot{m} = \rho \cdot Q$$

where:
$\dot{m}$ = mass velocity [kg/s]
Q = flow rate [m^3/s]
ρ = fluid density [kg/m^3]

When these two variables have been calculated, the force on the bit can be found by multiplying them.

$$F_n = \dot{m} \cdot v$$

where:
F_n = nozzle force on the bit [N]
$\dot{m}$ = mass velocity [kg/s]
v = fluid density [m/s]

2.2 Torque

Torque can be defined as the tendency of a force to rotate an object around an axis. The SI unit for torque is Nm – Newton meters. Torque is required in order to rotate the drill string while the hole is drilled. This is done in order to minimize the contact friction in the well in the axial direction.

Once the hook loads and weights for the different scenarios have been established, the torque can be calculated [1]. The torque for a vertical section will be 0, since ideally there is no contact between the drillstring and the borehole in this section.

In a straight inclined section:

$$T_2 = T_1 + \mu w \Delta s r \sin \alpha$$

In a drop-off section:

$$T_2 = T_1 + \mu r \{ (F_1 + C) |\alpha_2 - \alpha_1| - D \}$$

In a build-up section:

$$T_2 = T_1 + \mu r \{ (F_1 + C) |\alpha_2 - \alpha_1| + D \}$$

In a bending section:

$$T_2 = T_1 + \mu r |\phi_2 - \phi_1| (H - F_1)$$

where,

$$C = wR \sin \alpha_1$$

$$D = 2Rw(\cos \alpha_2 - \cos \alpha_1)$$

2.3 Fatigue

Fatigue is defined by the American Society for Testing and Materials (ASTM) as "*the process of progressive localized permanent structural change occurring in a material subjected to conditions that produce fluctuating stresses and strains at some point or points and that may culminate in cracks or complete fracture after a sufficient number of fluctuations*." [2] For metals, this means that fatigue is a progressive process, where damage develops slowly in the early stages, and accelerates very quickly towards the end [3]. This implies that the initial stage of fatigue is a crack initiation phase. For most fairly smooth materials, this initial state may encompass up to 90% of the fatigue life of the material. This initial phase is usually confined to a fairly small area which experiences high localized stresses, and thus accumulates damage over time.

The initiation process usually results in micro-cracks which begin to grow independently of each other. As they increase in size and begin to interact, however, the cracks will coalesce into one dominant crack. This crack normally grows slowly during normal loading conditions. When the remaining cross section is significantly reduced, however, the local stress field near the front of the crack increases, and this will accelerate the crack growth [3]. The final failure takes the form of an unstable fracture, and occurs when the remaining cross sectional area is insufficient to support the load it is subjected to. The precise behavior of these states depends to a great extent on the features of the material subjected to loading. To summarize, the fatigue process can be divided into the following stages:

- Stage I: Crack Initiation
- Stage II: Propagation of one dominant crack.
- Stage III: Final Fracture

Fatigue is another aspect which needs to be taken into consideration when using a steerable liner drilling system. Usually, the forces the connections on a given liner will see are those it experiences when it is run into the hole after a given hole section has been drilled. However, this is not the case when the liner in question is part of a steerable liner drilling system.

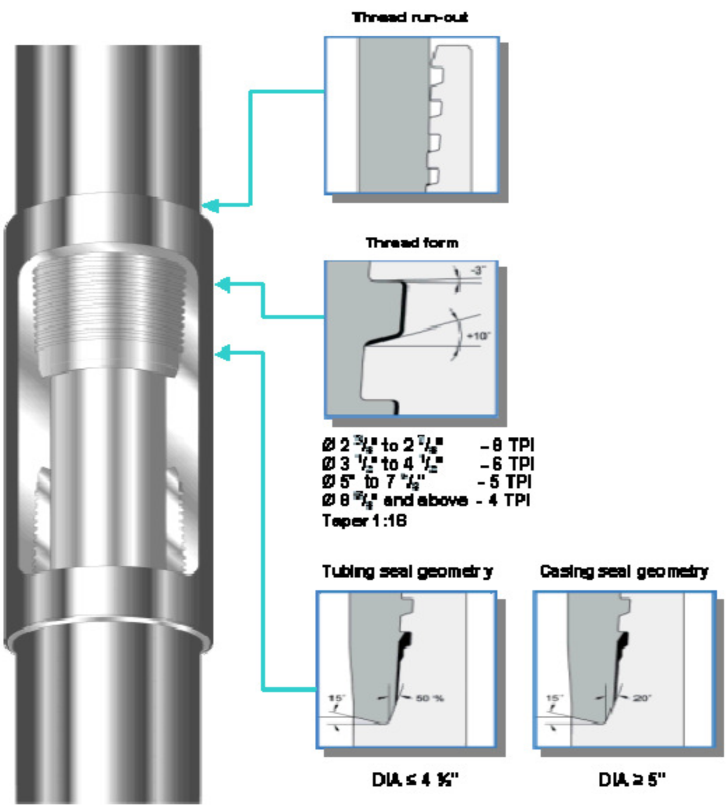

Figure 5: Typical Design of a Premium Threaded and Coupled Connection [4]

For a steerable drilling liner system, the connections and the liner will experience loading during drilling. This entails shock, vibration, increased torque, friction, and similar forces.

This exposes the connections of the liner to so-called load cycles. A load cycle indicates how many revolutions the liner has experienced, while exposed to a given side force.

Since the drilling system in question has steering and rotational capabilities, the side force becomes important. Depending on the dogleg severity (DLS), the number of load cycles a given liner connection can withstand before failure will vary greatly. The decrease in change for fairly small variations in the DLS will be almost exponential. This means that even slight changes in the DLS can significantly change the expected lifetime of a given liner connection [5].

Since the durability of the liner connection is given in terms of load cycles, the rate of penetration (ROP) becomes important. If a system can be created which has a sufficient ROP, high DLS sections may be drilled safely, because the liner connection does not stay in the dog leg area for a long time, and does therefore not experience as many load cycles there as it might otherwise have. This also means that a low ROP will cause the liner to rotate for longer periods in areas with presumably higher dog legs. This will hamper the effectiveness and range of the steerable liner drilling system. Ensuring sufficient ROP is therefore important in order for a steerable liner drilling system to be able to drill long distances.

The curves which display the given amount of cycles leading to failure for a given connection and DLS, also called S/N curves, have to be found for each separate connection type. Although calculations can be performed, they need to be backed by test data. Some S/N curves can be obtained from research papers, published by tubing manufacturers, and one example of such a curve is shown below, along with a figure which indicates the stress concentration in a connection experiencing bending stress.

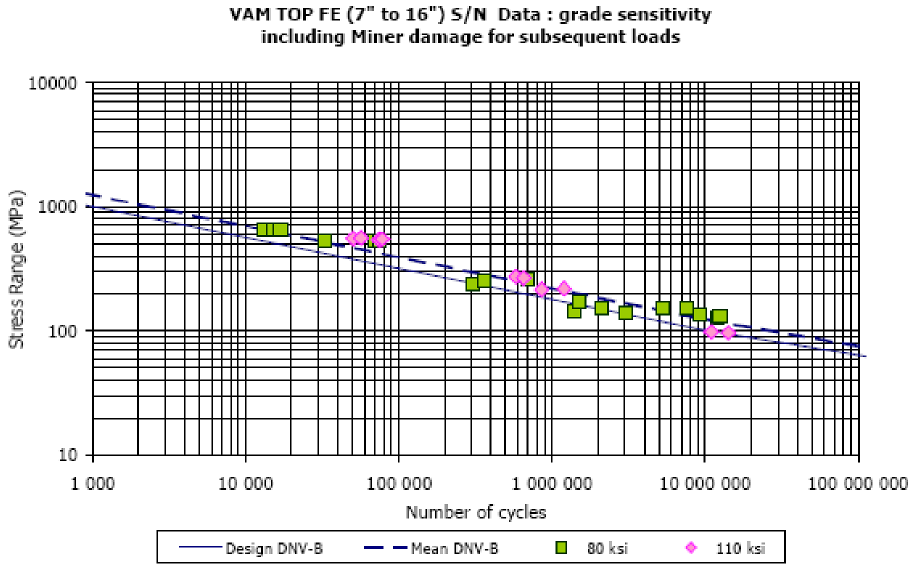

Figure 6: Example of a Typical Manufacturer's S/N Plot [4]

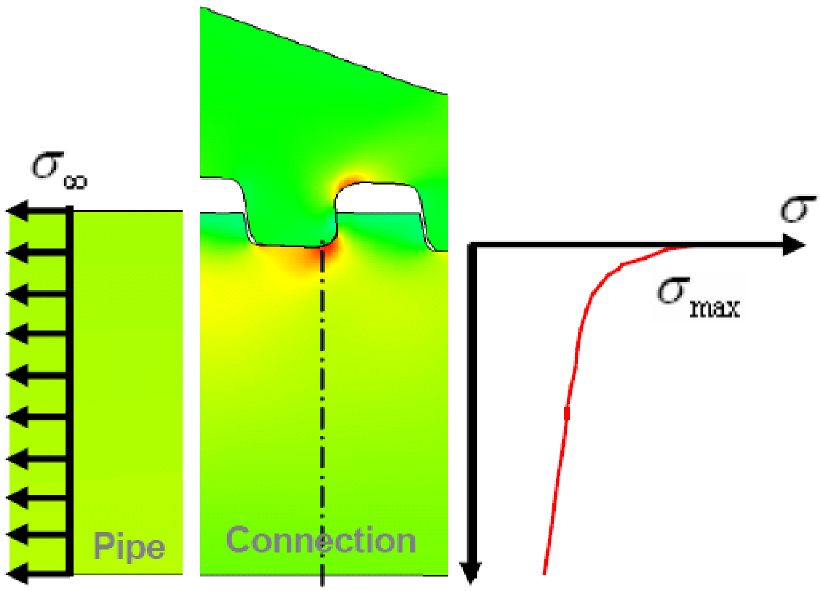

Figure 7: Stress Concentration in a Connection [4]

Based on these S/N curves, we see the significance of DLS and ROP on the liner connection durability. The exact curves for the liner connection used on the SLD system may not be divulged, because of manufacturer confidentiality issues.

On several S/N curves, there will many curves, each with a different name. Often, there will be a main curve called the DNV B mean. This means that it is based on the recommendations from Det Norske Veritas (DNV). However, after tests have been performed on the connections, connection behavior is assumed to be a parallel line to this curve, and is then expressed in terms of something called the Stress Amplification Factor (SAF) [6]. The SAF becomes the offset from which the reference curve is shifted either upwards, if the SAF is less than one and the connector is assumed to be better than the reference, or downwards, if the

SAF is greater than one and the connector is assumed to be poorer than the reference [6]. The relationship between the DNV curve and SAF can be seen in figure 8 below.

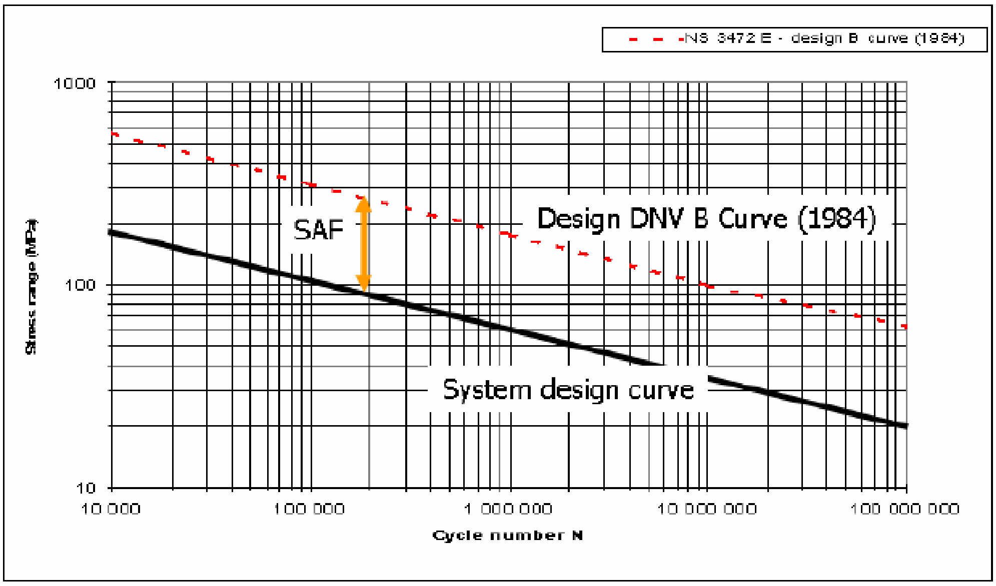

Figure 8: SAF vs. DNV Curves [6]

Furthermore, while the S/N curves show the amount of cycles before a given liner connection fails, this may not be sufficient in order to determine if the operation can be performed successfully. Depending on the placement and plans for the liner being drilled down, it may have to withstand high reservoir pressures and temperatures. It is therefore important that the liner retains full pressure integrity, even after being drilled down. With this in mind, it may not be sufficient that the material has not yet failed. The amount of fatigue experienced by the connection will also have to be investigated, in order to determine if the durability of the connection is sufficient after being exposed to loads during drilling.

Having said that, it might also be argued that reduced integrity may not be an issue, and that the focus instead should be placed on determining when the connection fails. The reason for this is that the fracture initiation phases can be quite long, while the phase from the fracture becomes critical and until failure is very short. It therefore appears as though the period from when the integrity is significantly reduced and until failure is relatively short, and therefore not as important as the failure limit itself. It may also be hard to determine the exact state of the connection at any given time, and it may thus not be very practicable. Determining the exact reduced strength levels will therefore not be attempted in this thesis.

Since most of the available test data correlates stress with number of cycles to failure, the stress data for the liner connections will have to be determined. For the curves used in this paper, static loads are already included, and one will therefore have to calculate the bending stress only in order to find the expected cycles to failure for the connection.

On the other hand, if one would like to find the total stress experienced by the connection in a given situation, one would probably have to calculate other stresses as well. Since the connection will most likely also experience some compression, the von Mises equation could be used in order to calculate the equivalent stress which is seen by the connection. Inside and outside pressure should also be included.

The von Mises stress equation is defined as follows [7]:

$$\sigma_E = \sqrt{\frac{1}{2}(\sigma_x - \sigma_Y)^2 + \frac{1}{2}(\sigma_Y - \sigma_Z)^2 + \frac{1}{2}(\sigma_Z - \sigma_X)^2 + 3\tau_{XY}{}^2 + 3\tau_{YZ}{}^2 + 3\tau_{ZX}{}^2}$$

where:

σ_n = the n component of the stress

τ_{mn} = the shear stresses between the m and n component

The effect of bending can also be calculated [8]. Since the stress will be at its highest at the outer diameter of the pipe, this is calculated as the maximum bending stress. The bending stress at the inside of the pipe may also be calculated, using the pipe inner diameter, if necessary.

$$\sigma_{max} = \frac{D_o}{2R}E = \frac{D_o}{2\Delta L}\Delta\alpha E$$

where:

D_o	= the outer diameter of the pipe	[m]
R	= the bending radius	[m]
E	= Young's Modulus	[Pa]
L	= the length over which the bending takes place	[m]
$\Delta\alpha$	= the change in angle	[rad]

In most cases, and especially for wells with a certain amount of inclination, the compressive force due to friction on the liner connections will be fairly small compared to the magnitude of the bending force. For this reason, and also for simplicity, only the bending force is used to calculate the stress the connection is exposed to in this case.

3 Hydraulics and Equivalent Circulation Density (ECD)

3.1 Equivalent Circulation Density

Normally, the density of a given drilling mud is given in specific gravity or in kg/m^3. However, during drilling, we have circulation and thus dynamic conditions in the well. This necessitates the use of the term known as equivalent circulation density (ECD). The ECD can be interpreted as the density of a fictitious fluid which in static conditions would give the same pressure as a certain drilling mud during dynamic conditions. The ECD, in other words, provides an indication of the circulating bottom hole pressure.

The bottom hole pressure given by the ECD will be higher than the same pressure given only by the mud density. This is because the dynamic conditions create a pressure drop, which makes the ECD larger than the original mud weight. The pressure drop seen can be calculated with the following formula from the Drilling Data Handbook [9]:

For the drillstring (assuming turbulent flow):

$$\Delta P = \frac{\Delta L \rho^{0,8} Q^{11,8} \mu^{0,2}}{901,63 \cdot D_i^{4,8}}$$

For the annulus (assuming turbulent flow):

$$\Delta P = \frac{\Delta L \rho^{0,8} Q^{11,8} \mu^{0,2}}{706,96 (D_o + D_i)^{1,8} (D_o - D_i)^3}$$

where:

ΔP	= pressure loss	[kPa]
ΔL	= section length	[m]
ρ	= fluid density	[s.g.]
Q	= flow rate	[l/min]
μ	= fluid viscosity	[cP]
D_o	= outer diameter	[in]
D_i	= inner diameter	[in]

Based on the formulas above, it is seen that a smaller annular area will give a higher frictional pressure drop. This will in turn increase the ECD. Therefore, all other factors being equal, the ECD for a casing drilling operation will be higher than for a conventional drilling situation, given the same flow rate. For liner drilling, this will also be true, although the effect will depend on the length of the liner relative to the total length of the drill string. Obviously, the longer the liner, the higher the ECD.

Once the pressure drop has been found, and when the static mud density is known, the ECD can be calculated [10]:

$$ECD = \frac{P_h + \Delta P_{fa}}{Dg} = \rho_h + \rho_{fa}$$

where:

P_h	= hydrostatic pressure	[Pa]
P_{fa}	= frictional pressure loss, annulus	[Pa]
D	= depth in TVD	[m]
ρ_h	= density of the fluid	[kg/m^3]
ρ_{fa}	= apparent increased density of the fluid because of friction	[kg/m^3]

In addition to the pressure drop because of fluid flow, the pressure drop when the dimensions of the annular area changes needs to be calculated [11]. It should also be noted that in addition to the method outlined in the Drilling Data Handbook, the pressure loss may also be calculated in another way [11].

$$\Delta P = \frac{4}{D} \cdot f \cdot \frac{1}{2} \cdot \rho \cdot U^2$$

where:

ΔP	=	pressure loss	[Pa]
D	=	hydraulic diameter	[m]
ρ	=	fluid density	[kg/m^3]
U	=	flow velocity	[m/s]
f	=	friction factor	

$$f = \frac{16}{Re} \qquad \text{for laminar flow}$$

$$f = 0{,}046 \cdot Re^{-0{,}2} \qquad \text{for turbulent flow}$$

The Reynolds number, Re, is equal to:

$$Re = \frac{\rho \cdot U \cdot D}{\mu}.$$

The Reynolds number can be used both in the pressure drop equation outlined above, as well as to determine whether the formula for pressure drop in turbulent flow can be used. Flow regimes are usually characterized as laminar for Reynolds numbers up to 2300. Above this number, and up to 4000, the flow is in a transitional phase between laminar and turbulence. For Reynolds numbers above 4000, the flow is usually characterized as turbulent.

3.2 Friction Caused by the Flow of Liquid

In addition to the mechanical friction described in section 2.1 about drag forces, there will also be a friction force caused by the liquid which circulates around the drillpipe [8]. The friction model assumes that there is a fairly narrow gap, compared to the pipe diameters, between an inner and an outer pipe, and that the inner pipe is rotating. The flow in the annulus can then be compared to the flow between two parallel plates with the same width as the circumference of the annulus. This circumference may be found by finding the average value for the inner and outer pipes [8]:

Note that SI units are to be used in all the formulas below, unless otherwise explicitly stated.

$$C = \frac{1}{2}\pi(D + d) = \pi(D - a)$$

$a = \frac{1}{2}(D - d)$ = the gap between inner and outer pipe
D = the inner diameter of the outer pipe
d = the outer diameter of the inner pipe

Since the assumption is that of a parallel plate model, the annulus cross sectional area is the same as the parallel plate model cross section area:

$$A_A = C \cdot a = \frac{\pi}{4}\left(D^2 - d^2\right)$$

The fluid velocity in the annulus can then be found if the volume flow rate of mud (Q) is known:

$$v_L = \frac{Q}{A_A}$$

Given the rotation of the inner pipe (f), the plate which represents the inner pipe is moving sideways with the velocity:

$$v_d = \pi df$$

Since the outer pipe is stationary, v_D can be said to be 0, and the average velocity between the two plates then becomes:

$$v_R = \frac{1}{2}\pi df$$

When the liquid flows along the pipe axis while the inner pipe rotates, there will be a resulting average velocity, consisting of two components. One component, v_L will be along the pipe axis, while the other component, v_R will be perpendicular to this axis. The resulting velocity, v, can be found by combining these two velocities. The angle between the pipe axis and the resulting flow direction can also be found.

$$v = \sqrt{v_L^{\ 2} + v_R^{\ 2}}$$

$$\varphi = \mathrm{Arc}\tan\left(\frac{v_R}{v_L}\right) = \mathrm{Arc}\cos\left(\frac{v_L}{\sqrt{v_L^{\ 2} + v_R^{\ 2}}}\right) = \mathrm{Arc}\cos\left(\frac{v_L}{v}\right)$$

The fluid will then rotate in a spiral, given by the angle φ, in the same direction as the rotating pipe and somewhat slower.

If the fluid flow is laminar, the friction gradient can be calculated with the following equation.

$$\frac{\Delta F}{\Delta L} = \mu C \frac{v_d}{a} = 2\mu C \frac{v_R}{a}$$

In order to find the velocity profile for the fluid between the two plates, the following formula is given, based on the fact that the flow profile between two parallel plates will be parabolic:

$$v(x) = 4\frac{ax - x^2}{a^2} v_M$$

If $\frac{1}{2}a$ is considered to be the middle point between two plates, the maximum velocity can be found for $a = \frac{1}{2}(D - d)$.

$$v\left(\frac{1}{2}a\right) = 4\frac{a \cdot \frac{1}{2}a - \frac{1}{4}a^2}{a^2} v_M = v_M$$

Based on this, the velocity gradient can be calculated by differentiating the expression for v(x):

$\dfrac{dv(x))}{dx} = 4\dfrac{a - 2x}{a^2} v_M$, where $\left(\dfrac{dv(x)}{dx}\right)_{x=0} = 4\dfrac{a - 2 \cdot 0}{a^2} v_M = 4\dfrac{v_M}{a}$ describes the velocity gradient at the wall.

In order to find the friction force gradient along the wall, the average velocity of the flow must be found. This is usually the measured velocity, which can be found as follows:

$v_A = \dfrac{1}{a}\displaystyle\int_0^a v(x)dx = \dfrac{1}{a}\int_0^a 4\dfrac{ax - x^2}{a^2}dx = \dfrac{1}{a}\left(4\dfrac{a\frac{1}{2}x^2 - \frac{1}{3}x^3}{a^2} v_M\right)_{x=a} = \dfrac{2}{3}v_M$, which makes sense, since the velocity profile is parabolic.

The velocity gradient at the pipe wall can then be used along with the average velocity in order to find the friction force gradient along this wall directly.

$$\frac{\Delta F}{\Delta L} = \mu C \frac{v}{a} = \mu C\left(4\frac{v_M}{a}\right) = 4\mu C\frac{v_M}{a} = 6\mu C\frac{v_A}{a}$$

Combining the above equations, the fluid flow friction can be expressed using pipe parameters, along with the flow rate (Q) and fluid viscosity (μ).

$$\Delta F = 6\mu C\frac{v_A}{a}\Delta L = 6\mu\frac{\pi(D+d)}{2}\cdot\frac{v_A}{\frac{1}{2}(D-d)}\Delta L = 6\pi\mu\left(\frac{D+d}{D-d}\right)v_A\Delta L = 6\pi\mu\left(\frac{D+d}{D-d}\right)\left(\frac{Q}{\frac{1}{4}\pi\left(D^2-d^2\right)}\right)\Delta L$$

$$\Delta F = 24\mu\left(\frac{Q}{(D-d)^2}\right)\Delta L$$

This fluid friction force can then be used to determine the pressure drop for laminar, or the pressure drop may be found in a source such as for instance the Drilling Data Handbook [9]. The equation has in this case been modified to accommodate SI units.

$$\Delta P = 192\mu\frac{Q}{\pi(D+d)(D-d)^3}\Delta L$$

The friction force against the inner surface can then be calculated. It is defined as half the total friction. The total friction is equal to the pressure force, and may therefore be calculated as follows.

$$\Delta F_{\text{friction}} = \frac{1}{2}\Delta P\cdot A$$

The equation for pressure loss may then be inserted into this equation in order to find the friction force on the pipe caused by liquid flow.

In drilling, however, the flow is usually considered to be turbulent. This entails a higher shear level, as well as the formation of whirls and eddies in the fluid. This means that fluid currents whose flow direction is not the same as the general flow are created [12]. The fluid moving forward is therefore a result of the net movements of the eddies, during turbulent flow.

The flow, which for laminar flow regimes is considered to be uniform in one direction, is for turbulence considered to be somewhat random, varying in direction as it flows.

For turbulent flow, the pressure drop equation has already been defined in section 3.1 of this thesis. In order to fit into these equations, however, it will be modified to accommodate SI units and the terminology used in this section.

$$\Delta P = 0.197006\frac{\rho^{0,8}Q^{11,8}\mu^{0,2}}{(D+d)^{1,8}(D-d)^3}\Delta L$$

Knowing the pressure drop, the fluid friction against one of the pipe surfaces can be calculated.

$$F_{Friction} = \frac{1}{2}\Delta P \cdot A = \frac{0.197006}{2} \cdot \frac{\rho^{0,8}\mu^{0,2}Q^{1,8}\Delta L}{(D+d)^{1,8}(D-d)^3} \cdot \frac{\pi}{4} \cdot \left(D^2 - d^2\right) = 0.0773640\frac{\rho^{0,8}\mu^{0,2}Q^{1,8}\Delta L}{(D+d)^{0,8}(D-d)^2}$$

Several different versions of this formula may subsequently be generated, if one should, for instance, wish to exchange the flow rate, Q, with for instance radial, average, or other fluid velocities.

Since the main point of interest is the friction force against the drillpipe surface, the combined velocities of the fluids close to this surface will be examined more closely. The combination of these velocities will provide a friction force equivalent to that of only axial flow with pumping, with an equivalent average velocity of:

$$v_{EA} = \sqrt{{v_A}^2 + \left(\frac{1}{3}v_d\right)^2} = \sqrt{{v_A}^2 + \left(\frac{2}{3}v_R\right)^2} = \frac{2}{3}\sqrt{2.25 \cdot {v_A}^2 + {v_R}^2}\ .$$

The earlier mentioned fluid friction force is proportional with the flow velocity to the power of 1,8, due to the way pressure drop is calculated for turbulent flow. Thus, the combined fluid friction force will be larger than the friction force due to axial flow only. The combined fluid friction becomes [8]:

$$F_{Ftotal} = \left(\frac{v_{EA}}{v_A}\right)^{1,8} F_{Friction} = \left(\frac{\sqrt{{v_A}^2 + \left(\frac{1}{3}v_d\right)^2}}{v_A}\right)^{1,8} F_{Friction} = \left(\frac{\sqrt{9{v_A}^2 + 4{v_R}^2}}{3v_A}\right)^{1,8} F_{Friction}\ .$$

This is the fluid friction which acts directly against the direction of fluid flow. Since there is both an axial and tangential component of the fluid friction force, the above force can be decomposed into these two directions [8]:

$$F_{Faxial} = \frac{v_A}{v_{EA}}\left(\frac{v_{EA}}{v_A}\right)^{1,8} F_{Friction} = \left(\frac{v_{EA}}{v_A}\right)^{0,8} F_{Friction} = \left(\frac{\sqrt{9{v_A}^2 + 4{v_R}^2}}{3v_A}\right)^{0,8} F_{Friction}$$

$$F_{F\tan gential} = \frac{\frac{2}{3}v_R}{v_{EA}}\left(\frac{v_{EA}}{v_A}\right)^{1,8} F_{Friction} = \frac{2}{3}\frac{v_R}{v_A}\left(\frac{\sqrt{9{v_A}^2 + 4{v_R}^2}}{3v_A}\right)^{0,8} F_{Friction}$$

The above equations should only be used when the drilling mud is circulated while the drill string is rotated. If only one of these events is taking place, the formula for $F_{Friction}$ should be used.

In order to use the above formulas, the maximum fluid velocity in the annulus must be known. In the case of cuttings transport in the annulus, turbulent flow is assumed. The maximum velocity can therefore be found using the formula [11]:

$$v_m = \frac{v_{avg}\left((n+1)(n+2)\right)}{2}$$

where,

v_m =	maximum annular velocity	[m/s]
v_{vg} =	average annular velocity	[m/s]
n =	ranges from 1/5 (weak turbulence) to 1/7 (strong turbulence)	

For this thesis, n = 1/6 has been assumed when performing these calculations.

3.3 Hole Cleaning

Hole cleaning is always important in drilling, and different types of wells and drilling systems pose different challenges. It can also be a challenge because of the wide range of variables which come into play when hole cleaning is to be considered. Some of the key variables which play a part in cuttings transport, and therefore also hole cleaning, are presented in the figure below.

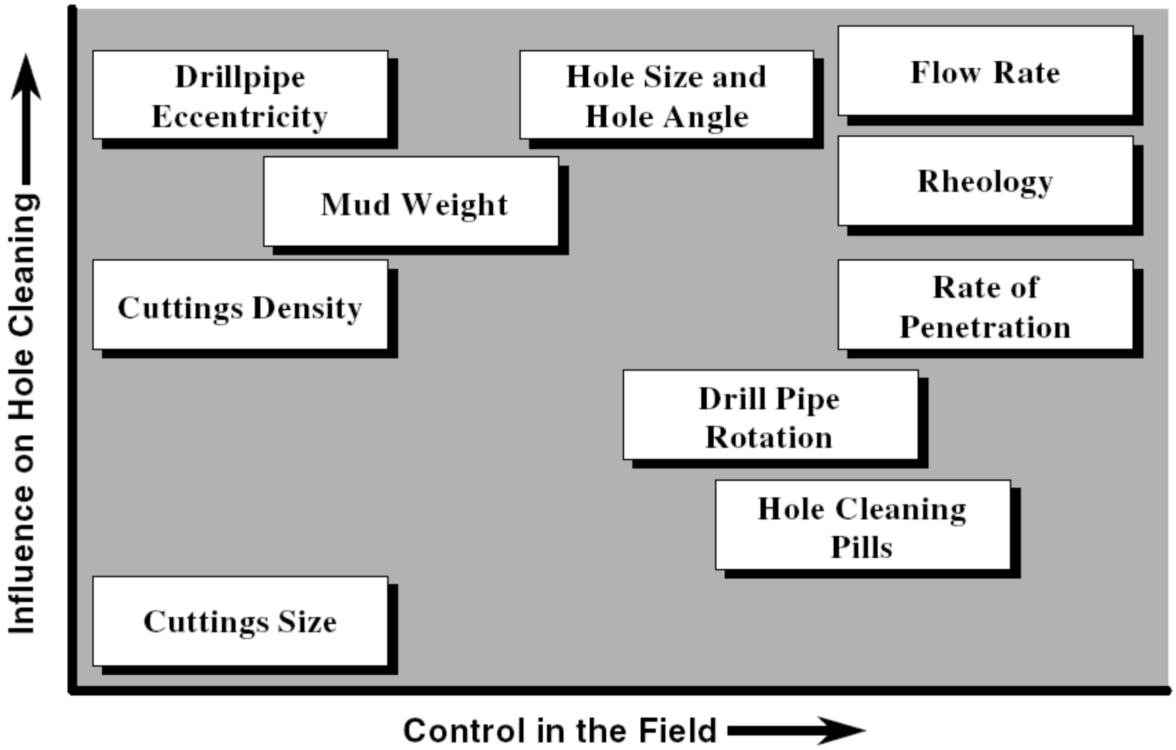

Figure 9: Key Variables Which Influence Cuttings Transport [13]

For fairly vertical wells, cuttings will be transported to the surface with the help of fluid viscosity and flow velocity [14]. If circulation stops, whether or not the cuttings will remain suspended depends on the rheological properties of the drilling mud, especially the gel strength. While the mud is flowing, it is important that the flow rate is equal to, or higher than, the drop rate of the cuttings.

As the angle of the well gets higher, approaching 45 degrees and above, the cuttings may start to form beds on the low side of the well. They are slowly transported upwards, and circulate up and down around the drillstring. The main challenge is that gravity pulls the cuttings downwards, while most of the flow takes place above the drillstring, It is therefore important to rotate the drillstring, in order to create sufficient shear in the drilling fluid to keep the cuttings moving upwards and prevent them from coalescing and forming beds [14]. As the inclination of the well becomes even higher, and approaches horizontal, pipe rotation becomes even more important in order to keep the hole clean.

Another area which will be affected by casing and liner drilling is hole cleaning. During normal operations the string will have practically the same outer diameter, throughout the entire hole, except for the BHA. In the case of for instance a 12 ¼” hole, the normal drillpipe size may vary between 5 ½" and up to 6 5/8". This would be the main outer diameter of a conventional drillstring when considering hole cleaning.

When drilling with casing or liner, on the other hand, the outer diameters will become larger. The most common casing/liner size for a 12 ¼" section is 9 5/8"; 50% to 70% larger than the drillpipe used. To further complicate matters, we have to differentiate between casing and liner drilling. For casing drilling, the casing outer diameter will be the same all the way to the top of the string; except for at the very bottom where a small part of the BHA sticks out if the system is retrievable. For liner drilling, however, there will be a noticeable change in diameter where the liner ends, and the drillpipe continues to the surface. This larger annular gap makes hole cleaning for liner drilling more challenging than for casing drilling.

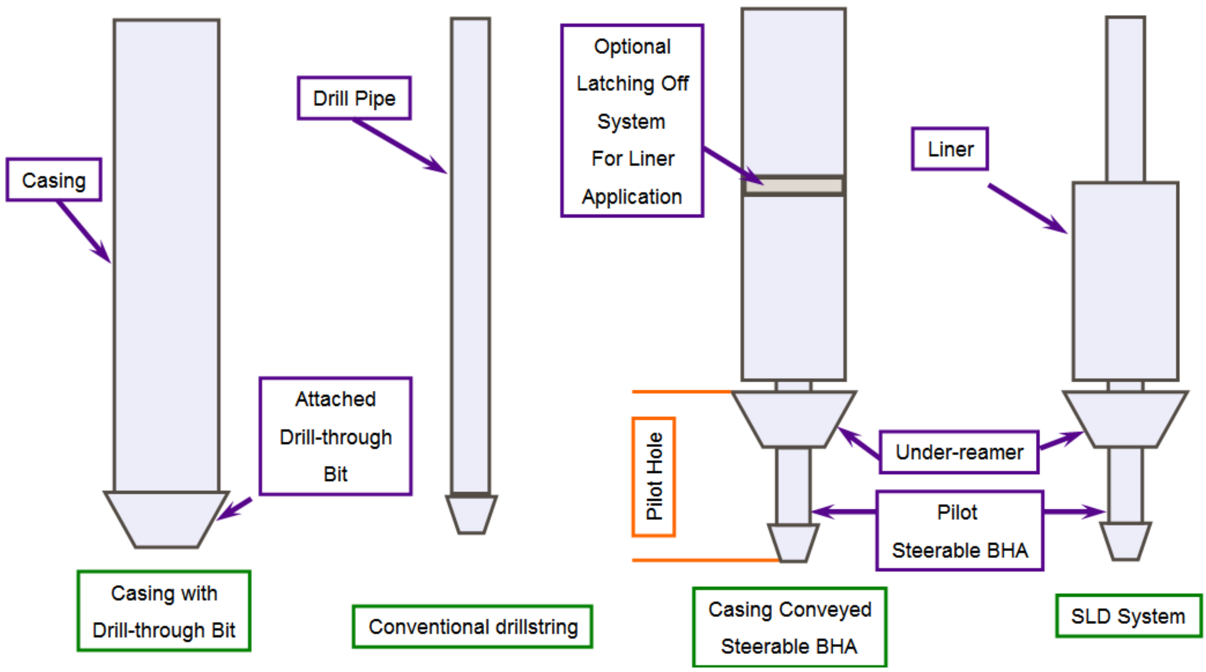

Figure 10: Different String Configurations [15]

There are different methods which may be used in order to determine the hole cleaning requirements of each system. One way would be to use software such as Drillbench or WellPlan. Another would be to look at company best practice and desired annular velocities.

In the case of StatoilHydro, there is a simplified way of calculating this, based on experience and best practice documents. This states that in order to ensure adequate hole cleaning, the annular velocity (v_{req}) should be kept preferably at 1 m/s or above, with 0,8 m/s as a recommended minimum [16]. If one then calculates the annular area for each section of the string, and then multiplies this with the desired annular velocity, the minimum required hole cleaning mud flow rates can be found.

$$A_{Annulus} = \frac{\pi}{4}\left(ID_{hole}^{2} - OD_{string}^{2}\right)$$

$$Q_{min} = A_{annulus} \cdot v_{req}$$

where:

$A_{annulus}$	=	annular area	[m^2]
ID_{hole}	=	inner diameter of the borehole	[m]
OD_{string}	=	outer diameter of the drillstring	[m]
Q_{min}	=	required flow rate	[m^3/s]
v_{req}	=	required annular velocity	[m/s]

This can be calculated, both for the 9 5/8" and 7" steerable liner drilling systems, and in turn be compared with the requirements of a conventional drilling system.

The case of the 7" steerable liner drilling system becomes slightly more complicated, however, as there will be more uncertainty related to the previously drilled and cased sections of the well than there will be for the 9 5/8" system, where it is generally assumed that the previous casing string is 13 3/8" casing set to surface. The 7" system may encounter the 13 3/8" casing as well, but is also likely to encounter 9 5/8" casing, either as a liner at the bottom of the well, or all the way to the surface, depending on the well design and previous operations.

In addition to the above calculations, hole cleaning considerations will also be made on the basis of simulation results from WellPlan. This is done in order to try to verify, or at least compare, the results of the different calculation methods.

4 Introduction to Casing and Liner Drilling

4.1 General Introduction

Casing while drilling (CWD) can be defined as the process of drilling a well by the use of casing instead of, or along with, regular drillpipe as the drillstring. Although some consider it a fairly recent technology, drilling with casing has in fact been around since the early 1900s [17]. It began with Reuben C. Baker, who patented a casing shoe which was tapered at the bottom to ensure that the hole diameter would be greater than the casing diameter. The shoe also had a cutting structure which was designed to remove ledges and debris in the hole that might otherwise cause problems. In the 1920s there were some experiments carried out both in the United States and in the Soviet Union. The method showed very low rates of penetration, however, and the projects were eventually abandoned in favor of other solutions. The technology re-emerged in the 1960s and 70s, and was once again put to use, although it would remain an exception [17].

The most common application of casing while drilling has usually been to increase the efficiency of onshore drilling operations. Several examples of this exist, but the most notable one is perhaps the Lobo field in the United States, where ConocoPhillips has used CWD quite extensively in order to save money on well construction related trouble time [18, 19].

Casing while drilling has not been applied offshore very often, however. Notable exceptions here are BP [20] on the Valhall field in Norway, ExxonMobil in Indonesia [21], and ConocoPhillips, who recently drilled a well with casing on the Eldfisk field [22]. Casing and liner drilling has also been used in the Gulf of Mexico, but not to a great extent [23]. Nevertheless, it is still a fairly new technology with respect to offshore use.
Drilling with casing and liner are fairly wide terms, and there are several different ways in which they may be carried out. Usually, however, the different casing while drilling systems can be classified as:

- Drilling with a non-retrievable bottom hole assembly (BHA)
- Drilling with a retrievable BHA

In order to understand casing while drilling better, both of these concepts will be explained, followed by a closer presentation of the system to be considered in this thesis.

It should also be noted that the terms casing drilling and liner drilling may be misleading. In some cases, the entire casing is drilled down, but the upper part of it is removed after reaching the planned end of the section, thus turning the casing string into a liner. For other systems, a liner may be included at the bottom, latched on to a retrievable drillstring. While the main focus of this thesis will be steerable liner drilling, it is important to include some background information which pertains to casing drilling as well, since these technologies are closely related.

4.2 Drilling with Casing

Drilling with casing means that the drilling process is carried out by using casing to transmit torque and weight to the bit. The entire drillstring is therefore made of casing, rather than drillpipe, as it would be in a conventional situation.

Depending on whether the system is retrievable or not, a full BHA with directional and measuring components may be employed. If the system is retrievable, the BHA may be retrieved either by wireline or on drillpipe. If the system is designed to be non-retrievable, however, there is no need to retrieve any inside components from the string, and the casing can be cemented in place right away, once it reaches its target depth. This is one of the most apparent advantages of a casing while drilling system, since being able to cement the casing in place without having to trip in and out of the well several times will save a lot of operational time. Risk with regards to not being able to run casing into the hole all the way to target depth due to borehole problems is also eliminated.

Because of this, drilling with casing is often done mostly for economical and time-saving reasons. One example of this is the Lobo field in Texas, where casing while drilling was seen as a way to increase drilling efficiency once the efficiency of conventional drilling methods seemed to have peaked.

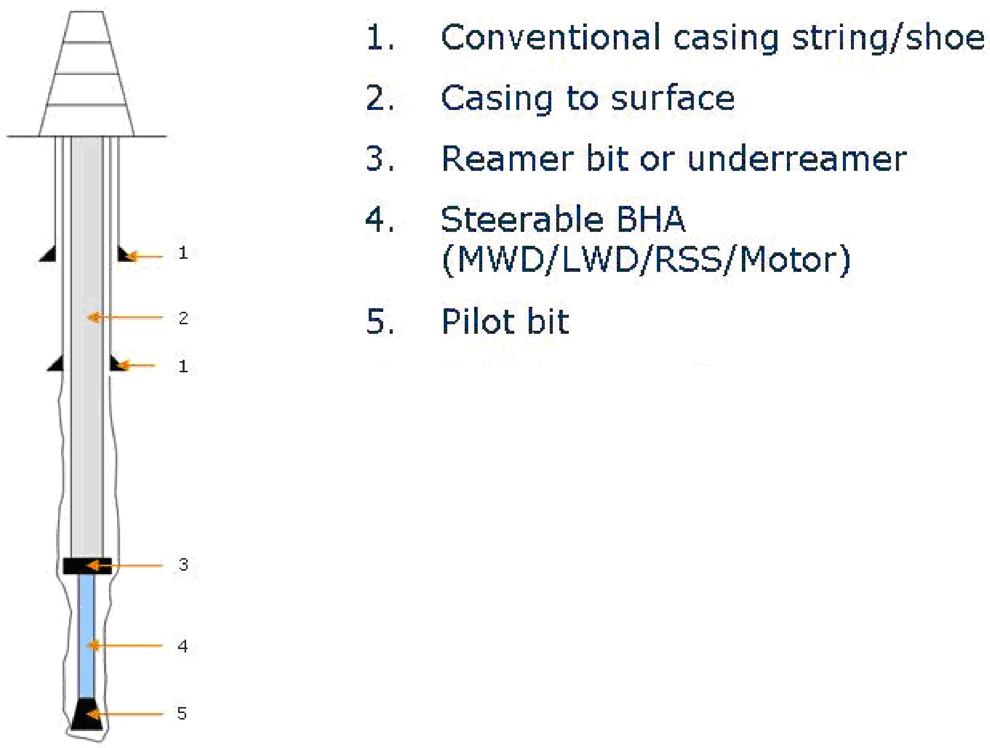

Figure 11: Drilling with Casing [24]

In addition to the reduction in time spent tripping, casing while drilling also offers several other advantages.

- Limiting open hole time: Casing drilling limits the open hole time when the formation is exposed, since we always have casing at the bottom of the well. This seems to have contributed to a reduction in lost circulation, wellbore collapse problems, as well as the number of kicks taken. The chance of getting a stuck pipe situation is also smaller when we have casing at the bottom all of the time. This may prove problematic if the casing is left static in the hole for too long, however. To mitigate this, circulation and pipe reciprocation should be performed when drilling is not taking place.

- The smear effect: Another reported benefit of casing while drilling is the so-called smear effect. The theory behind this concept is that as the casing rotates, cuttings which are travelling up the annulus towards the surface are ground and plastered by the rotating casing into the borehole wall. This creates a much more consolidated and smooth wellbore, while at the same time mitigating lost circulation problems.

  The smear effect has therefore allowed operators to circulate at lower rates and with lower mud weights. One reason for this is the narrow annulus, which will create fairly high flow velocities, and also provide a greater pressure drop which contributes towards the equivalent circulation density (ECD). In addition to this, the smear effect has also removed, or at least severely reduced, the amount of lost circulation problems reported in several cases. One reason for this is that fines may be created during grinding of the cuttings by the casing as they travel up the annulus. This creates a better and more consolidated filtercake around the borehole, thus stabilizing it. The smear effect will be discussed more thoroughly in section 4.7.

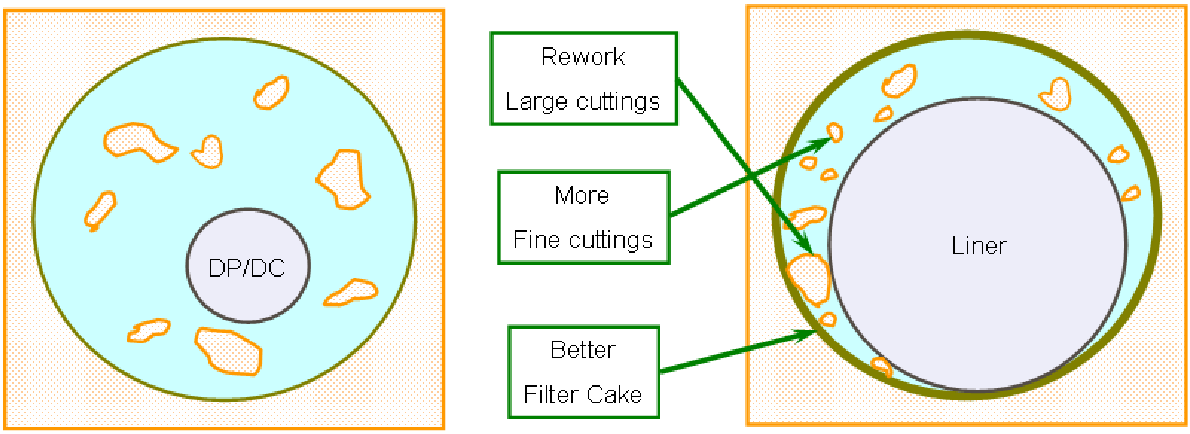

Figure 12: Illustration of the Smear Effect [15]

- Fewer casing strings: Casing while drilling may also allow for the use of fewer casing strings, and if combined with expandable tubular technology, this could prove to be quite a powerful combination.

Drilling with casing is not without its fair share of challenges, however.

- Torque is one of the challenges associated with casing drilling. At times, higher torque loads will be experienced at the surface when compared to conventional drilling. Also, the connections used on the casing will have to be strong enough to withstand the torque experienced by the casing string during drilling. While there are several reasons for the increase in torque, perhaps the main reason remains the increased weight of the drilling string. This is one of the topics which will be further investigated in later sections.

- Reduced ROP: Several operators have reported problems with a low effective rate of penetration (ROP). While there may be several reasons for this, one may be the increased time spent making connections at the surface during casing while drilling. Another issue is that limitations are often imposed on the amount of revolutions per minute (RPM) and the amount of weight on bit (WOB) which may be applied to the casing during drilling. The reason for these limitations is the use of casing as opposed to drillpipe. Since the casing used to drill the well must also retain its integrity and be operational for the rest of the lifetime of the well, a safety margin must be included in order to ensure that it is not loaded beyond its capacity. This will be discussed further in later sections, however.

- Becoming differentially stuck: Due to the larger surface area of the casing compared to normal drillpipe, the risk of becoming differentially stuck may increase. This is because the differential pressure between the wellbore fluids and formation fluids will get a greater area to act on. When the pressure acts on a greater area, the resulting force becomes greater, thus increasing the risk of getting stuck, and also making it harder to free the pipe if it does get stuck.

  If one gets stuck during conventional drilling and is unable to work the pipe free, action must be taken to continue the drilling operation. First of all, the part of the drillpipe above the stuck point must be retrieved. This is usually done by using explosive charges just above the stuck point, preferably at a connection, while applying torque simultaneously to the drillstring. After retrieving the pipe, there are several alternatives, depending on the situation. One alternative may be to set a cement plug, and use this cement plug to kick off into a new wellbore. Another option is to perform an open-hole sidetrack further up in the hole, and continue drilling. This requires certain formation characteristics and a rotary steerable system, however. The third option would be to place a whipstock in the well. The whipstock would then be used to kick off into a new wellpath to initiate a sidetrack. Regardless of the method used, the operation would be characterized as a technical sidetrack, since the sidetrack was a result of technical difficulties experienced during drilling.

- Extra equipment required: Another possible disadvantage of casing drilling is the increased amount of equipment which may be needed. Especially if the CWD system is retrievable, a lot of extra surface equipment has to be installed before operations may begin. This adds time, cost, and complications to the operations. The most visible requirement is that some sort of casing drive system must be installed. In addition to the casing drive system, wireline equipment may also be needed if the casing drilling system uses a wireline-retrievable BHA. This does not apply to casing drilling with non-retrievable BHAs, however. The concept of retrievable and non-retrievable BHAs will be discussed in sections 4.4 and 4.5.

4.3 Drilling with Liner

Drilling with liner means that the drilling process is carried out by using casing and drillpipe to transmit torque and weight to the bit. One exception would be where one first drills with casing and then turns the casing into a liner upon reaching TD. This is a special case, however, and will not be explored further in this thesis.

For a liner drilling system, the BHA will usually be retrievable. A liner drilling system may have many uses, but the most common one seems to be when drilling into unstable formations, or formations whose pressures vary greatly from its neighboring formations. This means that when drilling into a depleted reservoir, problems may be experienced. While drilling the overburden, normal or initial pore pressure will usually be experienced. The reservoir interval, however, has been produced, and the pressure here may therefore be significantly lower than when production drilling initially took place. Problems may therefore be experienced when entering the severely depleted zone from the overburden with normal pressures. One example of this will be mentioned in section 4.6.1.

Liner drilling can also be helpful in troublesome or unstable formations. This is due to the fact that the casing or liner is already in the hole allows one to isolate the formation from the wellbore when required. The next hole section can then be drilled, allowing the operation to continue as planned.

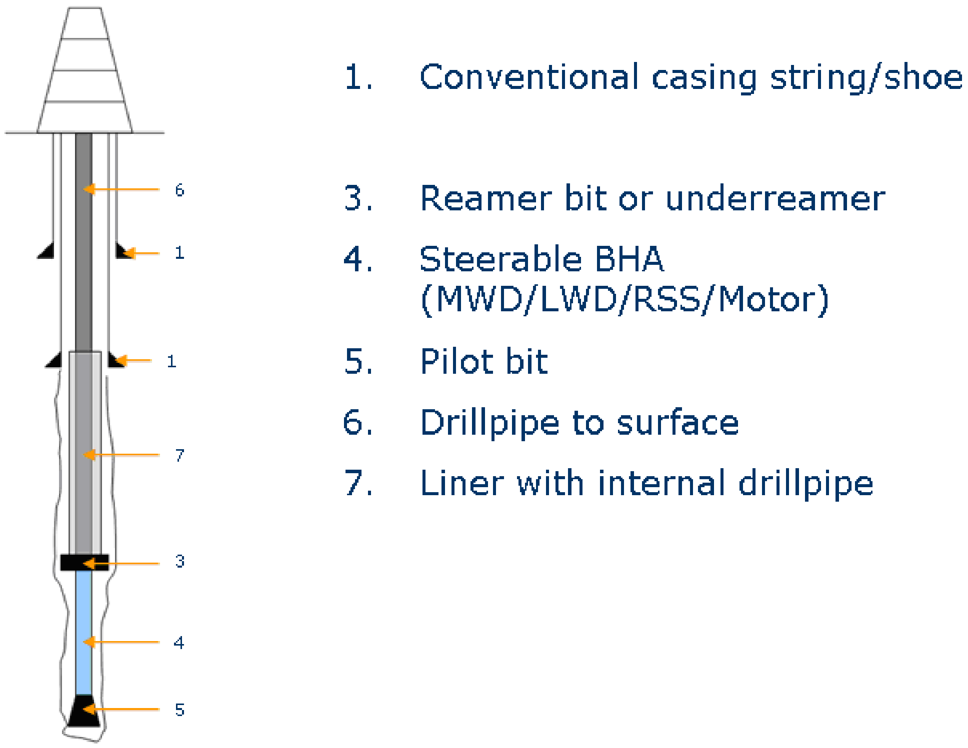

Figure 13: Drilling with Liner [24]

With liner drilling as shown above, a full directional BHA with MWD/LWD and other equipment can be run. This is beneficial because it provides accurate well placement information, and also allows steering the well where desirable. It is also necessary because of regulatory requirements on the Norwegian Continental Shelf, which require a survey to be taken every 30 meters drilled.

Furthermore, the impact of ECD is different for liner drilling than it is for casing drilling. This is because the length of the decreased annular space only applies to the length of the liner, as opposed to casing drilling where the entire length of the drillstring has a reduced annular area. Therefore, given the same flow rate for both liner and casing drilling, the ECD will be smaller for liner drilling. In reality, however, this may not be the case. The reason for this is that the liner drilling assembly requires higher flow rates for proper hole cleaning, because of the increased annular cross section area between the drillpipe and casing. This leads to an increase in the ECD.

One of the advantages of liner drilling compared to casing drilling is that it can be used with existing pipe handling equipment without any major modifications, apart from the need for a false rotary. This false rotary is only required when making up the liner and drillpipe system when tripping into the hole with the entire assembly for the first time, as illustrated below. It is also required if tripping the entire system out of the hole together with the liner.

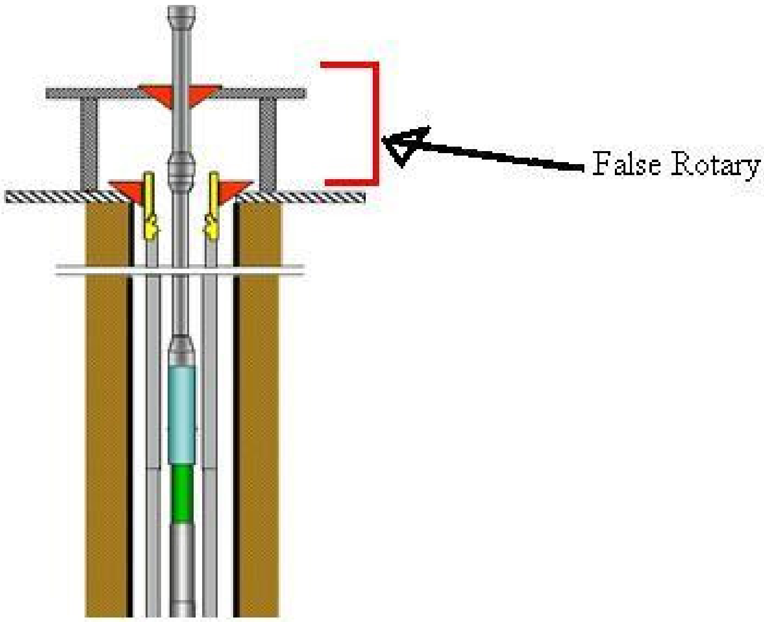

Figure 14: False Rotary Table used to make up the Liner Drilling System before running into the hole [25]

Another advantage of liner drilling compared to traditional drilling is that it ensures that the liner is always at the bottom. This reduces the risk of lost circulation, wellbore collapse, and kicks. The so-called smear effect is also a factor. This may allow lower circulation rates and mud weights, while still maintaining proper hole cleaning and well control. Wellbore collapse also becomes less of a problem, since the casing, as already mentioned, is always at the bottom of the well.

In other words, the likelihood of lost circulation and kick events becomes smaller, and the consequence of wellbore collapse becomes less severe. This is because the liner is at the bottom of the well at all times.

There are, however, disadvantages with the liner drilling system as compared to the casing drilling system. One of the most notable disadvantages is that the liner drilling system does not allow for circulation or reciprocation while pulling out the BHA with the liner left at the bottom of the well. If rotation, circulation, or reciprocation is required, the liner has to be pulled up to the rotary along with the entire BHA, and this negates some of the advantages of liner drilling. If the liner has to be left at the bottom of the hole, there is also an increased risk of the liner becoming differentially stuck during tripping out of and back into the well with the drillpipe.

As mentioned, the pipe handling is somewhat different from conventional drilling when making up the liner drilling assembly for the first time. This requires a false rotary table, since the drillpipe and BHA has to be run into the well with the liner hung off from the regular rotary table when running the system into the hole for the first time.

4.4 Drilling with a non-retrievable BHA

The arguably simplest form of casing drilling is done with a non-retrievable bottom hole assembly. Most commonly, the non-retrievable system will consist of a bit and a float collar mounted directly at the bottom of the casing. The bit will be especially designed for casing while drilling applications, and will usually be of the PDC type. This is to ensure sufficient durability of the bit, since it can not be replaced once it has been run into the hole, unless the entire section of casing is retrieved.

Figure 15: Weatherford EZCase non-retrievable [23]

Once the casing has been drilled down to TD, it can be cemented in place through a float collar, which is normally included in the string. Then, the next hole size may be drilled. For this reason, all BHA components used in non-retrievable systems must be designed to be drillable. One design employed by Weatherford also allows the cutting structure of the bit to be split into segments that are pushed outwards into the hole walls, making it easier to mill through the bit when moving on to the next hole size. It also allows for a more robust cutting structure, since drillability is no longer a concern.

Figure 16: PDC Casing Drilling Bit Pre- and Post-Expansion [26]

The advantage of non-retrievable systems is that they are fairly simple, and can usually be cemented in place immediately after reaching TD. There is also no need for an under reamer or hole opener, since the bit can be full gauge. This means that there are fewer components included in the BHA.

The disadvantage, however, is that should a BHA component fail or the bit become severely damaged, the entire string has to be pulled out of the hole to replace the BHA. This takes away all the advantages usually enjoyed by casing drilling, since the casing string will no longer cover the open hole sections.

Another disadvantage is that, in Norway, regulatory requirements demand that directional and inclination surveys are taken every 30 meters drilled. Since non-retrievable BHAs usually do not consist of advanced MWD equipment for cost reasons, this severely limits the application of non-retrievable casing drilling systems on the Norwegian Continental Shelf (NCS), unless some sort of wireline- or pipe-retrievable MWD unit could be developed.

Furthermore, the drillstring must also be rotated with the same RPM as the drill bit, all the way from the surface, and this limits the available torque, since the strength of the casing must be taken into consideration when considering the maximum amount of torque and rotation to be applied. While the casing itself may be able to withstand more or at least equal torque compared to the drillstring, fatigue considerations have to be made with regards to the number of cycles the liner connection can endure.

4.5 Drilling with a retrievable BHA

Drilling with a retrievable BHA, although done in different ways by different equipment manufacturers, offers several advantages over non-retrievable BHAs.

One of the most visible advantages is the increased flexibility in BHA design. While the BHA for a non-retrievable system will be very simple, largely due to cost, a retrievable BHA could in principle be designed with whatever tool combination required, just as in conventional drilling. A wide range of LWD and MWD tools may also be included in a variety of configurations.

Since the BHA is retrievable, some sort of latching mechanism is required, however. Some manufacturers, such as Tesco, have opted for a wireline-retrievable BHA, which latches into a drill lock assembly (DLA) at the bottom of the casing, and allows drilling to be done. The force is then transmitted to the BHA via the entire casing string.

Other manufacturers, such as Baker Hughes Inteq, have designed a retrievable system that is run on drillpipe and latches into the liner in several places. This system has so far been used mostly for liner drilling.

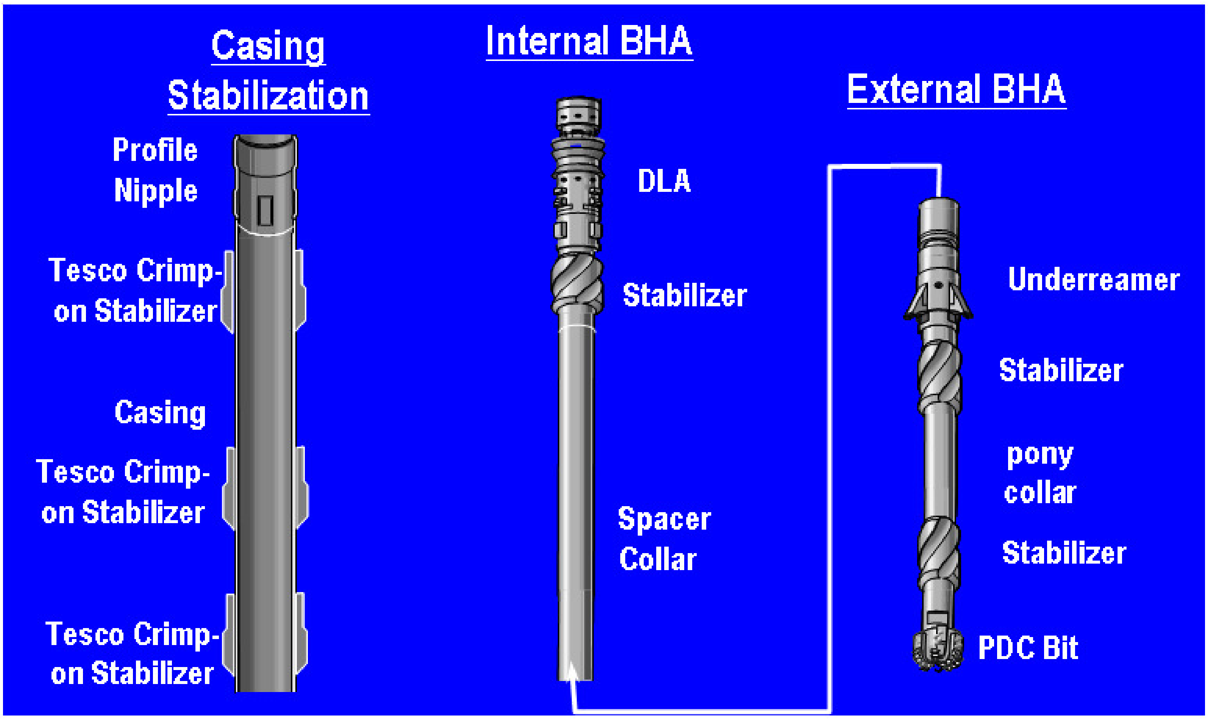

Figure 17: Typical Tesco retrievable CWD BHA [27]

Retrievable systems will usually incorporate a positive displacement motor (PDM) in the BHA. The reason for this is that it will allow the bit to rotate faster than the rest of the drillstring, making the drilling process more efficient. This allows the casing to be rotated slowly and thus avoid potential strength degradation due to fatigue induced while rotating the casing in a bend. At the same time, one must still maintain an acceptable RPM for the bit and BHA itself. This will help achieve a better rate of penetration (ROP).

Since a retrievable system does not have a float collar in place, this has to be pumped or run down after reaching TD before cementing can be performed. This is a disadvantage when compared to non-retrievable systems where cementing may take place right away.

Another aspect of retrievable BHAs is the need to use some sort of hole opening device in order to obtain a full-gauge hole which the casing may pass through. Since the BHA must be retrievable, it must be able to pass through the inner diameter of the casing. Therefore, the hole must be opened to full-gauge either by the use of under reamers or by reamers mounted on the casing shoe. Problems may also be experienced with failure of the reamer itself, or due to excessive balling.

4.6 Case Studies – Previous Use of Liner and Casing Drilling

In this section some of the applications so far of casing and liner drilling will be explained, in order to provide a brief overview of the different applications casing and liner drilling have been used for.

4.6.1 Offshore Liner Drilling on the Valhall Field

The Valhall field is an offshore field located approximately 150 miles to the southwest of Norway, outside Stavanger. It is currently operated by BP, but at the time of the initial liner drilling operations, the operator was called Amoco Norway Oil Company.

The problem faced by the operator on the Valhall field was that when drilling into depleted areas of the Tor chalk formation, there was an instantaneous reduction in pore pressure by 5-7 ppg from the Lista shale overburden and into the Tor chalk reservoir [20]. In this field, the shale overburden had to be cased off as close to the chalk reservoir as possible in order to prevent hole stability problems. This sudden decrease in pore pressure made it difficult to achieve this objective by conventional means, however.

Initially, the operator would drill to within a short distance of the top of the reservoir, and then cement the casing in place, some distance above where originally planned. Another approach was to drill into the reservoir, and then pump a gunk pill, consisting of diesel oil, bentonite, and lost circulation materials. This pill had to be taken into consideration when running the casing as well.

Using these methods to complete the well, the operator experienced problems such as hole enlargement, poor cuttings transport, stuck pipe, and well control incidents caused by gas influx [20]. This was mainly due to incomplete isolation of the Lista formation. From a long term perspective, there was also the potential for loss of production, resulting from the influx of mud, gunk, and cement into the producing interval. This was also observed as a trend over time.

One well which illustrated this in particular was Well 2/8 A-1. This had been the most stable Valhall producer since it came on stream in 1982 [20], averaging between 12,000 and 16,000 barrels per day from 1989 to 1993. It experienced casing collapse in the overburden, and consequently had to be sidetracked out of the 9 5/8" casing section. The objective of this operation was to drill Well 2/8 A-1A, which would be a "vertical twin" [20] to the original. Because of geological uncertainty, the depleted Tor section was penetrated earlier up than expected, and the well therefore experienced severe mud losses along with several gunk squeezes to remedy the situation.

After recompletion with several stimulation treatments, the current production of the well at the time of publishing had decreased to 5000 barrels per day, as opposed to the earlier figure of 12,000. While some of the cause might have been geological, there was a strong suspicion that the lost circulation incidents, and the actions taken to cure them, were in part responsible for this decrease in production, and therefore also loss of revenue.

On this basis, the operator felt that a liner drilling system could be beneficial, since it would make it possible to penetrate and isolate the Tor/Lista interface, without experiencing the situations which were seen during conventional drilling. A series of lab tests were performed, some with the aid of Baker Oil Tools, in order to determine the appropriate cutting structures, flow rates, and so on for the proposed liner drilling system.

The concept of the liner drilling solution was to first drill down to some distance above the Tor chalk formation with a conventional steerable assembly. Upon reaching this point, the BHA would be tripped out, and a liner drilling system would be run into the hole in order to enter the Tor formation.

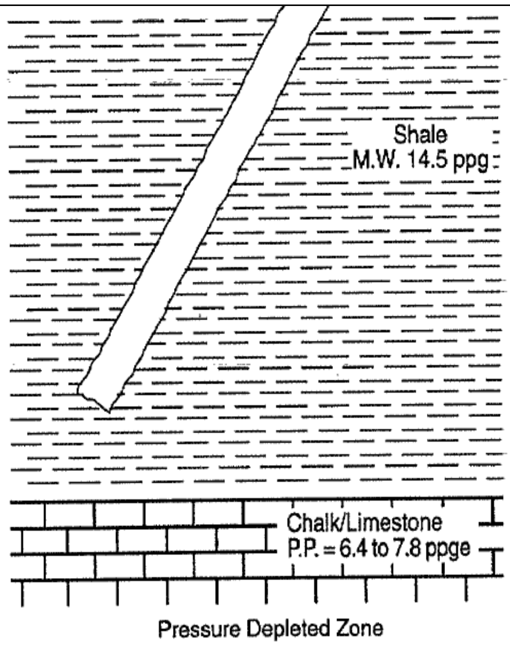

Figure 18: Conventional Drilling down to the reservoir [20]

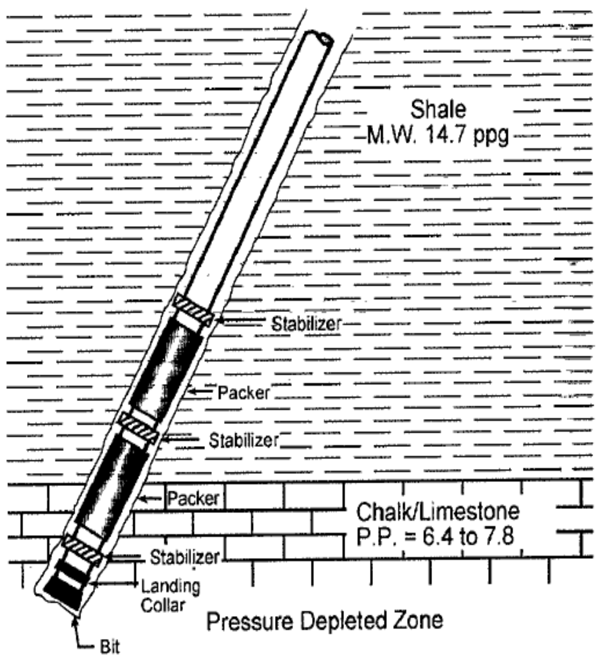

Figure 19: Drilling with a liner into the depleted zone [20]

Following the lab tests, several wells were drilled by the operator with the steerable liner drilling system. The first of these was Well 2/8 A-2A. In this well, a few meters of Lista shale and into the Tor chalk were drilled with a 7" rotary liner drilling system in order to isolate the overburden from the chalk formation.

A total of 51 ft were drilled in 3,2 hrs with the rotary liner drilling system in this well. The liner drilling approach on this well totaled 15,6 days. The same time consumption of a comparable well (A-1A) was 33,8 days, and the liner drilling approach therefore represented significant savings to the operator. Following this well, the lessons learned were used in order to further improve the liner drilling system design and procedures for subsequent operations, and on the next well drilled with a rotary liner, the time consumption was down to 12,1 days.

Several other wells were drilled by the operator on the Valhall field, and compared to the best conventionally drilled well into the depleted Tor formation, the liner drilling system presented a reduction in time spent of up to 50%. Unscheduled events also dropped by nearly 75% as experience was gained with the liner drilling system. In this instance, liner drilling has clearly been beneficial.

4.6.2 Onshore Casing Drilling in the Lobo Field

Since 1997, the operator ConocoPhillips has had sustained, multi-rig activity on its Lobo field in the south of Texas [18]. In the year 2001, ConocoPhillips had ten active rigs, drilling approximately 100 wells per year. Due to the significant number of wells drilled on the same field, there had been a quite steep learning curve up until this point with a lot of improvement.

After increasing up until 2001, the drilling efficiency of the field seemed to stagnate somewhat, with an average spud to rig release time for a 10500 ft well of 19,2 days [18]. It appeared as though the drilling efficiency had been improved up until the point where further improvement would be very difficult to achieve by conventional means, especially since downhole trouble time had been reduced to less than 10% of the overall drilling time. It was, however, necessary to increase the drilling efficiency, in order to make smaller reservoirs economically feasible to develop.

The operator identified the flat time at the TD of each hole section as an area that could be improved. It was also noted that stuck pipe and lost circulation were the cause of the majority of hole problems seen in the Lobo field [28]. Casing drilling was seen as a technology which had the potential to improve these problems, and Tesco's Casing Drilling system was chosen by the operator to perform the actual casing drilling.

Tesco's system, in brief, is a casing drilling system where the BHA may be installed and pulled by the use of wireline or drillpipe. The BHA is placed in a drill lock assembly (DLA) when drilling, and may be removed from this assembly if, for some reason, tripping the BHA is required.

An initial five well pilot program was initiated at first to see whether casing drilling could help solve the drilling problems seen in the Lobo field and thus reduce the drilling cost. The wells drilled in this first period were fairly simple wells, and their performance improved quickly, matching that of conventional drilling at the end of the five well pilot program. Because the operator believed that further improvement was possible, the program was extended further from 2001 and into 2002.

In phase two of the testing, the wells drilled were more challenging than in phase one. The results, however, were quite promising. Although wells were not drilled trouble-free, the trouble seen was associated with the equipment used, and not the formation being drilled.

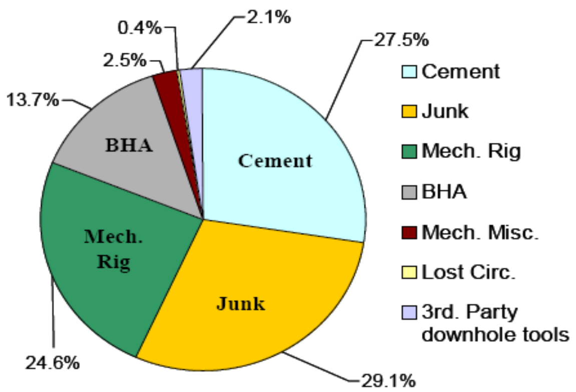

Figure 20: Trouble Time for two Casing Drilled Wells in the Lobo Field [18]

Thus, a third phase was implemented, in which the operator would employ three new rigs designed specifically for casing drilling from the beginning. Up until 2005, ConocoPhillips had drilled more than 94 wells using casing drilling in the Lobo field. Two of these wells had been drilled with conventional steerable motors as part of the retrievable BHA. They were not, however, competitive with regards to the performance of the rotary steerable systems commonly used offshore, and tests were also performed in order to see if RSS could be combined with casing drilling.

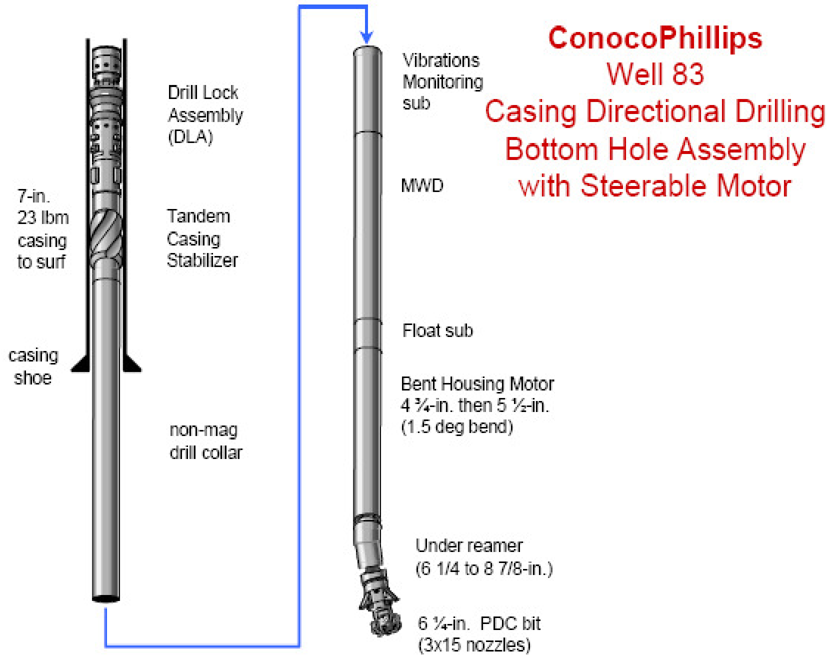

Figure 21: Casing Drilling BHA with Steerable Motor [28]

The first RSS and casing drilling test was successfully done on a vertical well. Although there were some equipment failures, these were judged not to be specific to casing drilling, and based on this it was concluded that directional wells could be drilled with casing using rotary steerable systems. While there are still improvements to be made on the system and procedures used, the fact remains that the operator in this case experienced that wells which might otherwise not have been economical to drill, could be drilled economically using the casing drilling system.

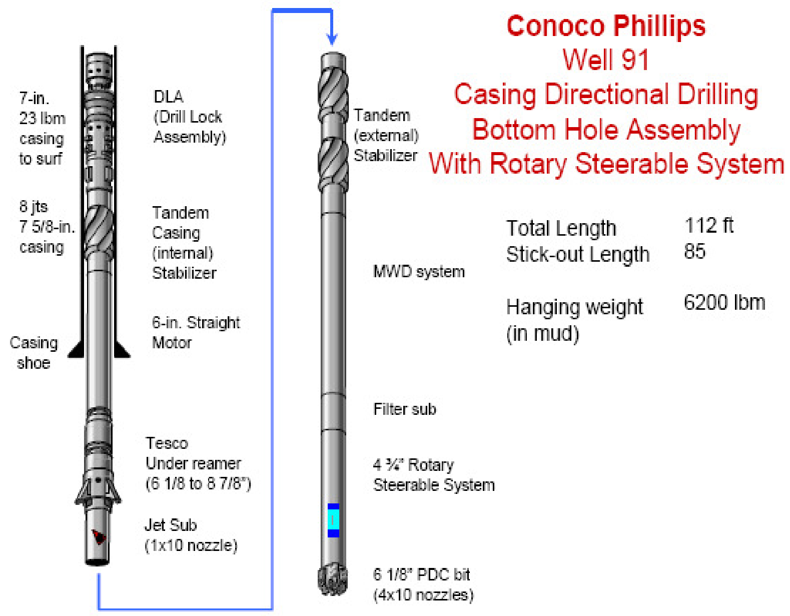

Figure 22: Casing Drilling BHA with RSS [28]

4.6.3 Offshore Casing Drilling on the Eldfisk Field

The Eldfisk field is located approximately 300 kilometers southwest of Stavanger, Norway, in the North Sea. It is operated by ConocoPhillips, which has previously implemented casing drilling on a large scale with great success in onshore operations [18], and had therefore decided to see if the benefits seen using casing drilling could be realized offshore as well as onshore [22]. A candidate well was subsequently found in Norway, on the Eldfisk Bravo platform. In order to gain some experience with casing directional drilling before testing it on the Eldfisk field, two land based tests were conducted prior to the operation planned for Eldfisk. At the same time, the planning process for well 2/7 B-16A was initiated.

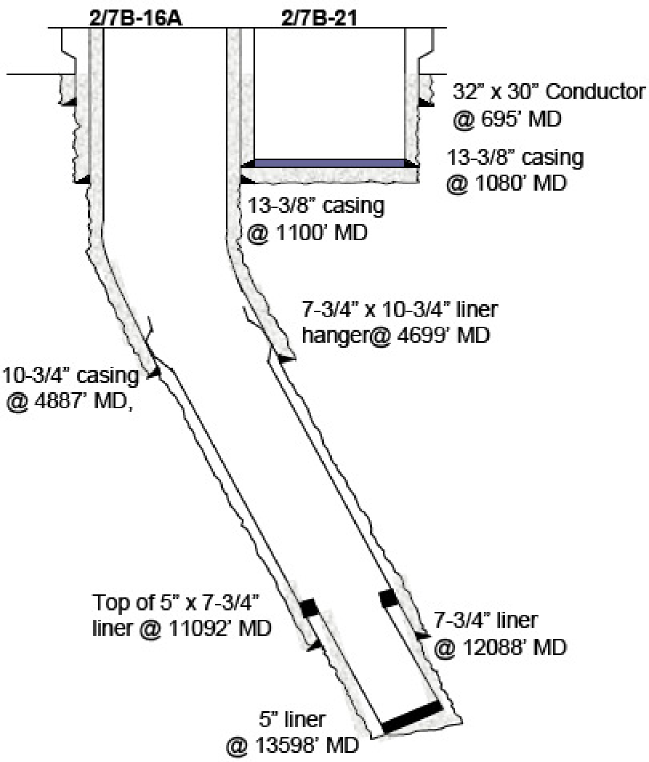

Figure 23: Eldfisk Bravo CWD Well Design [22]

The Eldfisk Bravo platform is a relatively small platform with 20 production slots and integrated drilling facilities. Constant drilling and intervention activities are performed in order to maintain the production of the field [22].

Among the drilling challenges usually faced are lost returns near the top of the reservoir, high levels of gas while drilling, and poor hole quality experienced during tripping operations. These problems made the field a good candidate for testing of the casing drilling system. It was therefore decided to drill both the 10 ¾" and the 7 ¾" sections of well B-16A with the casing drilling system.

The fact that the 7 ¾" production casing had to be converted to a liner upon reaching TD [29] further complicated the operations, although it did not directly impact the casing drilling operation itself .

The BHA used for drilling was mainly made up of standard components. All that set it apart from conventional drilling BHAs, was that it would be attached to the casing string by means of a locking assembly.

PDC bits with 13 mm cutters were used for both of the sections that were to be drilled with casing. 6 blades were included for the 10 ¾" section while the 7 ¾" bit had 7 blades. The BHA was set up with approximately 70 ft between the underreamer and the pilot bit [22].

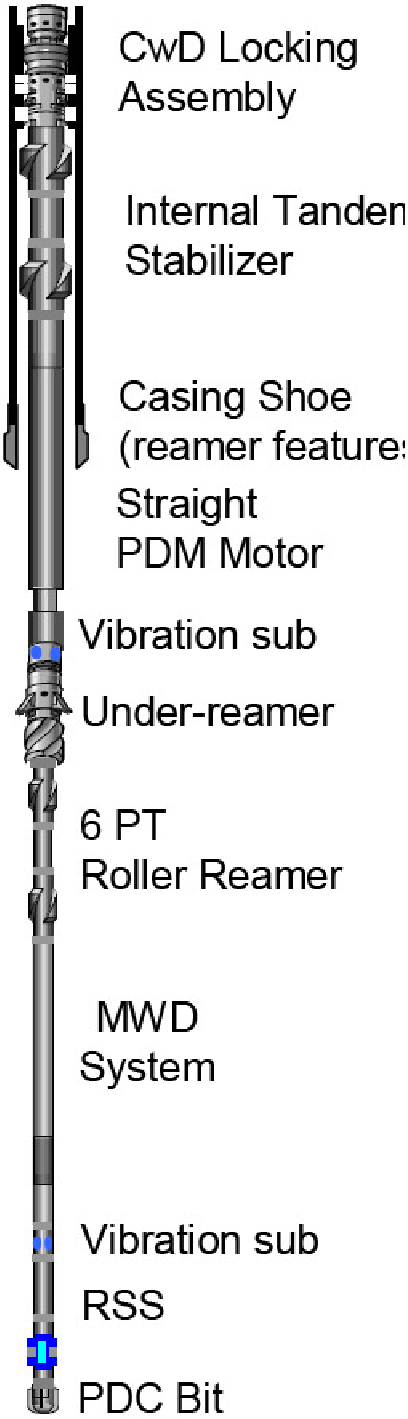

Figure 24: Eldfisk Bravo CWD BHA [22]

The underreamer was especially designed for casing drilling, with 19 mm cutters and 3 blades.

Aside from the CWD locking assembly, internal stabilizers and casing shoe with a reamer, the BHA of the casing drilling system did not employ any proprietary components. The MWD and RSS tools used were all tools which could have been used in conventional drilling assemblies as well.

The casing was rotated with 20-30 RPM from the surface during the operation, while the PDM would provide an additional 130 RPM to the lower part of the BHA [5]. This was done in order to minimize casing wear, while still maintaining sufficient rotation of the bit to ensure that a reasonable ROP is maintained.

As can be seen from the figure, non-magnetic drill collars were not included in the BHA. This was done in order to minimize the length of BHA sticking out below the casing. This was desirable in order to maximize the potential benefits and effects of the smear effect. Corrections for magnetic effects were made mathematically, and checked with gyro runs at the end of each hole section.

Both the 10 ¾" and the 7 ¾" sections were drilled and cased successfully. The overall time required to perform the operations was, however, somewhat longer than anticipated.

This was in part due to problems with the equipment and retrieval processes, but also due to quite slow average connection times. However, no significant hole problems were encountered, and it therefore appears as though casing drilling had a positive effect in the sense that hole problems were reduced, if not eliminated. The directional steering objectives were also met, and the system was seen to achieve build rates of almost 5°/ 100 ft.

Although there was seen to be significant room for improvement in the casing drilling operation which was performed on the Eldfisk field, the operation is still considered a technical success by ConocoPhillips [30].

4.6.4 Offshore Casing Drilling in Deepwater Gulf of Mexico

Shell is the operator of the Brutus tension leg platform (TLP) in the Green Canyon Block 158 in the Gulf of Mexico. The water depth in this area is 2985 ft, and the field has been in production since 2001 [31].

Since then, the production of the field has declined, and sidetracks are necessary in order to maintain the production at a satisfactory level. However, since the original development field, production has also lead to the depletion of several zones, and this is a complication which could lead to serious drilling problems during conventional drilling. Because of this, the wells on the Brutus field were seen as candidates for testing a rotary drill-in liner system [31].

Shell had previous experience from casing drilling from the South Texas Vicksburg field. In this field, the operator has combined casing drilling and underbalanced drilling in order to be able to maintain old wells and drill new wells which would otherwise either have been uneconomical, or caused a significant amount of drilling problems [32]. One of the reasons for the economical benefit of casing drilling in this case was the ability to eliminate a casing string, as can be seen from figure 25 below.

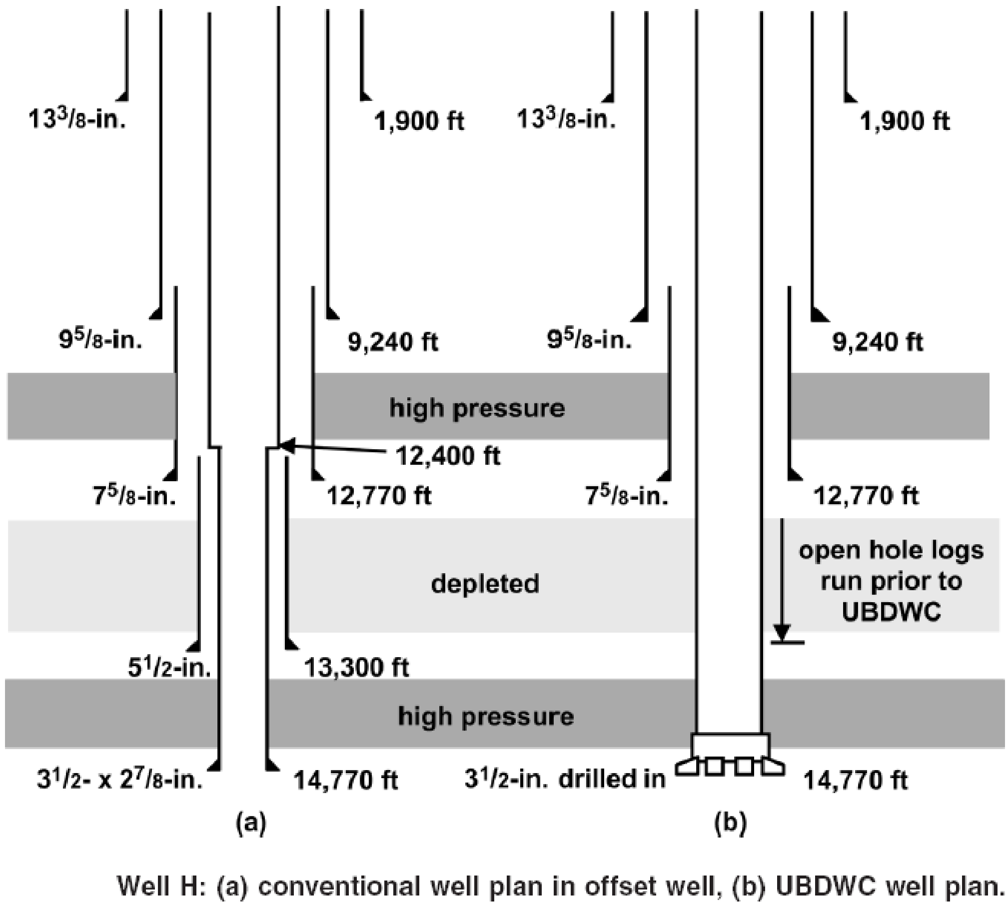

Figure 25: Shell South Texas Casing Drilling Well Plan [31]

Experience from the Vicksburg project, in particular with regards to connection design and testing, was also utilized in the deepwater application of liner drilling.

The liner drilling system components were as follows [31]:

- Roller cone bit
- Two joint shoe track
- Double valve float collar
- 5 ½” 20 lbs/ft P-110 casing
- Expandable Liner Hanger Assembly
- Sub-surface released high pressure liner wiper plug
- 4” 14 lbs/ft S-135 drillpipe

The first rotary liner drilling trial from the Brutus platform was unsuccessful. This was mainly because the expandable liner hanger component was unable to cope with the adverse hole conditions [31]. After modifying the liner hanger, a second attempt was made to drill with liner. This attempt was successful, and 97 ft of formation was drilled using rotary liner drilling in a time of 8,5 hrs, equivalent to 11,4 ft/hr.

The liner drilling assembly was rotated with up to 80 RPM, which was necessary in order to obtain an acceptable ROP as there was no positive displacement motor included in the BHA.

This trial showed the operator that rotary liner drilling is possible with an expandable liner hanger, and that the system is robust enough to be used.

4.7 The Smear Effect

The smear effect is quite commonly referred to in papers and reports dealing with casing and liner drilling. The fact remains, however, that the effect itself has not been investigated in great detail, even if it is reported as a benefit of casing drilling [19]. It may also be said to be a somewhat vague term.

The term smear effect in casing drilling is usually used to describe the process in which the cuttings are ground by the large casing or liner string, and then plastered onto the wall of the wellbore. The theoretical advantage of this effect is that it has the potential to strengthen the wellbore and filtercake, and therefore also mitigate, or perhaps entirely prevent, lost circulation problems. This has been the reported benefit of casing drilling in some fields, most notably the Lobo field in Texas where ConocoPhillips is the operator.

While some of the success of the casing directional drilling program in the Lobo field has been attributed to the smear effect and its ability to reduce lost circulation, it might be prudent to take a closer look at this claim. The reason for this is that in conventional drilling, a higher safety margin must be included in the drilling mud program, trip margins, to account for surge and swab pressures when running into and out of the well with drillstring and casing. For casing drilling, however, the margin appears to have been lower and the window between the pore pressure and fracture pressure gradient appears to be somewhat wider. In order to illustrate this, one might take a look at the attachments used in the papers by Warren *et al* [33] and Fontenot *et al* [34] describing the casing drilling operations in the Lobo field in Texas.

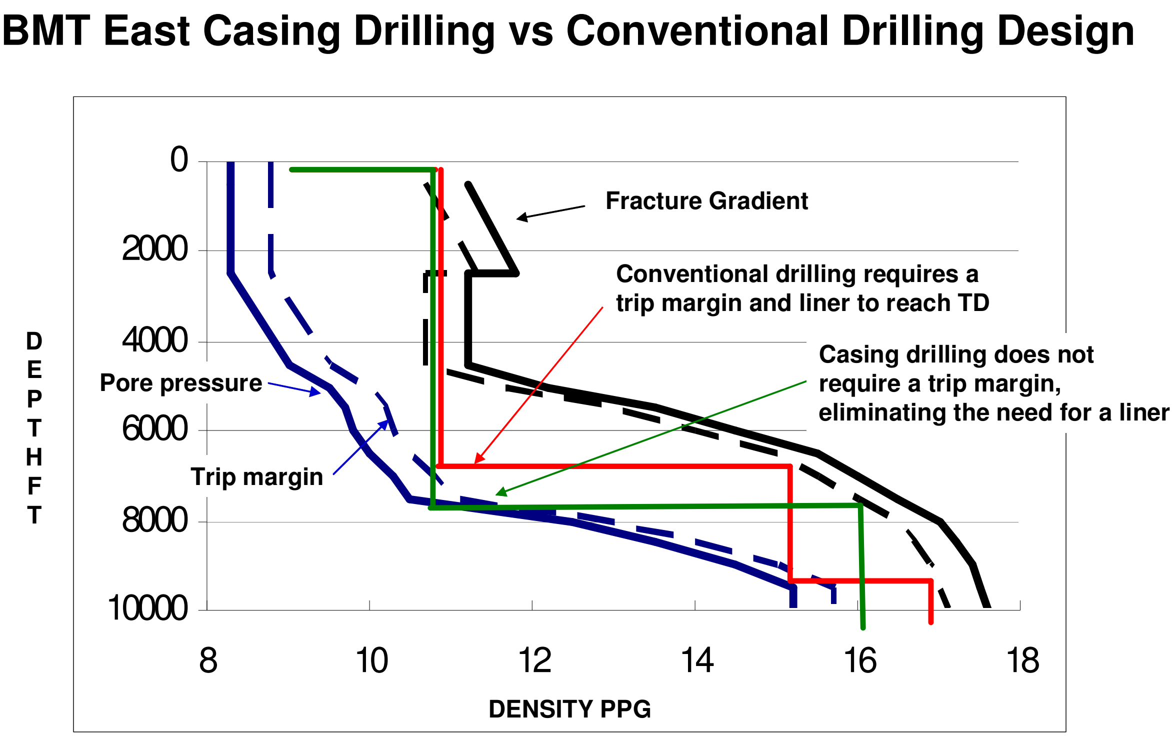

Figure 26: Pore- and Fracture pressure Analysis of the Lobo Field [34]

The same difference in the mud weight schedules versus the required trip margins are also illustrated in a similar paper by Warren *et al* [33].

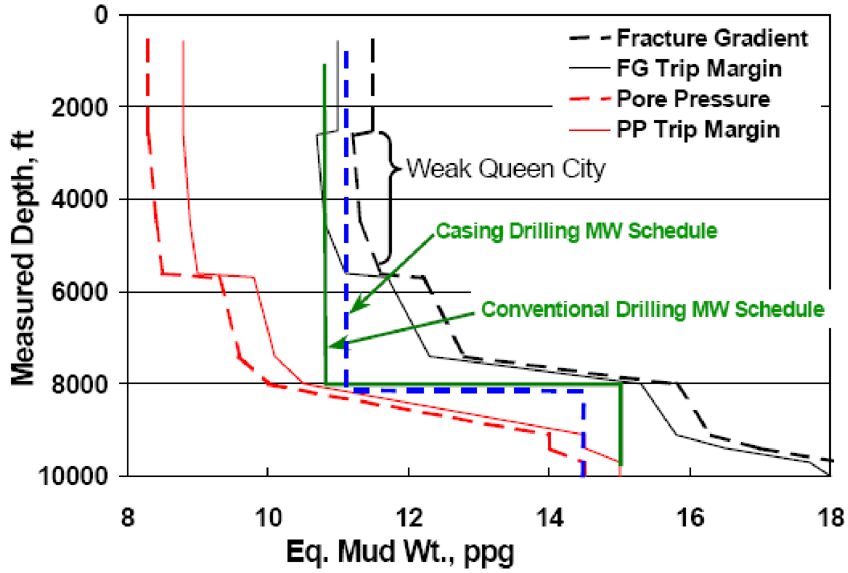

Figure 27: Lobo Pore and Fracture Pressures vs Mud Weights [33]

The same trend is seen in figure 27, as in figure 26 above.

Furthermore, an analysis of the cuttings particle size distribution from the cuttings of a casing drilled well on the Lobo trend was made.

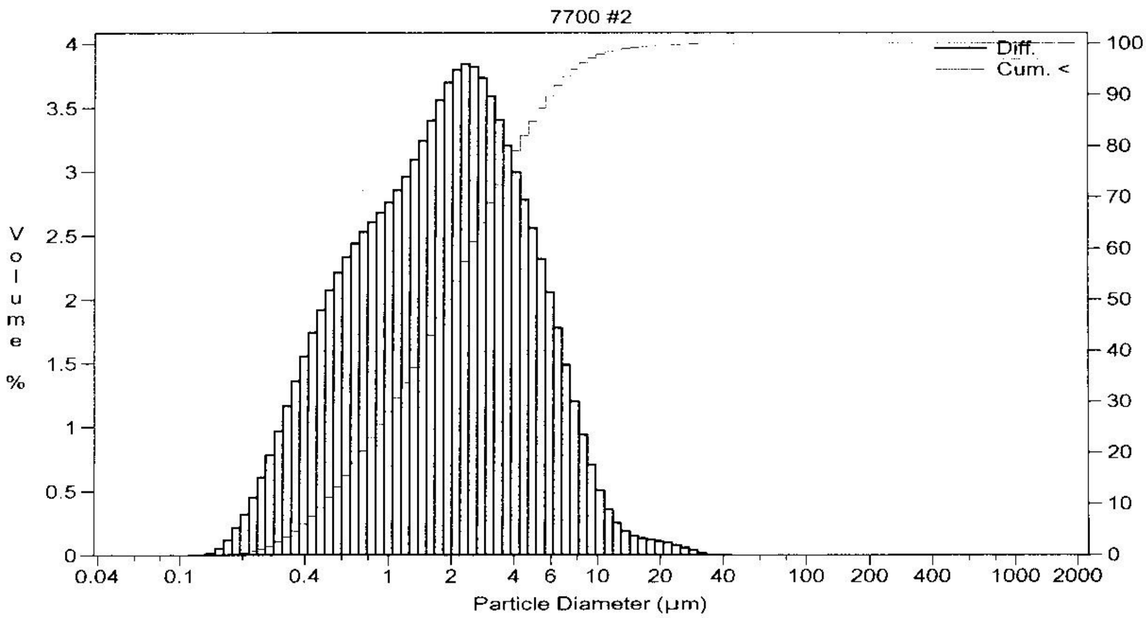

Figure 28: Particle Size Distribution for Lobo Trend Casing Drilling [34]

The main particle size distribution in the cuttings shown in figure 28 above, although wide, is concentrated from 0,4 µm to 10 µm. This is quite a bit lower than the particle size distribution of the particles which are usually added as lost circulation material to normal drilling mud in order to prevent losses. The particle size distribution of LCM for normal designer mud will usually be between 50 and 1500 µm.

Based on figures 28 and 29 seen above, it may therefore seem as though there are other partial explanations of why non-productive time (NPT) on the Lobo field was greatly reduced when drilling with casing was implemented. This does not, however, mean that there is no smear effect.

In theory, however, the smear effect does not seem like an unreasonable concept. It appears likely that the crushing of the cuttings by the liner or casing may provide a particle size distribution which would resemble that of LCM, and therefore be of help when encountering lost circulation scenarios. The cuttings will probably have to be crushed less than what seems to have been the case in some previous scenarios. The potential does exist, however, since the lower flow rates used during casing drilling when compared to conventional drilling gives a higher cuttings concentration in the well.

It should also be noted that of the different projects investigated which reported a beneficial smear effect, there are some which have no other probable explanation than the smear effect. This would again indicate that there actually is a smear effect, but the concept still seems to require further verification.

There are also other theories which attempt to explain the same effect as the one attributed to the smear effect. One theory claims that there may be a temperature effect seen with casing drilling. It states that there will be less cooling due to the mud flow during casing drilling, and therefore a smaller temperature change. This is claimed to cause less borehole stress and may therefore help prevent losses.

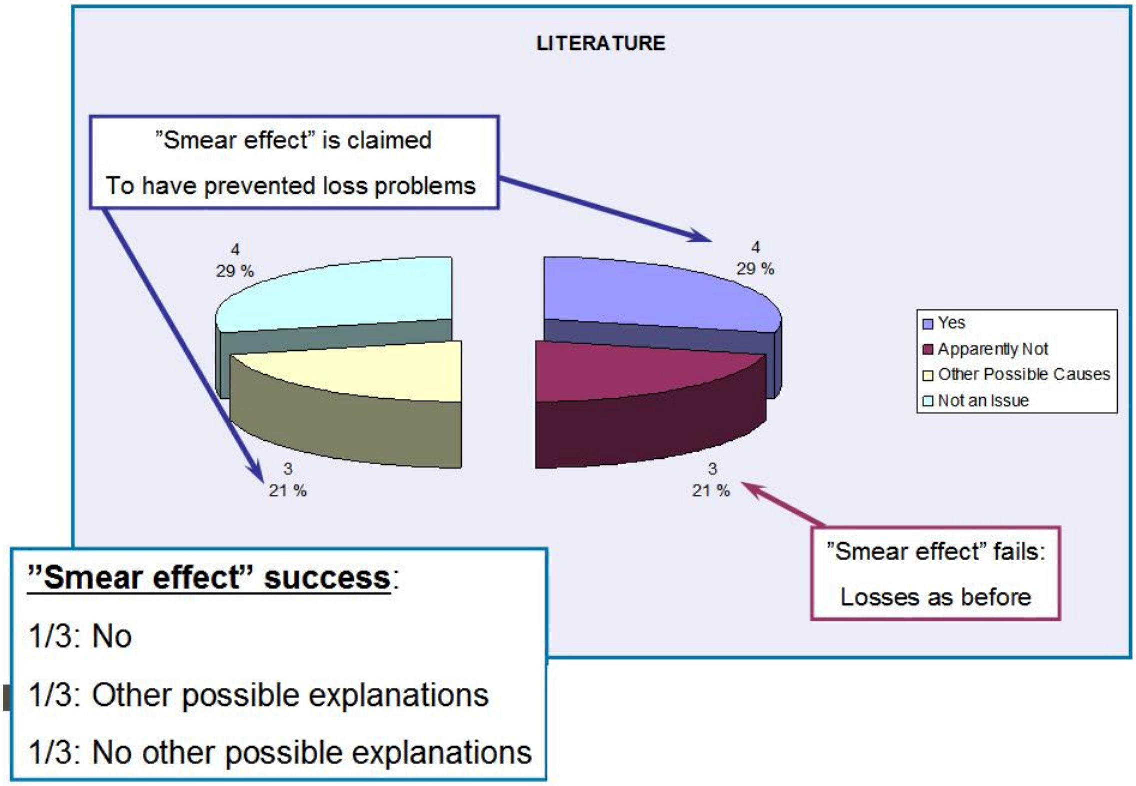

Figure 29: Smear Effect Success Rate [15]

Figure 30 above shows the results of a literature survey performed as part of the internal smear effect study. It should be noted that there may be cases which have not been included in this survey, and there may therefore be smear effect cases which have not been taken into consideration.

As for the liner drilling project, samples have been taken in order to attempt to verify the smear effect, but so far the samples investigated have proven to be inconclusive. It is therefore unlikely that there will be any more conclusive results until the system has been deployed in the field in an actual operation. Thus far, although the smear effect is advertised as a beneficial effect of casing drilling by some, conclusive evidence still appears to be lacking, even though it may very well be proven to be true in the future.

5 The Steerable Liner Drilling System

5.1 Introduction

While there have been successful casing drilling systems tested, a rotary liner drilling system with full steering and logging capabilities has yet to be developed and field proven.

In the past, there have been several other liner drilling systems in use. One example would be the different liner drilling systems developed by Baker Hughes at Valhall. The most commonly used liner drilling system at Valhall was originally developed for use in Arun, Indonesia [21]. The system was set up with the drillpipe extending all the way down to the bit as an inner string, with the liner on the outside. The liner could be rotated along with the drillstring, as there was a hanger and running tool assembly located at the top. In the end of the inner string, a positive displacement motor could be found, along with a latching and landing system where the drillpipe is landed to connect with the liner. There was also a pilot and core bit at the end of the liner.

This may be said to be the predecessor to the current liner drilling system to be used by BHI. The PDM allowed for an increase of the rotational speed of the bit, while not rotating the liner excessively. However, since no part of the BHA extended much outside the liner, there was no room for including directional steering or any type of logging tools. The advantage of this configuration, however, is that the BHA could easily be retrieved, even if the liner itself got stuck.

Over time, however, the need for a liner drilling system with steering capabilities became apparent. This will be discussed in more detail in the next section.

5.2 Needs and Capabilities

One of the primary reasons for developing a liner drilling system with steering capabilities is the current StatoilHydro field portfolio. Several assets are aging, and gradually becoming mature, depleted fields. Other assets have high initial pressures, but face a reservoir pressure which declines quite rapidly.

One example of this is the Kvitebjørn field, where production had to be shut down for a period of time. The reason for this was that the pore pressure declined so rapidly, that the planned drilling program could not continue, until Managed Pressure Drilling (MPD) was implemented.

As fields mature and become older, production zones also become depleted. There are, however, zones which retain their initial high pressures. This requires high mud weights in order to balance and control the formation pressure. When drilling through these depleted zones, problems such as getting differentially stuck or experiencing severe mud losses may occur. These types of problems may also be related to pressure variations in compartmentalized reservoirs.

The liner drilling system may also be regarded by some as a contingency, in case fluid losses occur. While some claim that liner drilling will decrease the likelihood of such events, it is also an advantage that the liner is already in place, and, as long as the liner is in a location seen as acceptable, may be set and cemented right away if losses should become too severe to continue. There are, however, scenarios where even a drilling liner may have to be abandoned and the wellbore sidetracked, unless it is acceptable to continue drilling the well, albeit with a lower inner diameter.

Furthermore, several fields have also experienced unstable formations. While casing and liner drilling in general is said to strengthen and stabilize the borehole, it is also an advantage that the liner is at the bottom of the well the entire time. This way, if hole problems become too severe to continue, drilling can be stopped and the liner cemented in place, thus isolating the problematic area.

In some fields, one may also be dependent on getting the production liner down to a minimum depth in the reservoir. This is the case on for example the Kristin field, where the production liner has to penetrate a certain length into the reservoir in order to achieve sufficient production capacity. A steerable liner drilling system could be beneficial in this case, because there would be no need for a separate liner run as long as one is able to drill to TD.

While liner drilling in itself is needed, requirements also exist with regards to steerability and data collection. Since the liner should preferably be drilled over an extended interval, there is a need for data collection to avoid collision, as well as steering tools in order to ensure optimal well placement. There are also regulatory requirements which must be adhered to.

In addition, there is also a need for the bottom hole assembly to be retrievable. Should tool failure or some other situation which would require tripping out of the well occur, one should be able to pull out and replace the BHA. It should also be feasible to reconnect with the liner and continue drilling once the BHA is back in the hole.

Another apparent advantage of the steerable liner drilling system is the idea of drilling and casing the well at the same time. Although this is not an advantage unique to this particular steerable liner drilling system, it is nevertheless an advantage which should be taken into consideration when considering cost and time consumption as a factor. A liner run is saved, in addition to the trouble time that may potentially be avoided by using this system.

The result of these needs was that an invitation was sent out from Statoil in April 2006, where contractors were to submit a project proposal for the shared development of a liner drilling system to meet these challenges. The system eventually chosen was the Baker Hughes Inteq steerable liner drilling system [35].

Hydro had been pursuing the same system from BHI almost simultaneously, and when the merger between Statoil and Hydro became effective, the project continued.

The system has so far been tested twice. The first test was performed on the 9 5/8" configuration of the system at Baker Hughes' BETA test facility in Tulsa, Oklahoma. In this test, only a few hundred meters of formation were drilled, and the steering and re-latching capabilities of the system were tested. Similar tests were performed on the 7" version of the SLD system during the spring of 2009.

The plan is that a pilot test with the 9 5/8" SLD system will be done on the Brage field, most likely during the summer of 2009. Therefore, calculations performed in this thesis are based on a typical Brage field wellpath and parameters, although some changes have been made.

5.3 The Components of the Steerable Liner Drilling System

While the basic principles for composing a string and bottom hole assembly remain unchanged, there are some differences with regards to the make-up of a steerable liner drilling assembly compared to conventional drilling assemblies.

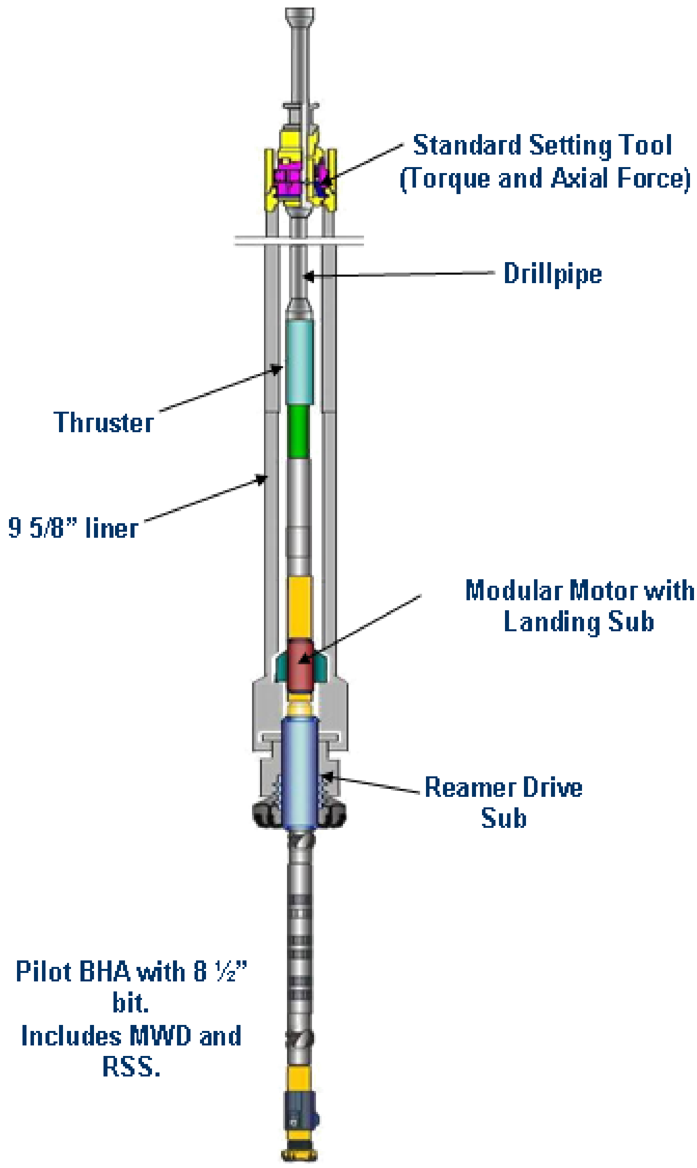

Figure 30: Overview of the SLD System [36]

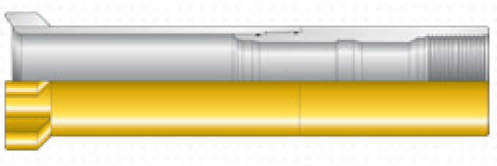

Figure 31: Liner Setting Sleeve [37]

From figure 31, it can be observed that when drilling with a rotary steerable liner, the system has an outer and an inner string at the bottom.

The outer part is made up of the liner, in this case a 9 5/8" liner. At the top of the liner, a Baker Oil Tools setting tool can be found.

This tool transmits torque and axial forces from the inner string to the liner. The setting tool is one of the areas where the inner string and liner connects, and it is therefore of vital importance to the functionality of the system that this component works properly. Otherwise, it will not be possible to connect the inner string to the liner, or to transmit torque and axial force.

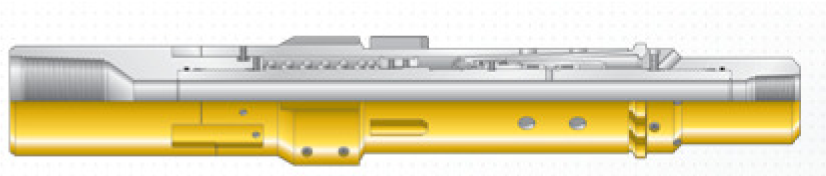

Figure 32: Pilot BHA Setting Tool [37]

The setting tool is also used whenever one wishes to disconnect from the liner with the pilot BHA. Hydraulically applied pressure, or left hand torque, may be used in order to release the setting tool. Furthermore, the setting tool is also useful when the desired section length has been drilled, and one wishes to set the liner and cement it in place.

Further down on the liner, a reamer bit is located. The purpose of the reamer bit is to enlarge the hole size from 8 ½” and up to 12 ¼”, so that the liner may pass through.

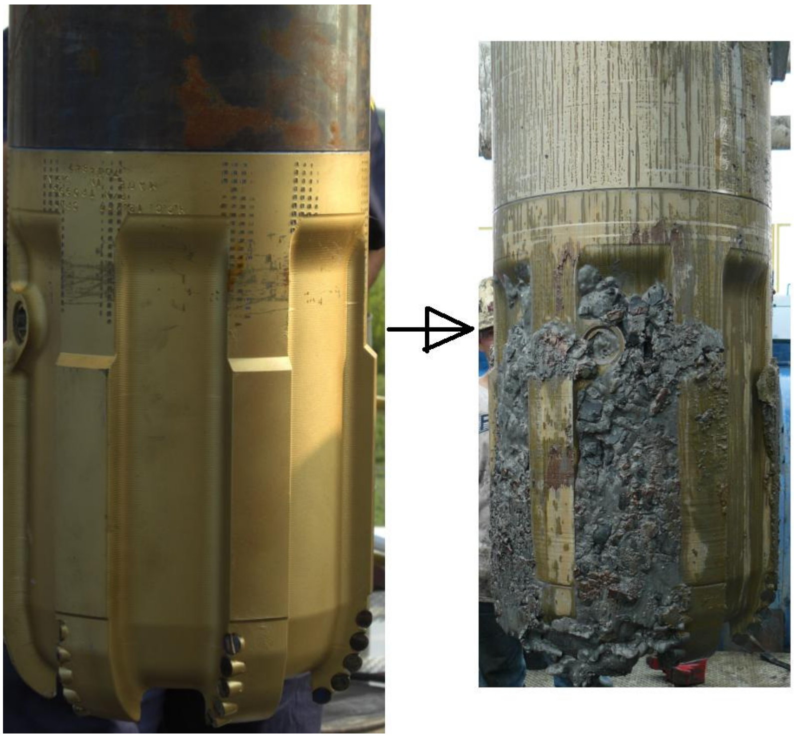

Figure 33: Reamer bit before run into hole and balled-up reamer after use [38]

In figure 33 above, the reamer bit can be seen in a photo taken from the BETA test carried out on the 9 5/8” system. This test displayed severe balling tendencies for the reamer bit in shale formations, and the reamer design was consequently altered to shorten the length of the blades. The mud system used was also altered, with the addition of more clay-inhibitive chemicals. Because of this, there were virtually no problems related to balling up the reamer during the 7” trials. Balling in shale to the extent that occurred during the first BETA trial may also be unlikely to occur in an offshore well in the Norwegian sector because of the use of oil based mud (OBM), as opposed to the test where water based mud (WBM) was used.

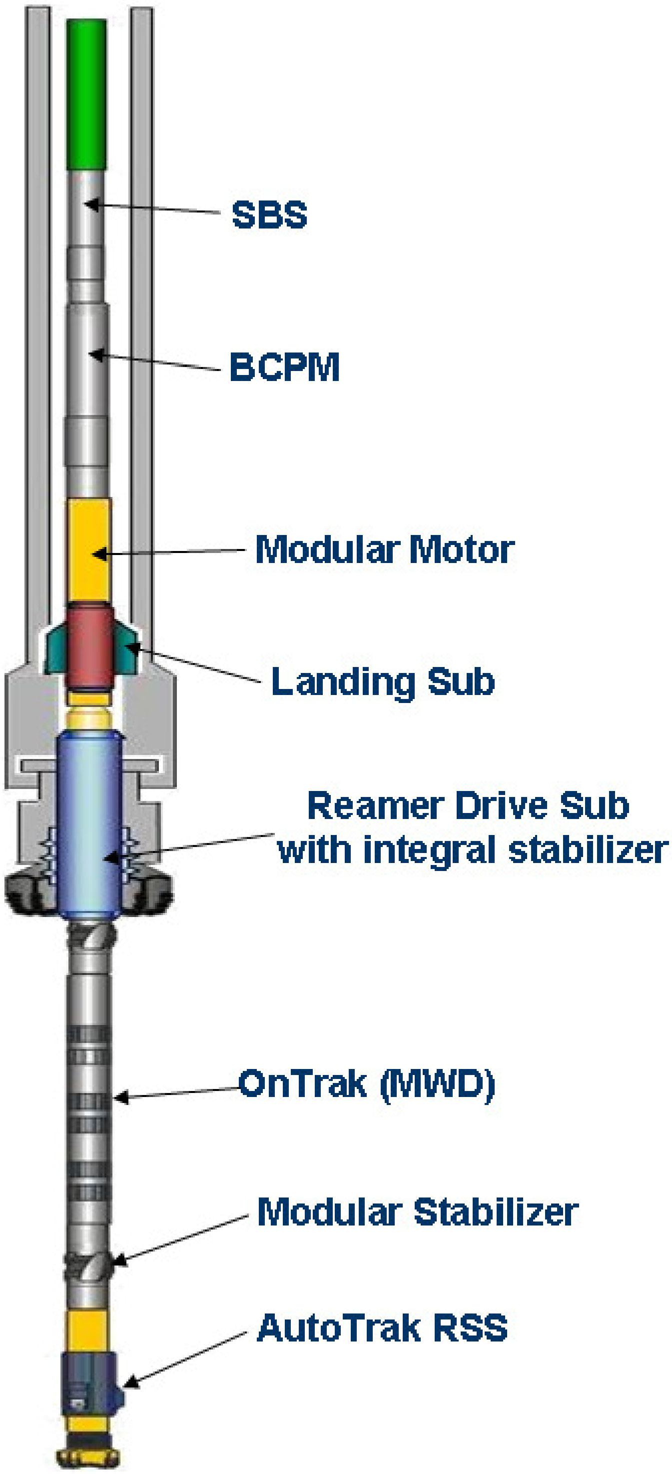

Figure 34: The Inner String and BHA in more detail [36]

The top of the inner string of the SLD system consists of normal drillpipe, as would be used for conventional drilling. Near the top of the inner string, a thruster will be placed. The thruster is needed for length compensation between the setting tool and the landing sub. It should also provide a compression force (downwards) which is higher than the maximum desired weight on bit (WOB).

Further down, the Smart Battery Sub, SBS, can be found. The purpose of this battery is to make it possible to perform surveys, even when there is no flow to run the equipment as usual. It also provides power for the clamping devices when there is no flow.

Below the battery sub, the bi-directional power and communications module (BCPM) is located. The purpose of this equipment is to enable transmission of signals and power in both directions.

After the BCPM a modular motor can be found. This is usually a conventional positive displacement motor. Because there are limitations with regards to the amount of rotation the liner can withstand over time, the drillpipe is rotated fairly slowly, with perhaps 30 RPM from the surface. Since this would be detrimental for drilling purposes, the mud motor is placed in the lower BHA in order to provide a higher RPM, without damaging the liner. The RPM of the BHA below this point, including the reamer, is usually around 150 – 180 RPM when the motor is active.

Thereafter, a landing sub is located on the string. The landing sub is a connection point for the inner string to sting into and connect with the liner. Below this, the reamer drive sub can be found. This is designed to be a connection point between the inner string and the liner. It also transmits torque to the reamer via a swivel. The reamer is connected to the liner with a bearing.

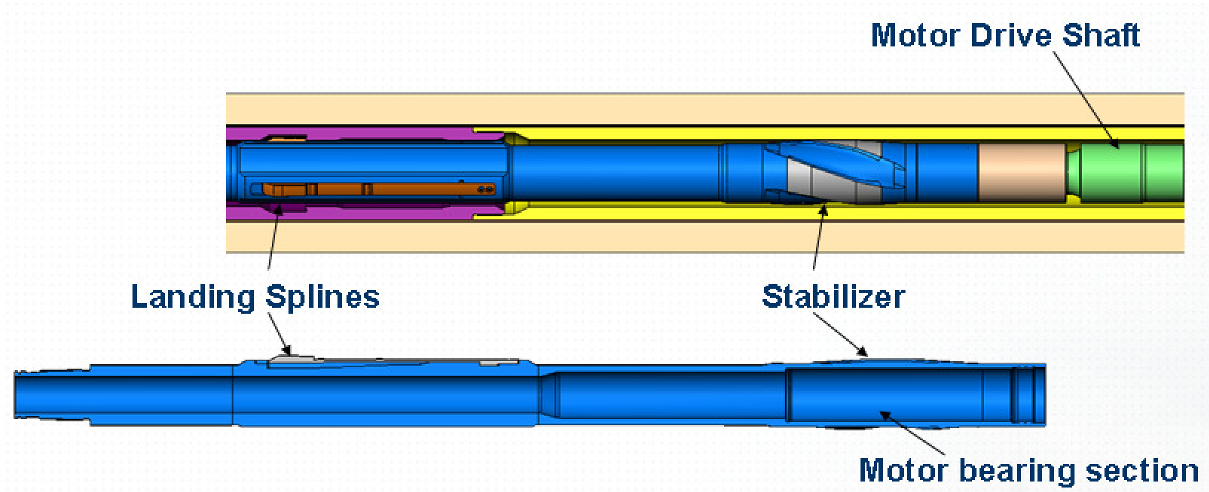

Figure 35: The Landing Sub [37]

As the inner string becomes the pilot section of the BHA, the MWD and RSS tools are located. The purpose of these tools is, as in conventional drilling, to ensure that the direction being drilled in is known, and to enable steering of the wellpath in the direction which is required.

The MWD package includes sensors which will measure the inclination, azimuth, gamma ray, resistivity, pressure, vibrations, and the temperature. The RSS tool is a version of Baker Hughes Inteq's AutoTrak.

For the BETA tests, different types of stabilizer designs were also used on the BHA, in order to evaluate the performance and longevity of differing designs. There was a noticeable variation in the performance of the different centralizers tested. Some centralizers came loose and shifted position during the trials, while some remained in place and displayed excellent performance characteristics. The results of the centralizer tests at BETA will most likely be a deciding factor for which centralizers will be used for the pilot test of the system.

5.4 Operating the Steerable Drilling Liner System

In order to understand how the steerable liner drilling system is actually used, this section will describe briefly how the steerable liner drilling system is operated.

Making Up and Run in Hole
To begin with, the 9 5/8” liner is picked up, and set in the rotary using slips. After the liner has been hung off, and in order to be able to run the inner string, a false rotary table is rigged up after hanging off the liner. This is shown in figure 36 below.

After rigging up the false rotary, the inner string is picked up, and run into the hole. When running into the hole with the inner string, the landing sub should be engaged when it is at the reamer drive. The thruster is then adjusted, and spaced out with pup joints, in order for the lengths to fit properly further down in the system. After this has been done, the system looks somewhat like in figure 37 below.

Once the thruster has been adjusted and spaced out properly, the false rotary is removed, and the thruster is then compressed. The setting tool can then be engaged, and the steerable liner drilling system can be run into the hole. Before reaching the bottom of the well, before drilling may commence, a downlink must be performed using mud pulse in order to activate the reamer drive. Once this has been done, the system is ready to drill, and looks like in figure 38.

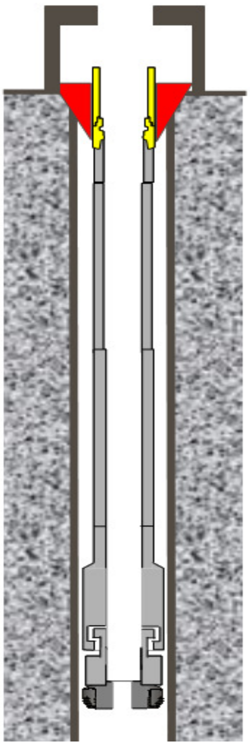

Figure 36: Liner Hung Off and False Rotary Rigged Up [39]

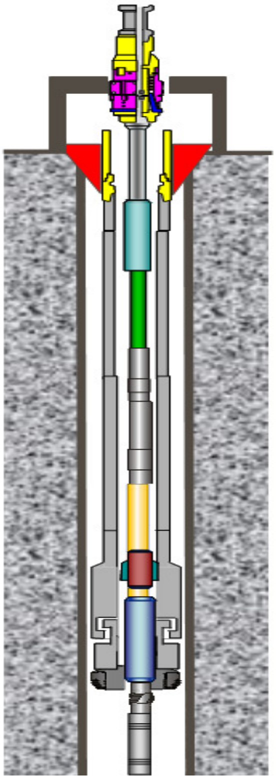

Figure 37: Thruster Spaced Out and Landing Sub Engaged [39]

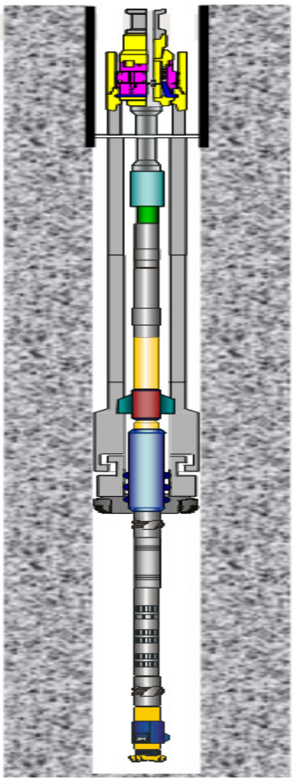

Figure 38: Thruster compressed, Setting Tool Engaged [39]

Retrieving the inner string:
There are two main scenarios where the inner string and all of the BHA components may be retrieved. One reason may be that the drillstring has reached its target depth, and that the inner string will be pulled out of the hole so that the liner can be cemented in place.

Another possible reason is that there has been a component failure in the inner string or bottom hole assembly. Since the BHA used for this operation contains several advanced logging and steering tools, there is always the potential that a component may fail. It is therefore important that it is possible to trip the system out of the hole to replace failed components, while still keeping the liner in place.

Once it has been decided to retrieve the inner string, a signal is sent via mud pulse telemetry in order to deactivate the reamer drive. If it is not possible to get the reamer drive to disconnect by downlink, it will automatically disconnect after 20 minutes without circulation. After the reamer drive has been disconnected, a ball is dropped in order to release the setting tool. This can be seen in figure 39 below. If for some reason the ball fails to release the setting tool, left hand torque may be applied to the setting tool, in order to release it.

Once the reamer drive and setting tools have been deactivated and released, the inner string may be pulled out of the hole, while the liner remains in place, as seen in figure 40 below.

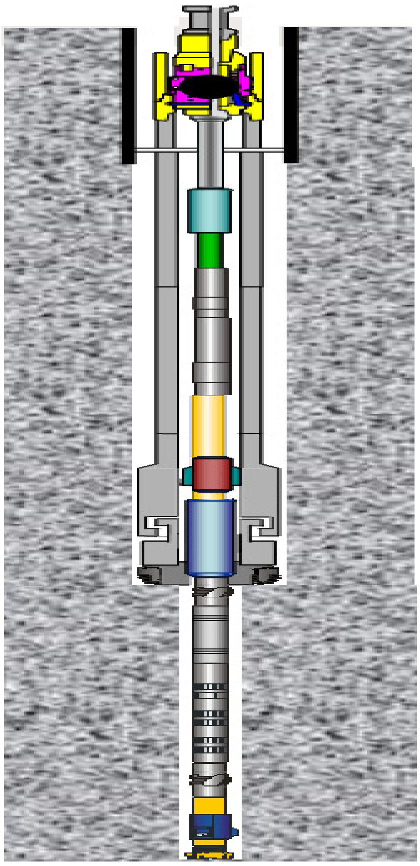

Figure 39: Ball dropped to release Running Tool [39]

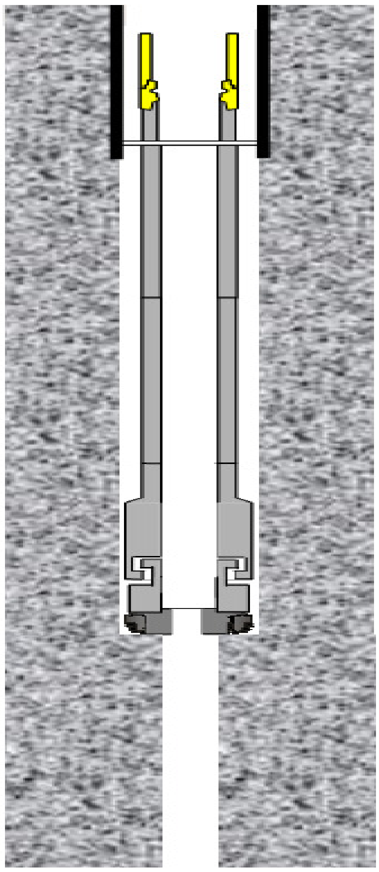

Figure 40: Inner String retrieved - Liner left in Hole [39]

Re-connecting with the liner downhole:

If, for some reason the inner string of the steerable liner drilling system has to be retrieved to the surface, it becomes necessary to have a means of reconnecting with the liner downhole. To do this, the inner string is first run into the hole itself.

In many cases, the pilot hole below the liner which had previously been drilled may have collapsed to some degree, or at least be filled with a certain amount of debris or cuttings. Therefore, before anything else is done, the pilot hole below the liner must be worked and re-drilled as necessary with circulation.

Once the pilot hole is clear of obstructions, the landing sub may be engaged. Once the sub has been engaged, the thruster may be compressed. After the thruster has been compressed, the setting tool will be engaged to latch on to the liner.

With all components in place and connected, the reamer drive is then activated via mud pulse telemetry from the surface. Once this has been done, drilling may continue as planned, as demonstrated in figures 41 and 42.

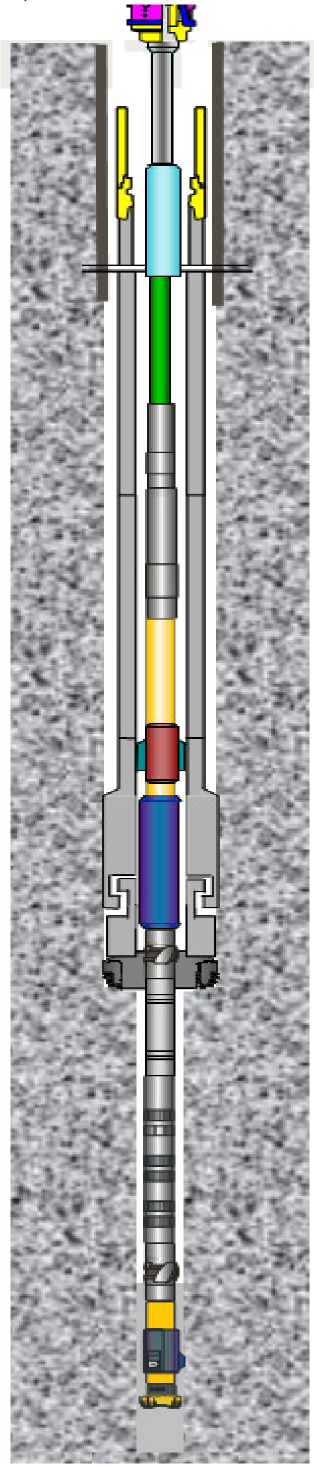

Figure 41: Re-working the Pilot Hole [39]

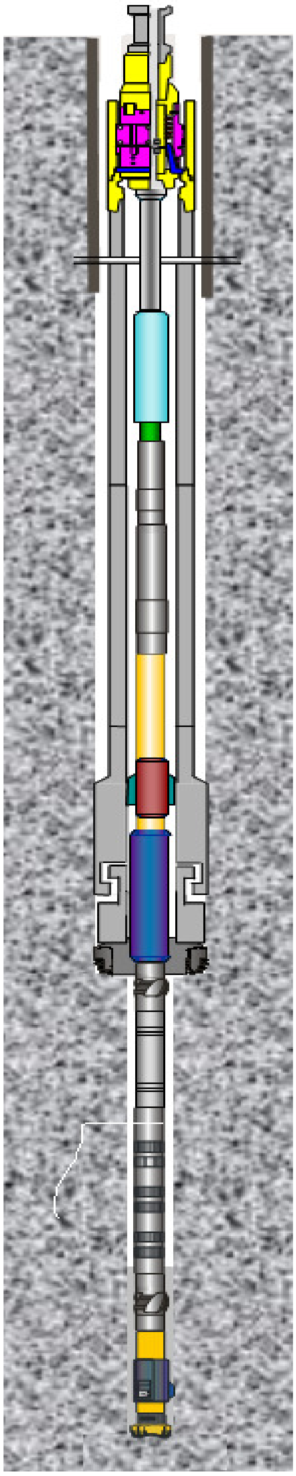

Figure 42: Ready to Drill [39]

6 Torque, Drag, and Hydraulics Calculations for the Steerable Liner Drilling System

The simulations presented for torque, drag, and hydraulics have been performed in the EDM Landmark software package using WellPlan. This program does not have built-in support for the steerable liner drilling system, and an ad-hoc solution had to be found with regards to entering the components of the system into the program. The solution used was to use the OD of the liner and ID of the drillpipe as the defining size parameters, and then add the weight of both liner and drillpipe combined when entering the weight of the assembly. This has several drawbacks, and the results of the simulations should therefore be looked upon critically.

It is believed that this program should provide fairly realistic results with regards to the hydraulics calculations. This is because the hydraulics will mainly be affected by the interior properties and dimensions of the drillpipe as well as the exterior dimensions of the liner and drillpipe. These properties are fairly well and realistically included in the WellPlan simulation model, and the results should therefore be reasonably reliable. WellPlan does, however, have a reputation for underestimating the ECD.

Torque and drag simulations in WellPlan may be a bit more dubious however. These have been performed using the same system layout as explained for the hydraulic simulations. The drawback here is that the system had to be put into WellPlan as though it was one string, and not a liner with drillpipe inside. While this probably provides insufficient detail with regards to the properties of the two strings, it also does not allow for any interaction between the two strings.

In order to try to mitigate these problems, the calculations have also been performed manually, using methods which have been described in chapter 2 and 3.

The calculations performed using the WellPlan simulation software have calculated torque and drag values for the depth of the well. This means that hook load and torque values have been calculated for each position in the well that the drillstring will pass. Since this would be impractical and very time consuming to do with manual calculations, the manual calculations have focused mainly on the situation which occurs when the string is at its deepest point. The hook loads and torque values calculated manually are therefore only valid for when the string is at the bottom, whereas the simulation software has calculated the hook load values all the way down towards the bottom of the section.

6.1 The Brage Pilot Well

During the summer of 2009, the 9 5/8” steerable liner drilling system will be used to drill parts of a well section in the Brage field that would normally be drilled with a conventional 12 ¼” drilling system. For this reason, it was decided to base most of the calculations in this thesis on this case. It should be noted, however, that the actual wellpath had to be simplified somewhat, in order to make it practical to perform manual calculations on. This means that the sections where azimuth and inclination changed simultaneously were changed, in order to have only one of these changing at any given time.

The planned well design for this well is illustrated below:

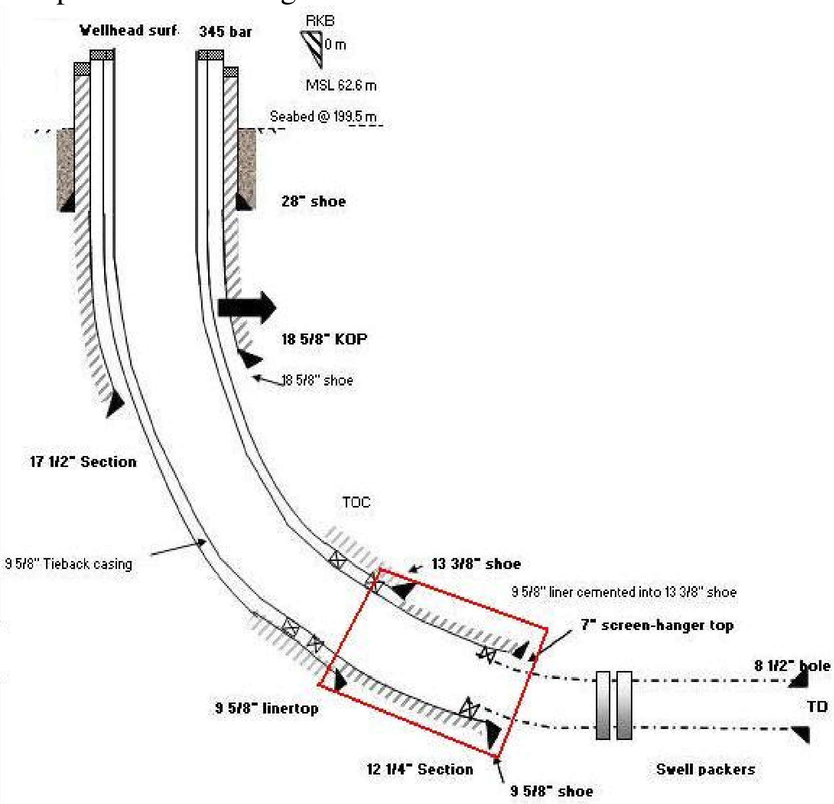

Figure 43: Planned Well Design

On figure 43 to the left, we see the planned well design for the Brage well to be drilled partially with the SLD system.

An old well will be plugged and abandoned, and then a sidetrack will be made from the 18 5/8” casing, followed by the drilling of a 17 ½” section.

Once the 17 ½” section has been drilled and cased, drilling of the 12 ¼” section, indicated with red on the figure, will begin. The first part of the 1000 m long section will be drilled with a conventional assembly.

The last part, most likely around 200 to 300 m, will be drilled using the steerable liner drilling system, along with a 1000 m long liner. The reason for not drilling the entire section with a liner is mainly to be conservative, since this is, after all, the first proper field deployment of the 9 5/8” steerable liner drilling system.

The planned wellpath to the bottom of the 12 ¼” section is given in the Appendix to this thesis. The cased hole friction factor has been assumed to be 0,25 and the open hole friction factor has similarly been assumed to be 0,30. A base mud weight of 1,4 s.g. has been used, since this is the plan for the well. Since oil based mud (OBM) is used to drill this section, the friction factors used might be somewhat conservative.

The detailed survey for this well can be found in the Appendix.

6.2 Drag and Friction Calculations

In addition to the formulas listed in section 2.1, the drag values in this section are based on WellPlan simulation results.

Since the values calculated manually relate to the hook load while hoisting and running into the hole, these values have been plotted for the different cases in WellPlan, and will be compared with the manual values. First the hook load when running into the hole is plotted, and then the hook loads when pulling out of the hole are shown.

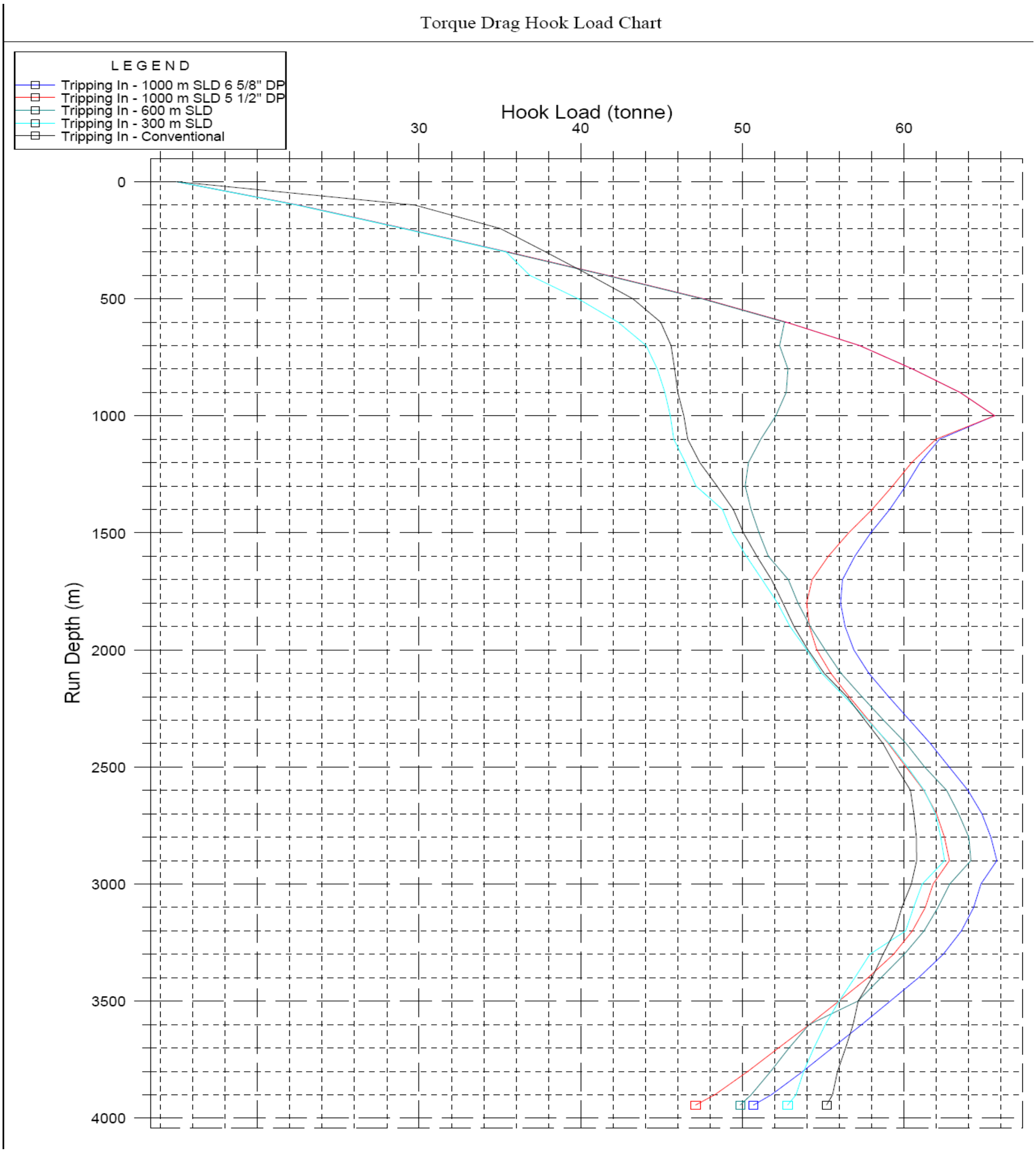

Figure 44: Hook Load - Running into the Hole

There is, at least for the heavier drilling systems, a noticeable decrease in the hook load while running into the hole at around 1000 m and 3000 m. This is believed to be because the inclination of the well begins to increase at these points, and the friction from the pipe and liner being pushed into the well therefore increases accordingly.

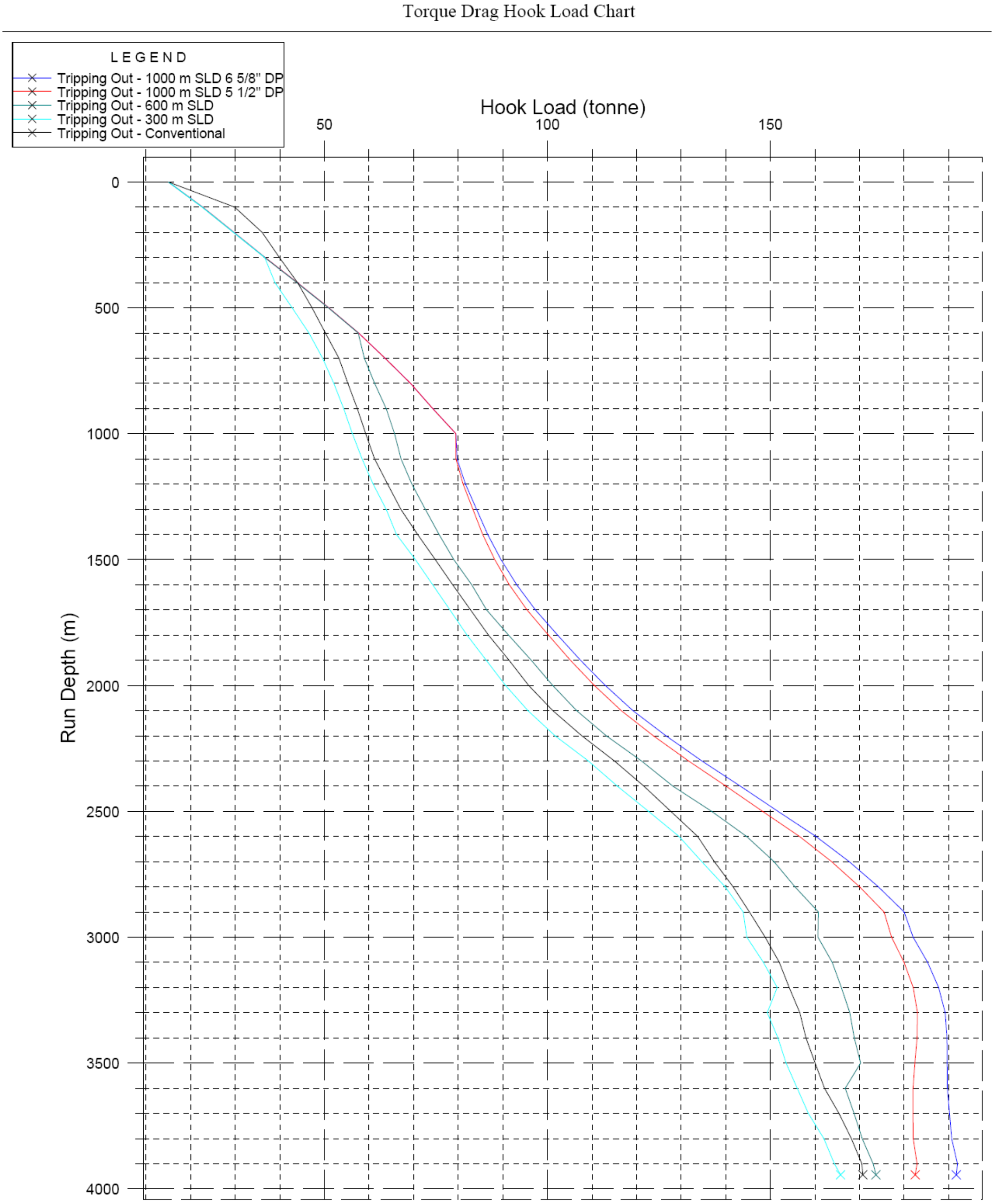

Figure 45: Hook Load – Hoisting

As expected, it is the drilling assembly with the longest liner which has the highest hook load in both cases. It can also be seen that the lowest hook loads are actually given by the SLD system with 300 m of liner. This is because the conventional system is heavier with its drill collars and heavy weight drillpipe when the liner becomes sufficiently short.

Manual calculations have also been performed on these two parameters, in order to see how they compare with the simulations. The simulated values for the drag at TD have been inserted into a table, and compared with the manual calculations:

Liner Length	1000 m 6 5/8" DP	1000 m 5 1/2" DP	600 m	300 m	Conventional
Simulation, Lowering	51 tonnes	47 tonnes	50 tonnes	53 tonnes	55 tonnes
Simulation, Hoisting	193 tonnes	183 tonnes	177 tonnes	169 tonnes	172 tonnes
Manual, Lowering	63 tonnes	59 tonnes	53 tonnes	52 tonnes	49 tonnes
Manual, Hoisting	255 tonnes	247 tonnes	216 tonnes	192 tonnes	173 tonnes

Table 1: Hook Load Values Calculated Manually

	1000 m 6 5/8" DP	1000 m 5 1/2" DP	600 m	300 m	Conventional
Percent Difference, lowering	22.91 %	25.53 %	5.91 %	-2.54 %	-10.30 %
Percent Difference, hoisting	24.38 %	25.91 %	18.11 %	11.94 %	0.47 %

Table 2: Percent Difference - Manual vs. Simulations (Simulations as base case)

While it is apparent that the manually calculated hook load values are somewhat higher than their simulated counterparts, there is still a certain degree of similarity here. In most cases, however, the manual calculations are approximately 20 to 25 % higher than the simulated values. In order to see the difference more clearly, they have been plotted against each other in a bar chart. Another difference is that the manual calculations are analytical, and take into account fewer parameters than the simulation software does. One example of this is the effect of centralizers, which the manual calculations do not take into account.

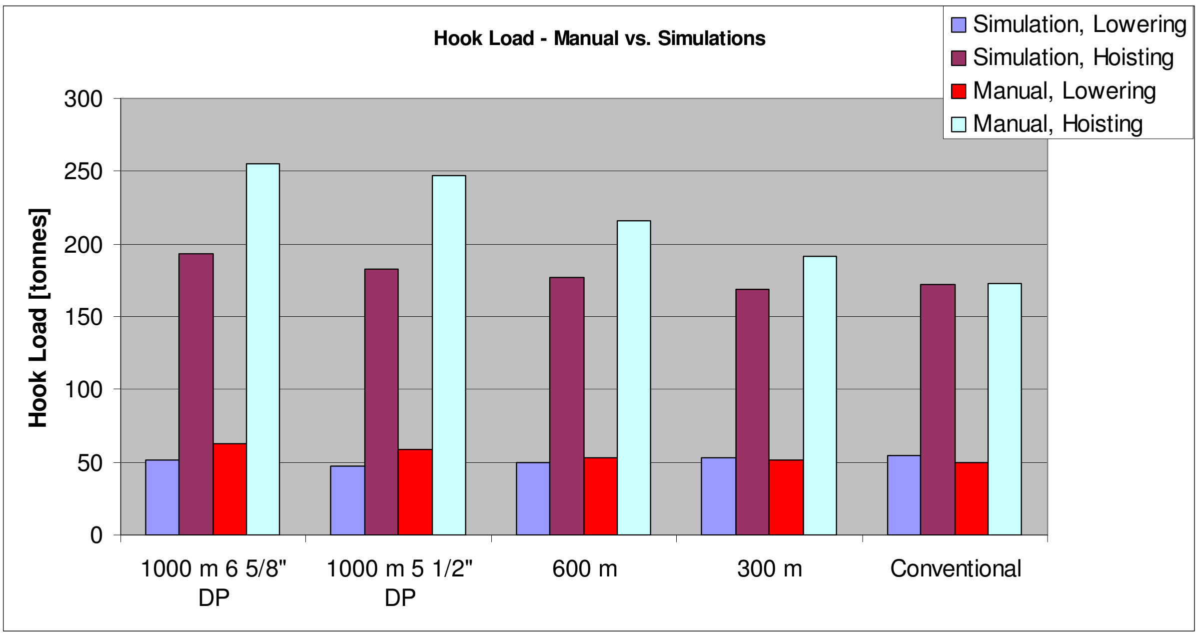

Figure 46: Hook Loads - Manual vs. Simulations

Since there is a great deal of uncertainty related to whether or not the simulation program is able to calculate the drag forces on the steerable liner drilling system properly, it is nevertheless interesting to see that the simulation results and the manual calculations seem to be fairly similar with regards to the hook loads during hoisting and lowering.

Another trend, at least for the manual calculations, seems to be that the longer the liner, the higher the drag values are, both for hoisting and running into the hole. The conventional drilling system does, however, approach the values of the SLD system with a 300 m long liner.

Since the hook loads are known, one may then also calculate the highest axial stress seen at the top of the drillpipe; the hook load while hoisting. While the actual hook load value can be compared to the yield limit of the drillpipe, one may also divide it by the cross sectional area of the drillpipe, in order to find the stress.

$$\sigma_{axial} = \frac{F_{hookload}}{A_{cross\,sec\,tion}}$$

In order to examine the most severe cases, the 6 5/8" drillpipe with a maximum hoisting load of 250,4 kN and the 5 ½" drillpipe with a maximum hoisting load of 247 kN are used. The cross sectional area of the different drillpipes can be calculated based on their dimensions, or simply found in the Drilling Data Handbook [9] to be:

$A_{6\,5/8} = 0{,}004593\ m^2$
$A_{5\,½} = 0{,}004277\ m^2$

Based on these areas, along with the hook loads, the stress values can then be calculated.

$\sigma_{6\cdot 5/8} = 5452$ bar
$\sigma_{5\cdot 1/2} = 5775$ bar

These stress values are quite high, and it is therefore apparent that a fairly high grade drillpipe without very much wear should be used for this operation. Grades S-135 and S-105 can be used with some wear, but when approaching grades such as S-95, very little degradation can be tolerated. This can be found both using the actual hook load values, as well as the calculated stresses.

6.3 Torque Calculations

The torque values are calculated based on section 2.2. In addition to this, torque values for different scenarios have been calculated using WellPlan. Manual calculations of torque have only been performed using string tension and one scenario. Only the comparable manual calculations and simulations will be shown here. Note also that, mainly due to space considerations, only the torque values for the 6 5/8" 1000 m SLD system and 5 ½" 1000 m SLD system are shown here.

To begin with, the results of the torque simulations are shown below.

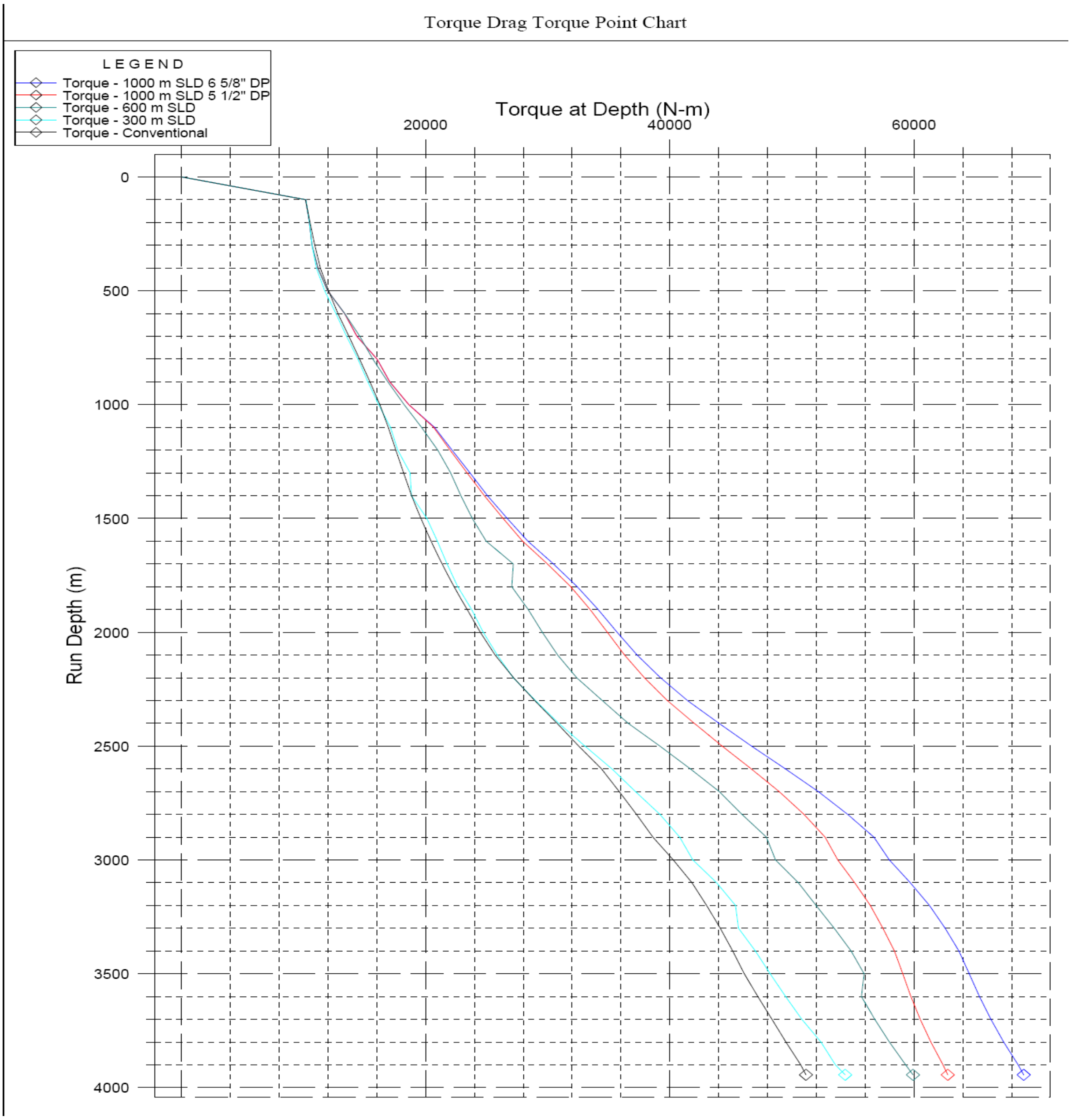

Figure 47: Simulated Torque Values

Figure 47 above shows that, as for the drag calculations, the torque values for the system with the longest liner are the largest. This applies to both the 6 5/8" and 5 ½" drillpipe versions of the 1000 m SLD system. Again it can be seen that the 300 m SLD system and the conventional system display very similar characteristics. This is also in line with the previously calculated parameters.

In addition to the simulated torque values, manual calculations have also been performed in order to find the torque which the system will be exposed to. This was first done for the base case; the 1000 m SLD system. Note that as opposed to the simulation results listed above in figure 47, which shows the surface torque at each point on the way down to TD, the manual and simulated torque values below in figures 48 through 51 show the torque loading when the system is at the bottom. Also note that for the manual calculations, the liner and drillpipe have been calculated separately, whereas this was not possible for the simulation software.

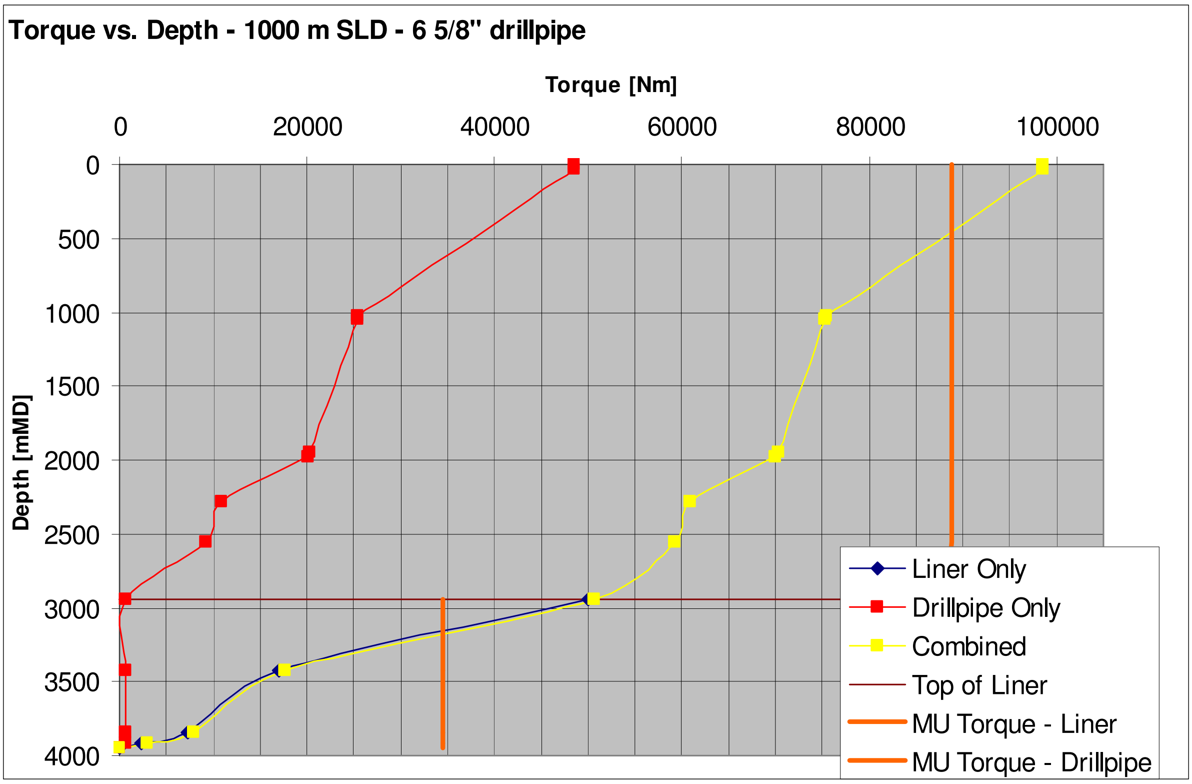

Figure 48: Manual Torque Values for the 6 5/8" drillpipe 1000 m SLD System

First, the torque values for the liner only were calculated, and then the same was done for the inner string and drillpipe. It should be noted, however, that there is no torque acting on the inner string inside the liner above the mud motor. This is because the drillstring and liner will rotate at the same speed above the mud motor. At the top of the liner, the two torque loads were added, and this shifted the torque curve for the entire SLD system to the right. The highest torque value calculated for this system is approximately 98,5 kNm, which is quite high. The highest torque which the liner itself will be exposed to is 50 kNm near the very top of the liner. The HRD setting sleeve will be exposed to 50,7 kNm. The make-up torque values for the liner connections and the tool joints of the 6 5/8” drillpipe have been included. Note that these lines do not necessarily represent the absolute torque limits of the system.

The same calculations have been performed using the WellPlan simulation software, and the results can be seen in figure 49 on the next page.

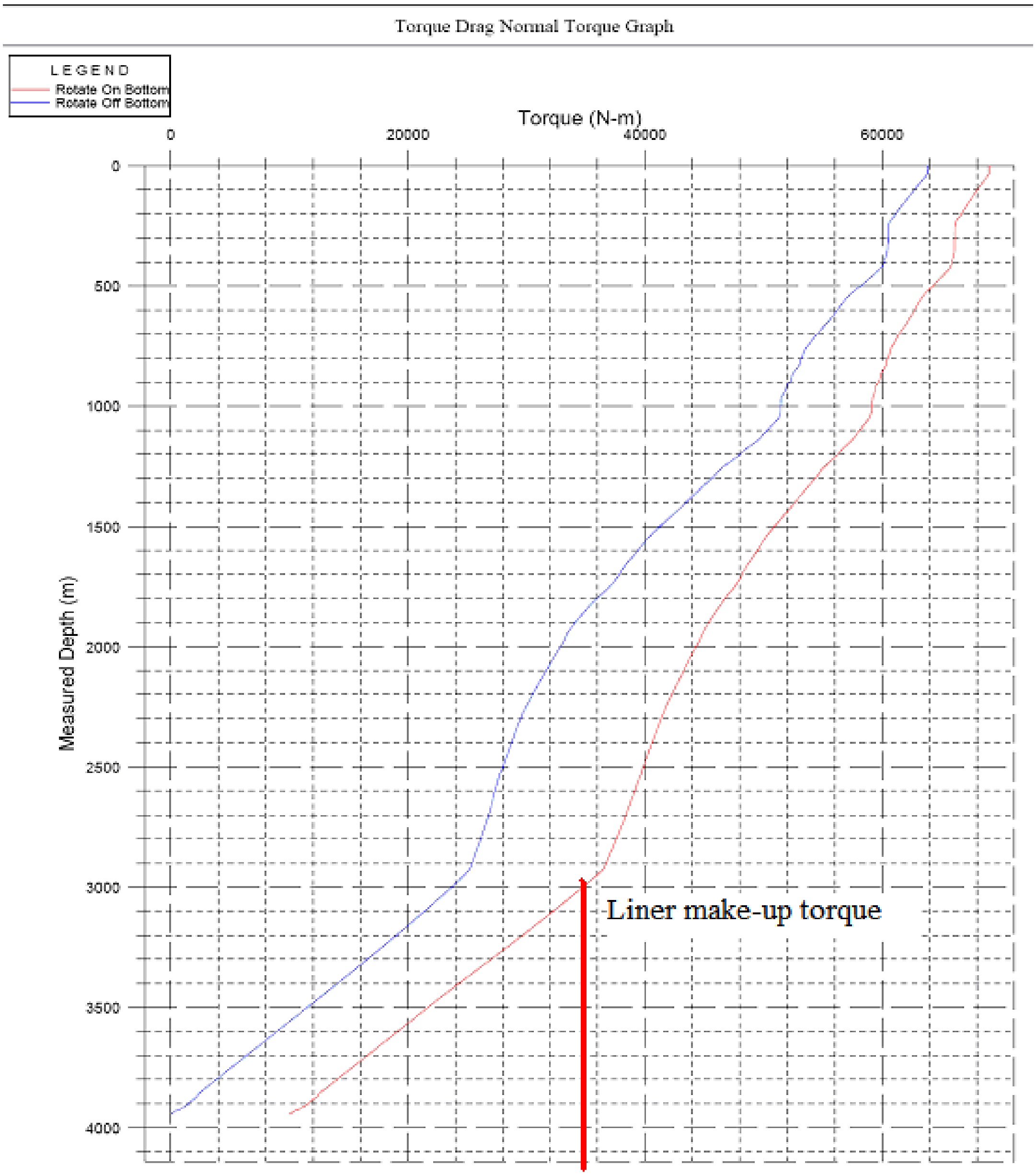

Figure 49: Simulated Torque for the 6 5/8" 1000 m SLD System

While the simulated torque values differ somewhat from the manual calculations, it is still interesting to observe that the trend with regards to how the torque increases for each section seems to be the same. Obviously, the torque at the bottom is higher than when rotating off bottom, due to the torque-on-bit input into the simulation software as 5 kNm.

We also see that the top of the liner experiences loading of up to around 36 kNm or slightly below.

In order to see how changing the drillpipe type would affect the torque, a similar graph has been constructed for 5 ½" drillpipe. It is shown below in figure 50.

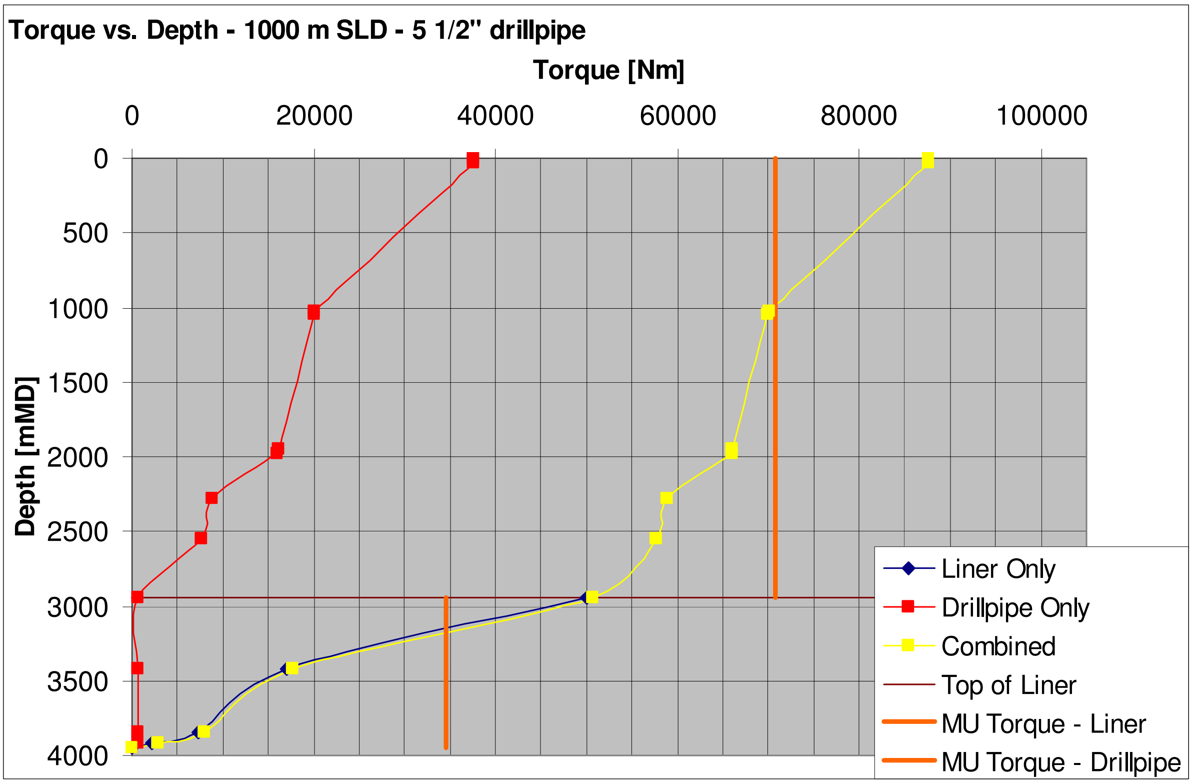

Figure 50: Torque Values for the 5 1/2" drillpipe 1000 m SLD System

While the final torque values for the 5 ½" drillpipe 1000 m SLD system are slightly lower than the 6 5/8" system, reaching 87,6 kNm, this is still a fairly high number. Since the liner and inner string in the lower section remain the same, the loading at the top of the liner remains the same. The make-up torque values for the liner connections and the tool joints of the 5 ½" drillpipe have been included. Note that these lines do not necessarily represent the absolute torque limit of the system.

Simulations were also performed on this system, similar to those performed on the 6 5/8" drillpipe version of the SLD system. As with the manual calculation shown above, the make-up torque values have been included for the liner. The drillpipe tool joint make-up torque values are not shown on the simulation graphs, however. This is because the value of 88 kNm is too high compared to the x-axis of the chart below.

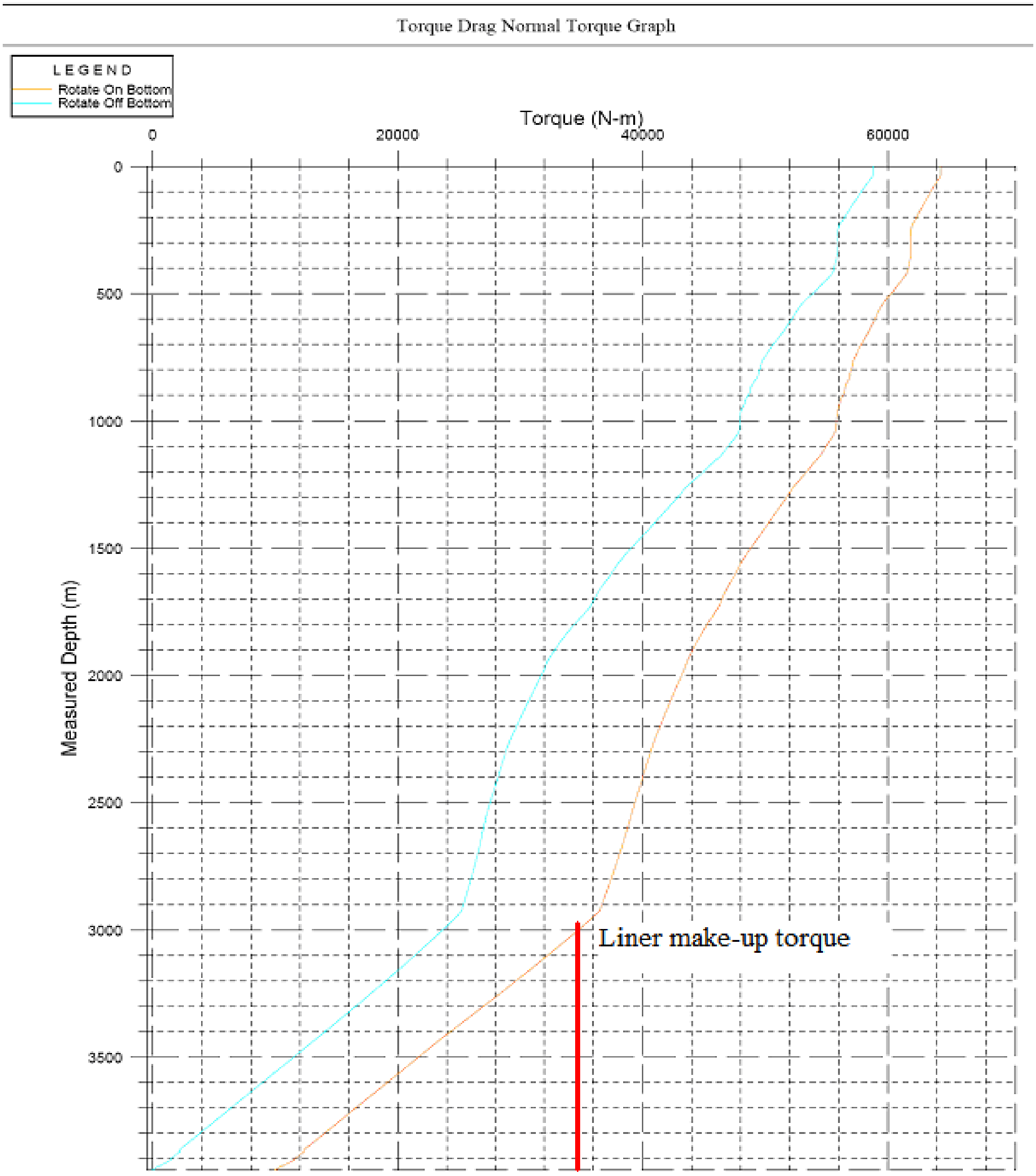

Figure 51: Simulated Torque Values for the 5 1/2" 1000 m SLD System

Similar to the simulations for the 6 5/8” drillpipe system, the trends here can also be said to be the same, both with regards to the simulation and manual results. For the 5 ½” drillpipe system, the loading at the top of the liner is approximately 35 kNm. Theoretically, one would expect the torque to be the same at the top of the liner for both the 6 5/8” and 5 ½” drillpipe systems, since the components of the systems are identical all the way up to the top of the liner at the running tool. It does appear as though the simulation software agrees with this, even if the exact torque values are slightly different.

Liner Length	1000 m 6 5/8" DP [kNm]	1000 m 5 1/2" DP [kNm]	Conventional [kNm]
Torque, Simulation	69	63	52
Torque, Manual	98.5	87.6	91.2

Table 3: Torque Values Compared

Torque	1000 m 6 5/8" DP	1000 m 5 1/2" DP	Conventional
Percent Difference	42.75 %	39.05 %	75.38 %

Table 4: Torque, Comparison with Simulations as Base Case

It is evident from tables 3 and 4 above that the torque values calculated manually are significantly higher than the ones calculated using the simulation software. The manually calculated values are from 40 to 75% higher.

The drillpipe itself in grade S-95 and upwards, should be able to withstand these torque values, as long as it is not excessively worn. The tool joints could be a problem, however, with the Drilling Data Handbook quoting 88 kNm [9] as the make-up torque, which is below what it would be exposed to in both of the above mentioned liner drilling scenarios, based on manual calculations. There are, however, high torque drillpipe connections capable of dealing with these forces.

The challenge therefore becomes the liner, which has to face torque values of up to 50 kNm calculated manually and 36 kNm simulated. While most regular liner connections have a maximum make-up torque of around 30 kNm, there are liner connections, such as the VAM High Torque Flush (HTF) [40] connection, which are capable of handling loads up to around 250 kNm. Regular connections, however, will probably not be able to handle the loads seen in the steerable liner drilling system.

6.4 Fatigue and Connection Life

In order to investigate the fatigue and life span of the liner connections, one must first determine what wellbore geometry the liner will be exposed to. When this is known, the bending stress can be calculated, using the formula given in section 2.3. When the bending stress has been calculated, an S/N curve will be used.

For the steerable liner drilling system, VAM TOP liner connections are most likely to be used. The manufacturer of these connections usually provides the customer with S/N curves for the product, but for this thesis the actual curve may not be used for confidentiality purposes. Instead, the S/N curve from figure 6, publicized in a paper by the same company will be used. The actual numbers will be somewhat different than what is calculated here, but the process will nevertheless be the same, while also providing a rough estimate of what is realistic.

First of all, the bending forces are calculated, as per the equations given in section 2.3. Since the bending stress depends mainly on the dogleg severity, a graph can be constructed which shows the bending stress as a function of this variable.

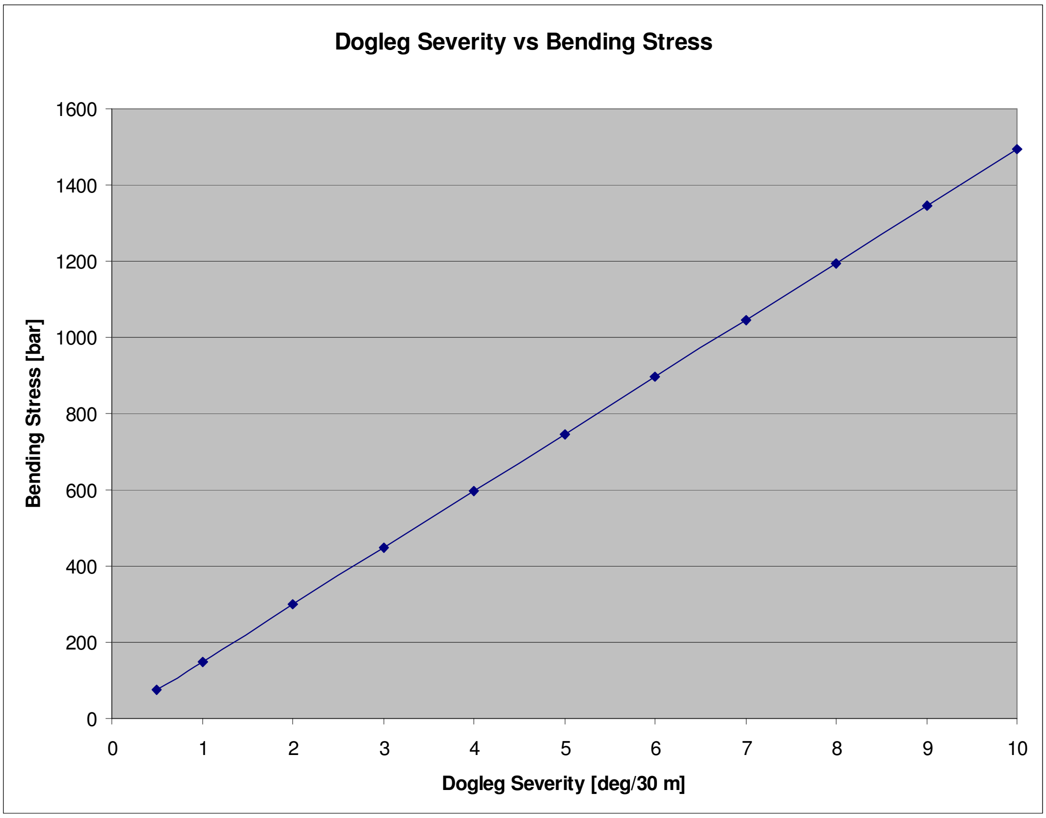

Figure 52: Dogleg Severity vs. Bending Stress

Once the bending stress has been calculated, the question becomes what type of S/N plot is available. If the S/N plot in question has a y-axis which requires only the dynamic bending stress to be used, then one may proceed to the S/N plot in order to find the number of cycles to failure. If this is not the case, additional stress values must be calculated and combined in order to use the plot. In this case, it has been assumed that the bending stress can be used on the y-axis of our example S/N plot.

Because the bending force will depend on the actual dogleg severity, there will obviously be different answers to the number of cycles to failure. However, if one assumes a dogleg severity of 5 degrees per 30 meters, one will get a bending stress of approximately 747 bar.

When this bending stress is applied to our example S/N plot, the number of cycles we get is 25 million. This is a fairly high number, and even with a safety factor of 2 applied, we still get 12,5 million cycles. Based on 30 RPM string rotation and an ROP of 10 meters per hour, this makes it possible to drill more than 69 km. This is, of course, an unrealistically high number, but may be in part due to the fact that the loading curve used is not related to the actual connection which will be used on the steerable liner drilling system.

It should be noted, however, that if the dogleg severity is increased to 8 degrees per 30 meters, the bending stress becomes 1195 bar, which in turn gives a number of cycles to failure of 750000. With a safety factor of 2, this becomes 375000 cycles. With the same assumptions as above, this would enable us to drill 2083 m. This significant decrease is related to the logarithmic nature of the S/N curve, where an increase in the bending stress will give an exponential decrease in the number of cycles to failure.

It may, however, be slightly wrong to calculate the actual fatigue life of a liner connection in this way. The reason for this is that the liner is only actually exposed to the bending forces in the bends, and most wellbores are not curved uniformly, with the same dogleg severity all the way. Therefore, what is actually calculated in the paragraphs above is how long one could drill with constant dogleg severities of 5 and 8 degrees per 30 meters, respectively. This is thus also seemingly a quite conservative estimate of how far one may drill with a liner.

One might therefore then attempt to investigate whether the total length the liner has travelled through a given dogleg severity throughout the well seems to approach the fatigue limit of the liner, given the bending stress from the dogleg. This can be done by checking how many revolutions the liner has had during the time it was exposed to the bending forces. When the bending force is known, the S/N plot can then be used similarly to before, in order to determine the total number of cycles to failure, with a given safety factor.

6.5 ECD Calculations

The configuration of the 9 5/8” steerable liner drilling system, along with the configuration of a conventional 12 ¼” drilling system for a similar section, was programmed into WellPlan, in order to calculate the equivalent circulating density (ECD) of the drilling fluid. The pore and fracture pressure prognosis from the Brage field for this well was also inserted into the simulation software, in order to see how the calculated ECD fits within the available drilling window. The flow rate used was 2200 lpm, as this was given as a likely estimate for the operation on the Brage field. The results of the ECD simulations for the different drilling systems are shown in the figure below.

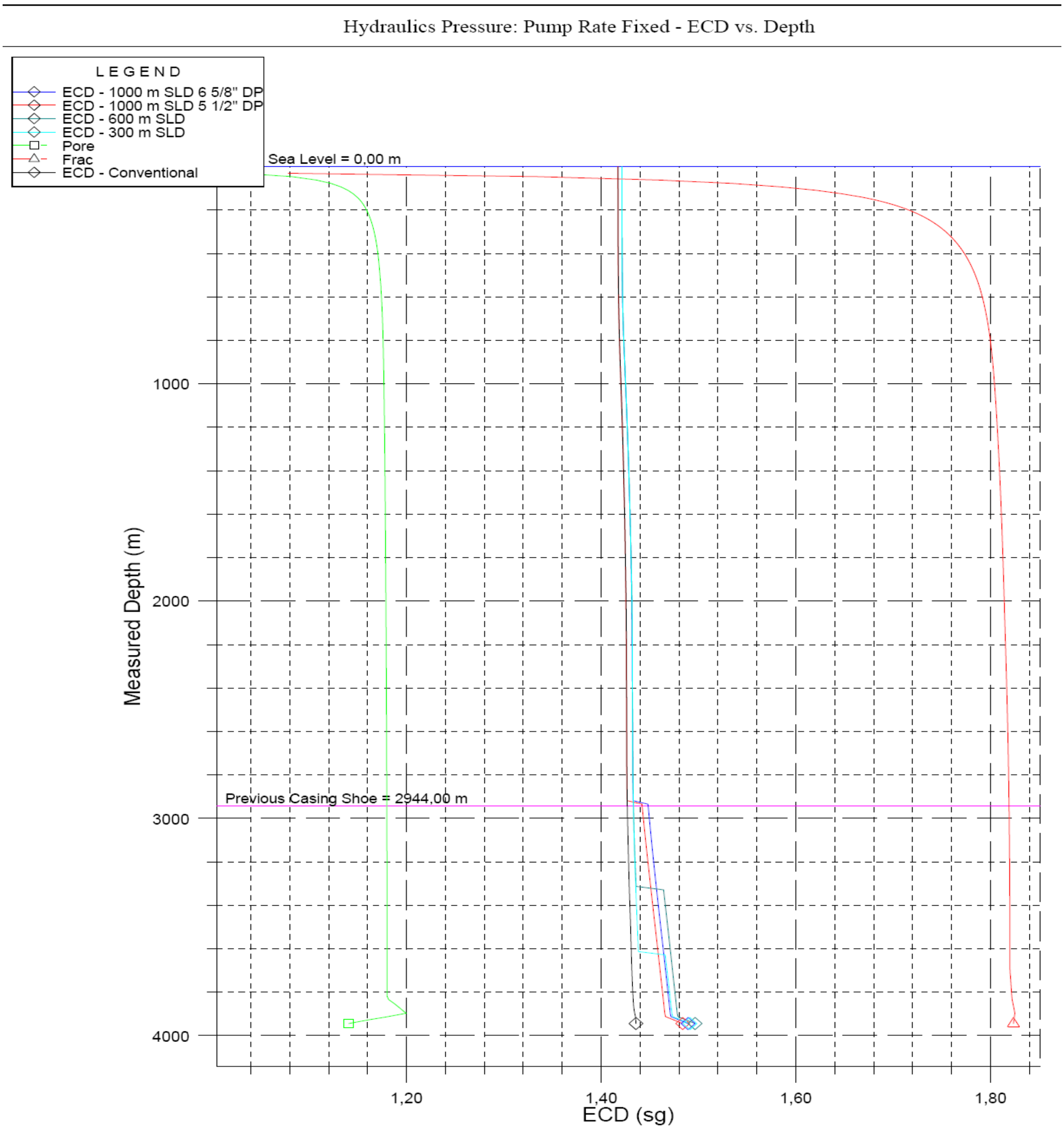

Figure 53: Simulated ECD Values for the different systems

Based on the pore pressure and fracture pressure prognosis for this well, the ECD does not seem to approach values where it might be a danger in itself. It is clearly seen, however, that the ECD values during liner drilling are higher than they would be for a comparable conventional drilling operation. This is as expected, however.

In order to perform manual pressure drop and ECD calculations, an excel spreadsheet was made, based on the formulas listed in section 3.1.

First of all, the pressure drop values for each section are calculated, assuming that the liquid flow occurs in turbulence. This assumption is supported by the Reynolds number which can be calculated. Although the actual Reynolds number for each section of the string varies, due to the different annular areas and flow velocities, flow was seen to be turbulent, with flow rates above 1500 lpm in just about all sections outside the drilling assembly.

Once the pressure drop values are known, the resulting ECD for each scenario can be found. The ECD can also be calculated for different scenarios, for instance with or without stabilizers taken into account.

Once the ECD has been found, the liquid friction for each scenario can also be calculated. Although the liquid friction itself may not necessarily represent a major force compared to the drag values, it is nevertheless a parameter to investigate.

First, the pressure drop for each section will be analyzed based on the base case represented by the 1000 m SLD system and 2200 lpm. The effect of including centralizer pressure drop is also shown.

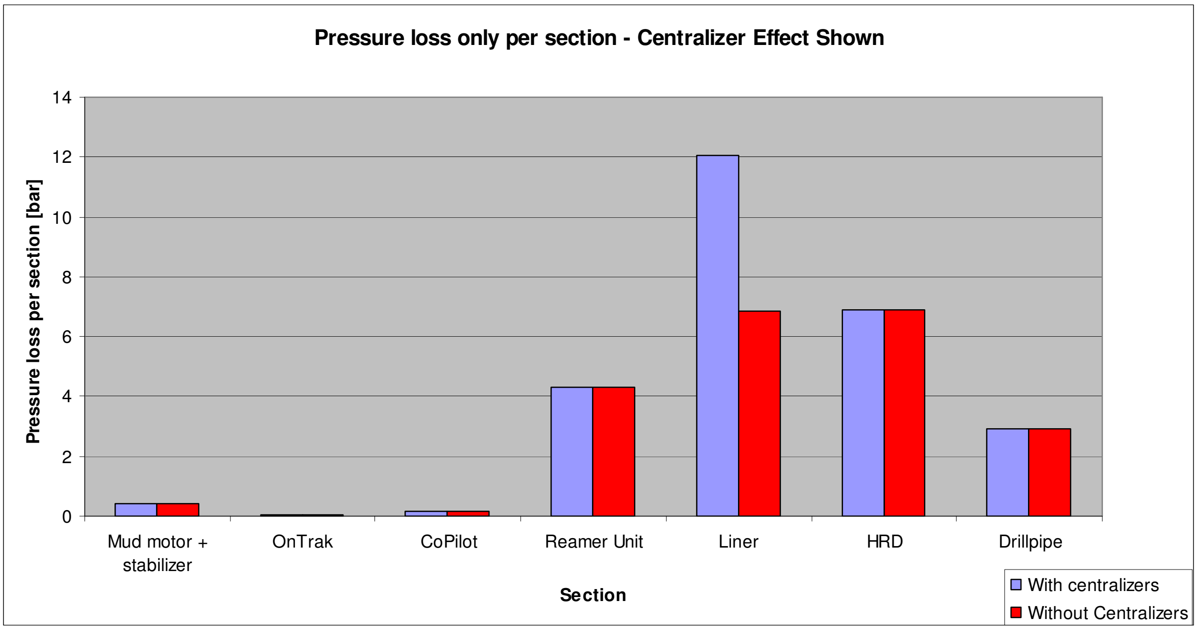

Figure 54: Pressure Loss per Section of the 1000 m SLD System

As can be seen in figure 54 above, the major pressure loss contributors are mainly the reamer unit, liner and HRD setting sleeve. The drillpipe also contributes, but that is to be expected since more than 2/3 of the total system length is made up of this. It is worth noting, however, that that the HRD setting sleeve, although only 3,2 meters long, gives a larger pressure loss than the drillpipe, which is 2923 meters long. It also comes close to giving the same pressure drop as the liner section, without centralizers included. When centralizers are included, however, the liner becomes, by far, the main pressure loss contributor, as expected due to its fairly large OD and the centralizer OD. The pressure loss for the same system, with 5 ½" drillpipe would be very similar, although the pressure loss would be slightly lower in the drillpipe only section. As shown below, however, this does not constitute a major increase in the ECD, although it does increase some.

In addition to examining the pressure loss for each section of the steerable liner drilling system, the resulting ECD has also been calculated, both with and without the centralizers included. The ECD values for the different SLD alternatives, along with that of the conventional system, have been calculated and shown in the table below.

Liner Length	1000 m 6 5/8" DP	1000 m 5 1/2" DP	600 m	300 m	Conventional
ECD without centralizers	1.504	1.499	1.491	1.481	1.413
ECD with centralizers	1.529	1.524	1.506	1.488	n/a

Table 5: ECD Values for the different configurations – Flow Rate: 2200 lpm

As can be seen from table 5 above, the system with the highest ECD is the one with the longest liner attached to the drillstring. The ECD is quite high for all of the liner drilling systems, however, compared to the ECD of the conventional drilling system. This is also shown in figure 55 below.

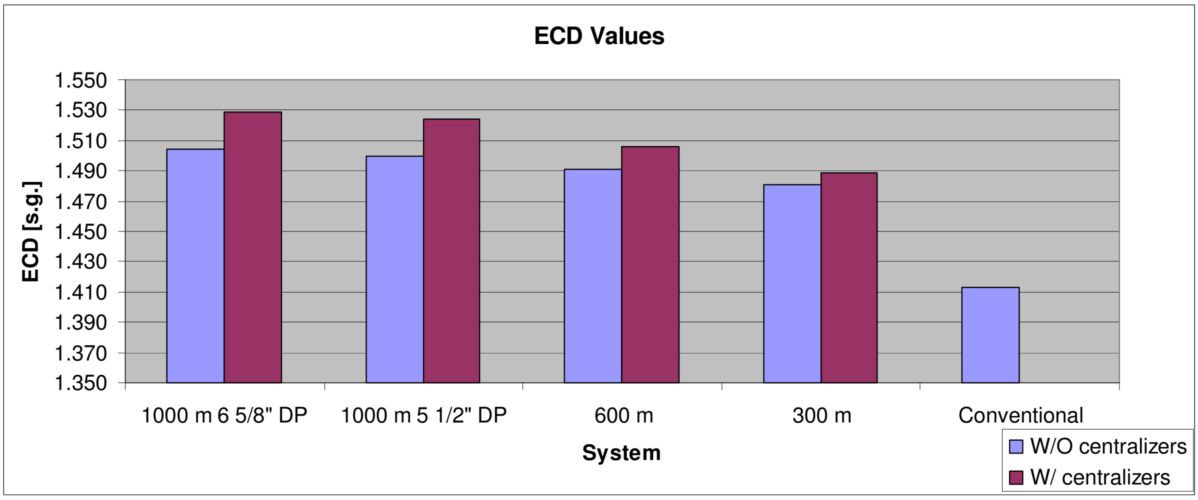

Figure 55: ECD Values for the different drilling systems

In figure 55 above, it is seen that the longer the liner is, the greater the pressure loss increase, and consequently also the ECD, becomes.

It also becomes apparent that the ECD values calculated manually are somewhat higher than those found by the simulation software. What the exact reason for this might be is uncertain, although the simulation software in question has in some cases had a reputation for under-estimating the ECD. It is therefore, although interesting to note, not very surprising.

Since the first use of the steerable liner drilling system will be using a 1000 m liner and 6 5/8" drillpipe, it was also decided to perform some simulations with this as a constant, while varying the flow rates. The purpose of this would be to combine the results of this simulation with the simulations to come later on to find the minimum required hole cleaning flow rate, along with its resulting ECD.

This was first done in WellPlan, and the result can be seen in figure 56 below.

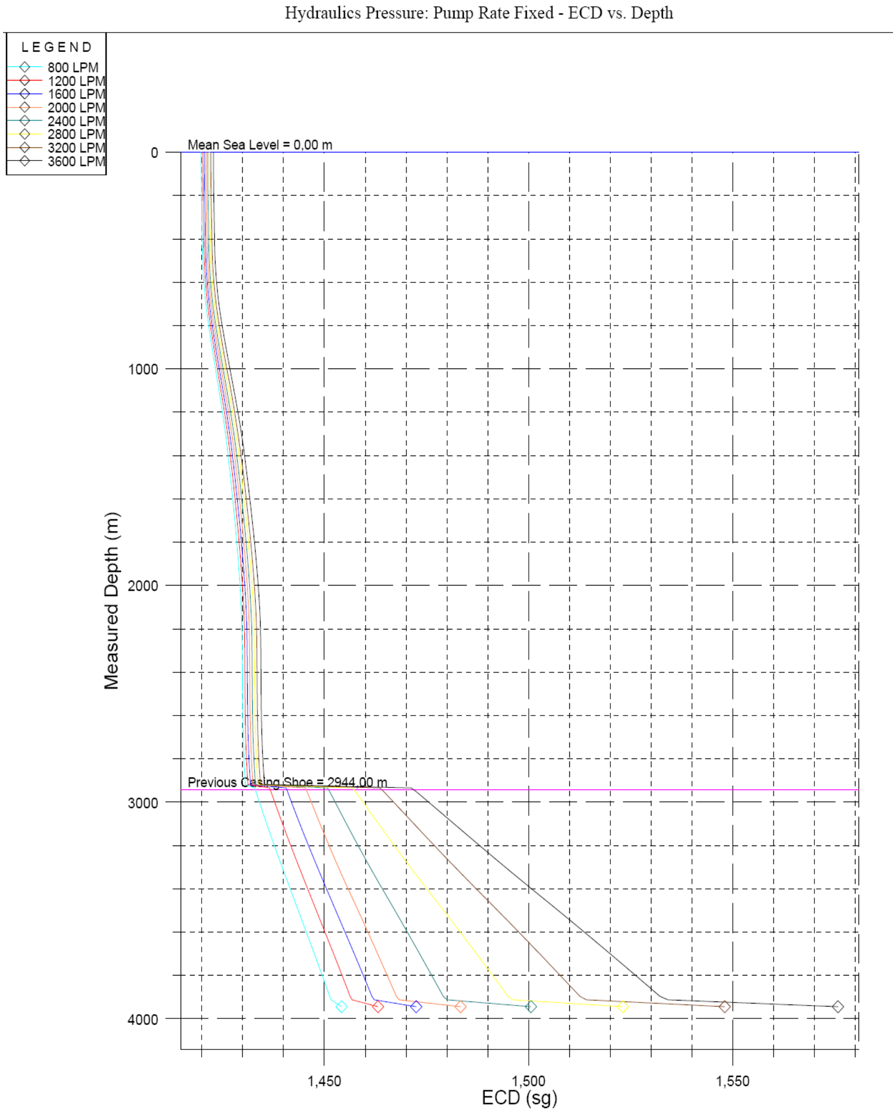

Figure 56: ECD Values for Different Flow Rates for the 1000 m SLD System

Based on the results seen in figure 56 to the left, we see that the resulting ECD will vary between approximately 1,45 and up to almost 1,6 s.g., depending on which flow rate is chosen. The pore- and fracture pressure curves have been removed from this plot, but even though the ECD has increased noticeably up to the highest flow rate, it does not appear to present a danger with regards to fracturing. In order to do this, it would have to reach values of about 1,8 and above.

In addition to the simulation results, the same calculations have also been performed manually.

It was decided that the ECD calculated manually for this case would include the pressure loss as a result of the centralizers. The reason for this was that this would make the calculations more conservative, and also that the WellPlan simulations used this assumption as well.

The results of the manual ECD calculations are tabulated below, and can be seen on the next page in figure 57 as a graph.

Flow Rate [lpm]	6 5/8" DP	5 1/2" DP
800	1.421	1.420
1200	1.443	1.442
1600	1.473	1.470
2000	1.509	1.505
2400	1.551	1.545
2800	1.599	1.592
3200	1.653	1.644
3600	1.713	1.701

Table 6: Flow Rate vs. ECD for the 1000 m SLD System with 6 5/8" and 5 ½" drillpipe

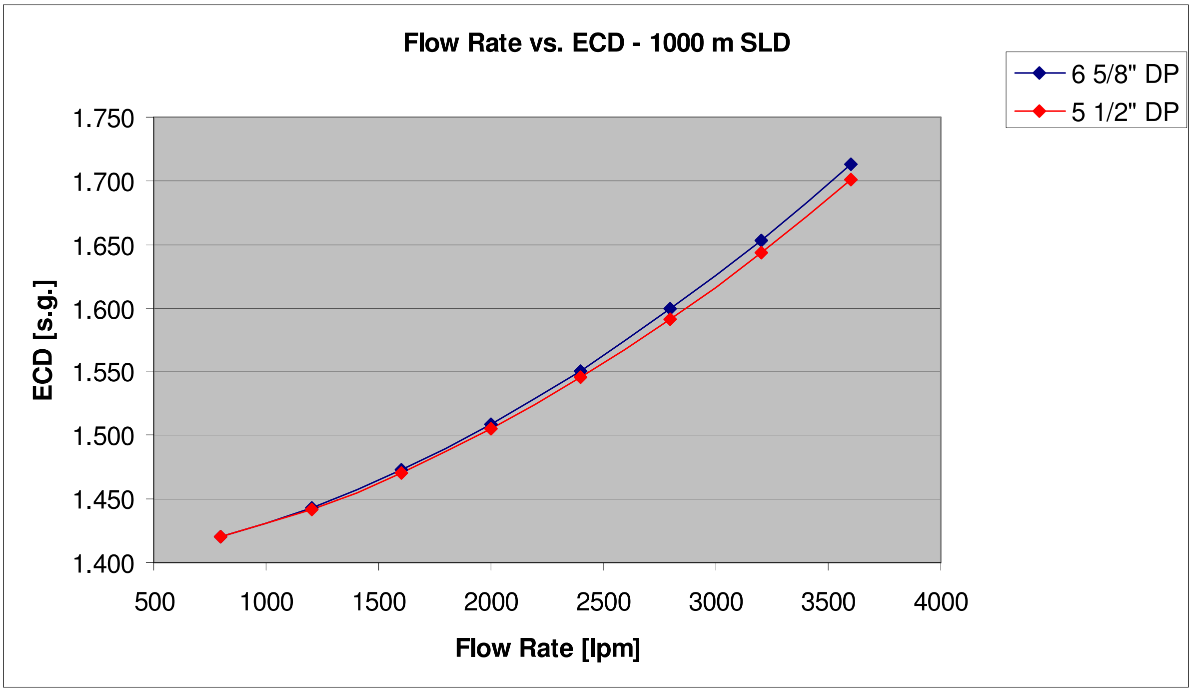

Figure 57: Flow Rate vs. ECD - 1000 m SLD with 6 5/8" and 5 ½" drillpipe

As seen in figure 57 above, the ECD increases in a slightly exponential way. This is consistent with the pressure drop formula, which has a power of 1,8. It is also apparent that the manual calculations give higher ECD values than the simulations do. This is also consistent with the other ECD calculations performed in this thesis.

6.6 Friction Caused by Liquid Flow

In addition to the mechanical friction forces, the friction caused by the actual flow of liquid in the annulus between the pipe and hole wall has been calculated. Since this force was not believed to be very large, it was decided to only calculate it for the base case of this thesis; the SLD system with 6 5/8" drillpipe and a 1000 m long liner.

The axial liquid friction force, acting upwards, has been calculated, both for simultaneous pumping and rotation, along with the axial force present when only one of these occur. The resulting torque has also been calculated. Note that the torque will act against the already found rotational torque, similar to how the axial fluid friction will make the string slightly lighter.

Axial Friction, pumping OR rotating	24.28 kN
Axial Friction, pumping AND rotating	28.92 kN
Torque	2.24 kNm

Table 7: Liquid Friction

Based on the values in table 7 above, it is apparent that the effects of liquid friction do not appear to be very large. While it will decrease the hook load somewhat, and also decrease the torque, it does not change either the hook load or the torque to the extent that it significantly affects the design requirements of the steerable liner drilling system.

6.7 Hole Cleaning

The outer and inner dimensions of the steerable liner drilling system were programmed into the WellPlan simulation program in order to calculate the ECD to begin with.

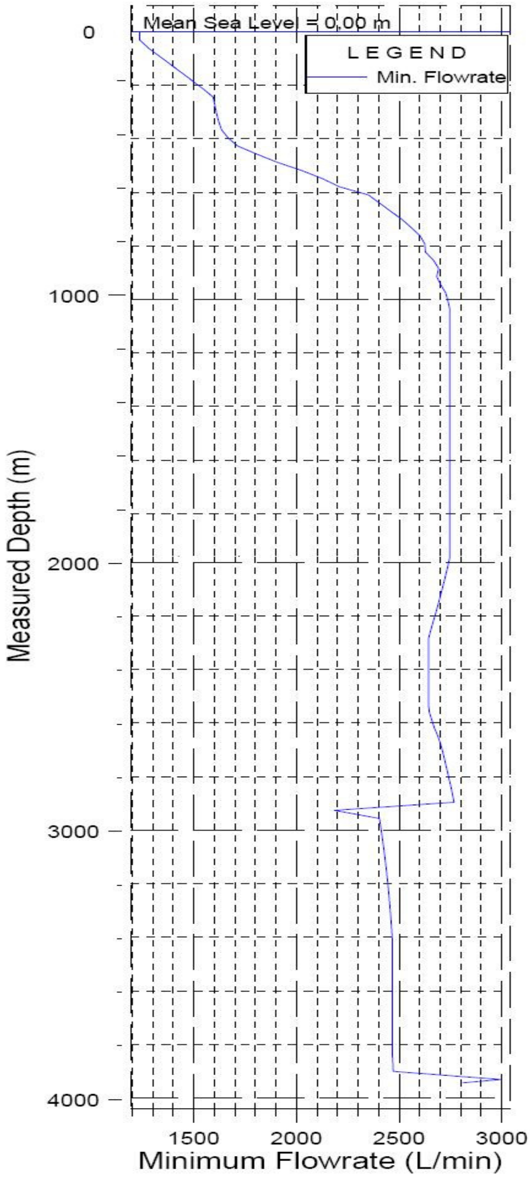

Figure 58: Minimum Required Hole Cleaning Flow Rate

As part of the hydraulics and ECD simulations, hole cleaning simulations were also performed.

Since there are a variety of different flow rates which may be chosen, it was decided to focus mainly on the minimum required flow rates for proper hole cleaning, instead of evaluating the actual hole cleaning performance given a certain flow rate. This was also done for practical reasons, since simulating a wide variety of flow rates for four different cases would entail very many graphs and results which would not necessarily be very valuable in the context of this thesis, although it would be wise to do in order to evaluate a given operational plan.

Therefore, the minimum required flow rate for proper hole cleaning was investigated for the given depths in the well. The resulting figure 58 can be seen to the left. It clearly shows that in several sections of the well, flow rates well in excess of 2500 l/min are required, all the way up to 3000 l/min.

In addition to the minimum required flow rates for each depth, it is also possible to show the minimum required flow rate vs. the hole inclination. Although the manual calculations to follow will not take this into account, it is still something to be aware of.

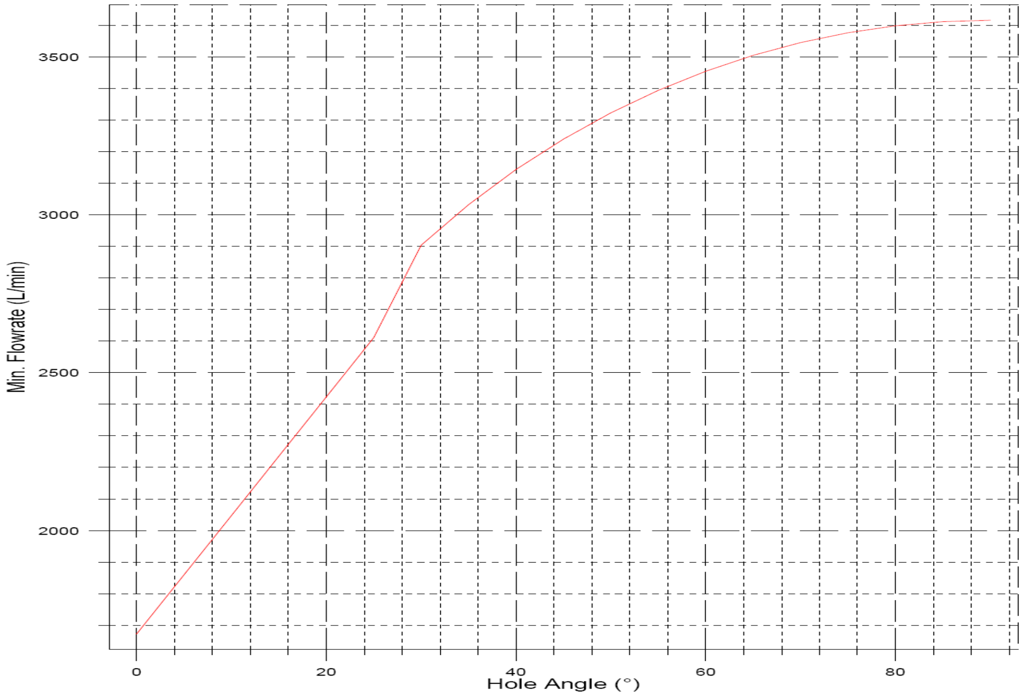

Figure 59: Hole Angle vs. Minimum Required Flow Rate

Manual calculations have also been carried out in order to determine the minimum and recommended flow rates in order to ensure sufficient hole cleaning. While the method for obtaining the minimum flow rates manually are less advanced than the WellPlan simulation software, it still gives an indication of what the flow rate should be. Note that this method is based on StatoilHydro internal best practice [16], and that the required minimum flow rates therefore also may vary somewhat from the requirements of other companies for this reason. The results of the calculations are summarized in the tables below:

9 5/8” SLD System	**Minimum Flow rate [lpm]**	**Recommended Flow rate [lpm]**
13 3/8" casing and 6 5/8" drillpipe	2640	3300
13 3/8" casing and 9 5/8" liner	1455	1818
12 1/4" open hole and 6 5/8" drillpipe	2582	3228
12 1/4" open hole and 9 5/8" liner	1397	1746
8 1/2" pilot hole	608	760

Table 8: Recommended Flow Rates for the 9 5/8” SLD System with 6 5/8" Drillpipe above the Liner

As seen in table 8 above, the highest required flow rates are seen in the area between the drillpipe and 13 3/8” casing. The reason for this is that this is where the annular area is largest, and therefore a higher flow rate is required to maintain a sufficient annular velocity. The difference between the required flow rates in the pilot hole, and further up between the drillpipe and casing, is quite noticeable. This also creates contradictory requirements, since a high flow rate is required for hole cleaning while it may not be desirable due to ECD.

9 5/8” SLD System	**Minimum Flow rate [lpm]**	**Recommended Flow rate [lpm]**
13 3/8" casing and 5 1/2" drillpipe	2972	3715
13 3/8" casing and 9 5/8" liner	1455	1818
12 1/4" open hole and 5 1/2" drillpipe	2914	3643
12 1/4" open hole and 9 5/8" liner	1397	1746
8 1/2" pilot hole	608	760

Table 9: Recommended Flow Rates for the 9 5/8” SLD System with 5 1/2" Drillpipe above the Liner

As seen in table 9 above, the highest required flow rates are seen in the area between the drillpipe and 13 3/8” casing. This is consistent with the findings for the other SLD system. The only difference here is that the drillpipe outer diameter has been decreased to 5 ½”. As is expected, this increases the recommended flow rates required for proper hole cleaning.

Conventional 12 1/4" System	**Minimum Flow rate [lpm]**	**Recommended Flow rate [lpm]**
13 3/8" casing and 5 1/2" drillpipe	2972	3715
12 1/4" open hole and 5 1/2" drillpipe	2914	3643
12 1/4" open hole and BHA	2093	2617

Table 10: Recommended Flow rates for a Conventional 12 1/4" Drilling System

The flow rates required for the conventional system are seen in table 10 above. Because the largest annular area is the same as for the SLD system with 5 ½” drillpipe, the minimum required flow rate is also just as high. Fewer ECD problems would be expected for a conventional system, however, since the OD remains fairly low, even in the lower sections of the drillstring.

7" SLD System	**Minimum Flow rate [lpm]**	**Recommended Flow rate [lpm]**
13 3/8" casing and 4 1/2" drillpipe	3215	4019
9 5/8" casing and 4 1/2" drillpipe	1513	1891
8 1/2" open hole and 6 5/8" drillpipe	1265	1581
6" pilot hole and BHA	327	409

Table 11: Recommended Flow Rates for the 7" SLD System with 4 1/2" Drillpipe

In addition to the 9 5/8” SLD system and conventional 12 ¼” systems, the recommended flow rates have also been calculated for the 7” SLD system in table 11. This has been done in order to show the variation in required flow rates in order to maintain a sufficiently clean hole. The exact flow rate requirements will depend on the previous casing strings, and whether the 9 5/8” section is a casing or liner, as is reflected in table 11.

7 Discussion of the Results

7.1 Discussion

While it should be pointed out that there is a great deal of uncertainty related to the calculation of the drag and friction forces, the fact that both the simulation software and manual calculations provide fairly similar answers does indicate that the results are not too far off. Having said that, the hook loads calculated, especially for the 6 5/8" drillpipe SLD system with 1000 m of liner, are fairly high, especially when tripping out of the hole. This imposes restrictions on the types and grades of drillpipe material which can be used, while still maintaining a safe operation.

While the calculated axial stress values of up to 5700 bar do not seem to be a problem with regards to the steel grade, it may be a problem for the drillpipe. Therefore the Drilling Data Handbook's Drillpipe Torsional and Tensile Data table was consulted, in order to see how the different material grades and pipe specifications would deal with the calculated tensile loads.

It was decided to base these considerations on the highest hook load value calculated, which was based on the 6 5/8" drillpipe 1000 m SLD system and manual calculations. If these calculations are inaccurate, so will the following statements be. This number is believed to be conservative, however.

Based on the tabulated [9] tension data for 6 5/8" 27,7 lbs/ft drillpipe, the following is observed:

- E-75 drillpipe is not strong enough, neither as New, Premium, nor Class 2.
    - No safety factor.
- X-95 drillpipe is strong enough as New, but not as Premium or Class 2.
    - New safety factor: 1,2
- G-105 drillpipe is strong enough as New, and barely as Premium as well. It is not strong enough as Class 2, however.
    - New safety factor: 1,33
    - Premium safety factor: 1,05
- S-135 drillpipe is strong enough as New, Premium, and Class 2.
    - New safety factor: 1,7
    - Premium safety factor: 1,35
    - Class 2 safety factor: 1,17

Care must therefore be taken in order to ensure that the drillpipe chosen for the operation is strong enough to withstand the tensile loading it will be exposed to at the top. It should also be noted that if the simulation values had been used in order to determine acceptable drillpipe grades, the outcome would have been slightly different. This is because the simulations show a hook load of 20 – 25% less than the manual calculations do.

When using 5 ½" drillpipe, the hook load becomes somewhat lower, calculated manually to be 247 tonnes. Similar considerations can be made for this drillpipe size, as was done for the 6 5/8".

Based on the tabulated [9] tension data for 5 ½" 24,7 lbs/ft drillpipe, the following is observed:

- E-75 drillpipe is not strong enough, neither as New, Premium, nor Class 2.
  - No safety factor.
- X-95 drillpipe is strong enough as New, but not as Premium or Class 2.
  - New safety factor: 1,13
- G-105 drillpipe is strong enough as New. It is not strong enough as Premium or Class 2, however.
  - New safety factor: 1,25
- S-135 drillpipe is strong enough as New, Premium, and Class 2.
  - New safety factor: 1,61
  - Premium safety factor: 1,26
  - Class 2 safety factor: 1,10

For the drilling systems with a shorter liner, the hook loads will be lower, and there will thus be a wider variety of drillpipes to choose from. The conventional drilling system, whose highest hook load was calculated manually to be 173 tonnes, would also be able to use a somewhat wider range of drillpipe grades.

With regards to torque, the steerable liner drilling system also has several challenges. The first such challenge is that the top of the liner, along with the setting tool, will be exposed to high torque loads. This point in the string has also been identified as critical by others who have looked into performing casing and liner drilling operations [22, 29, 31].

In this case, with a 1000 m long liner, the torque loading at the top of the liner becomes approximately 50 kNm based on the manual calculations, and 36 kNm based on the simulations. The connections on this liner are supposed to be conventional VAM TOP C-95 connections, which have a make-up torque of 31,4 kNm, with a maximum make-up value 10% higher, at 34,5 kNm. The liner connections will therefore be exposed to torque above its maximum make-up torque. This is supported both by the simulations and manual calculations.

The maximum make-up torque does not tell the whole story, however. For most connections available, there is also a value which indicates how much torque the connection is able to withstand before it actually fails. This might be called the ultimate torque tolerance of the connection. It is not a publicly available figure in most cases, however. Therefore, the performance evaluation made with regards to the connections in this thesis will have to be made based solely on the make-up torque values. In reality, the actual torque tolerance will be somewhat higher, but it still seems reasonable to assume that if a connection will be loaded substantially above its make-up value, it might also be a problem with regards to its maximum allowable torque tolerance. This will, however, have to be evaluated internally, and can not be discussed here.

Should it not be possible to use regular connections, there may be several connections capable of handling higher torque. One example of such a connection is the VAM HTF connection [40], which is supposedly capable of handling loads up to 250 kNm.

It should also be noted that even though the simulated torque values are higher than the manually calculated ones, these values also indicate that there may be a torque challenge with regards to the torque loading on the liner connections.

Another concern would be the torque rating of the running tool, as well as the torque rating of a potential setting tool, should this be implemented some time in the future. For the moment, this is not the case, but it seems likely that this is something which will be developed in the future. The torque rating of such a tool must also be able to withstand the maximum loading at the top of the liner; in this case 50 kNm or 36 kNm. Further up the string the drillpipe will be exposed to up to 98,5 kNm at the very top for the 6 5/8” drillpipe with 1000 m liner.

Based on the tabulated [9] torsional data for 6 5/8” 27,7 lbs/ft drillpipe, the following is observed:

- E-75 drillpipe is strong enough, as New, but not as Premium, or Class 2.
  - New safety factor: 1,05
- X-95 drillpipe is strong enough as New and Premium, but not as Class 2.
  - New safety factor: 1,33
  - Premium safety factor: 1,06
- G-105 drillpipe is strong enough as New, Premium, and Class 2.
  - New safety factor: 1,47
  - Premium safety factor: 1,18
  - Class 2 safety factor: 1,01
- S-135 drillpipe is strong enough as New, Premium, and Class 2.
  - New safety factor: 1,89
  - Premium safety factor: 1,51
  - Class 2 safety factor: 1,29

Similar considerations can also be made for the 5 ½” drillpipe. Based on the tabulated [9] torsional data for 5 ½” 24,7 lbs/ft drillpipe, the following is observed:

- E-75 drillpipe is not strong enough, neither as New, Premium, nor Class 2.
  - No safety factor.
- X-95 drillpipe is strong enough as New, but not as Premium or Class 2.
  - New safety factor: 1,11
- G-105 drillpipe is strong enough as New. It is not strong enough as Premium or Class 2, however.
  - New safety factor: 1,22
- S-135 drillpipe is strong enough as New, Premium, and Class 2.
  - New safety factor: 1,57
  - Premium safety factor: 1,23
  - Class 2 safety factor: 1,07

It is therefore apparent that the choice of drillpipe is further limited due to torque considerations, in addition to the limits already imposed by tension loading. Note that the above mentioned limitations apply for tensional or torsional loading separately, and that the pipe should not be loaded to the maximum in tension and torsion at the same time.

The tool joints of the drillpipe must also be able to withstand the loads of 98,5 kNm and 87,6 kNm for the 6 5/8” and 5 ½” versions of the steerable liner drilling systems, respectively. This may imply that tool joints with higher torque tolerances than usual may be required. None of the weld-on type tool joints listed in the Drilling Data Handbook have make-up torque values which would indicate that they will tolerate the loads manually calculated for the 1000 m SLD system, neither in 5 ½” configuration, nor as 6 5/8”. As for the liner connections, the actual torque tolerance may be somewhat higher than what is listed in the Drilling Data Handbook. Even so, one might still at least consider using drillpipe connections with a higher torque rating, such as for instance the “H-Series Hi Torque” connections made by Grant Prideco [41]. This tool joint has a listed torsional capacity of 112 kNm. Other manufacturers may also be considered, of course, as this is only an example. The availability of drillpipe tool joints with high torque ratings is believed to be higher than it is for casing and liner at the moment.

It should also be noted that the torque calculations are where the simulation software and manual calculations seem to diverge the most. The manually calculated torque values are consistently higher than the simulated ones. One reason for this may be that the simulation software does not fully support the steerable liner drilling system’s configuration with an inner string. There is, however, also room for the possibility that the manual calculations of torque are higher than the actual values will be, and the calculations in this thesis might therefore be regarded as somewhat conservative. This applies to both hook load and torque.

Another aspect to be considered is fatigue. The reason why fatigue becomes important is that liner and casing connections, as opposed to drillpipe connections, are not designed to withstand great torque loading, and are therefore weaker in torsional strength. Therefore, it is important to know the fatigue strength of the liner connections used, and have the S/N curves available in order to find out the amount of cycles the connection can withstand in a given state of stress until it fails.

In this thesis, the way of finding the expected fatigue life of a liner, given an example S/N curve and the calculated side force, has been demonstrated. With regards to the specific case in question, however, there is not much to be said which will be useful in a real life operation. The reason for this is that the S/N curve for the liner connection used on the steerable liner drilling system is kept confidential, at the request of the manufacturer, and even though this is a confidential thesis, it may not be published here. Thus, the fatigue results calculated based on an example plot would have little value with regards to evaluating a specific operation. Even so, the general principle remains the same.

On a general basis, however, it may be said that a not too aggressive wellpath, with no planned dogleg severities exceeding 5 degrees per 30 m, and a length of 1000 meters where only the last 200 to 300 m will actually be drilled by the liner drilling system, should not present a major risk with regards to fatigue failure of the liner connections, provided they are strong enough to withstand the torque the system is exposed to in the first place.

ECD is also an area of concern typically expressed during casing and liner drilling operations. The reason for this is that the annular area is narrower during casing and liner drilling, and the flow velocities generated for similar pump rates will therefore be much higher. If the formulae for frictional pressure drop are considered, we see that they depend on the annular velocity to the power of either 1,8 or 2,0 depending on which formula is used. Consequently, the frictional pressure drop in the annulus will increase, and when the frictional pressure drop in the annulus increases, so does the equivalent circulation density, or ECD.

Obviously, the ECD for the steerable liner drilling system will depend on which flow rate is chosen. This is in turn decided by hole cleaning considerations, which will be addressed later in this chapter.

Having said that, based on the wellpath and pore pressure prognosis in the field where the 9 5/8” steerable liner drilling system is to be field tested, the ECD will not be problematic until flow rates begin to approach 3800 lpm, where the ECD is 1,713 s.g. from a base mud weight of 1,4 s.g., and above. Should the fracture pressure prognosis for some reason change, this will have to be reconsidered, however. As a side note, it might also be mentioned that it is believed that the 7” steerable liner drilling system may have greater challenges with regards to ECD than the 9 5/8”. This is because the running tool OD on the 7” system is somewhat larger, compared to the hole size, than is the case for the 9 5/8” system. This creates a significant pressure drop, even though it is a short section.

ECD considerations will, of course, have to be made on an individual basis for each well and liner drilling system, but in the case examined in this thesis, it does not seem to represent the most critical parameter.

Liquid friction is another parameter which has been investigated. While this may seem like a strange term, it implies that the drillstring is subjected to a certain force, both axially and tangentially, when fluid is circulated in the annulus around the drillpipe. Both the axial force and torque from the liquid has been calculated. However, these forces are not very large compared to the other forces the system is subjected to. Adding or subtracting them would therefore make little or no difference with regards to the design requirements of the system itself. It is nevertheless something to investigate, in order to verify whether or not this is the case.

Hole cleaning is another concern, both for conventional and steerable liner drilling systems. The minimum required hole cleaning mud flow rates have been calculated, both using the simulation software and manual calculations based on StatoilHydro Best Practice [16]. Based on these calculations, the actual minimum required hole cleaning flow rates do not differ significantly between the steerable liner drilling system and the conventional alternative.

For the 9 5/8” SLD system with 6 5/8” drillpipe, the minimum recommended flow rate is 2640 lpm, while the recommended flow rate is 3300 lpm. For the same system with 5 ½” drillpipe, the same flow rates become 2972 lpm and 3715 lpm respectively. The highest flow rates required are in the upper section where there is drillpipe inside the 13 3/8” casing. This is the area with the highest annular cross sectional area, and thus where the flow rate needs to be the highest in order to achieve the required flow velocity. This is also why the minimum flow rate requirements are the same for the 9 5/8” SLD system with 5 ½” drillpipe and the conventional system, which also used 5 ½” drillpipe.

Usually, one does not wish to increase the flow too much, due to ECD concerns. In this case, however, it does not appear as though the recommended flow rates for hole cleaning will cause unacceptable ECD values, especially not if one stays a little bit below the highest recommended value. How this ECD compares to the pore and fracture pressure will vary on a case to case basis, however, and will need to be evaluated as such.

It should also be mentioned that for the field trials which will take place of the SLD system on the North Sea well this summer, the maximum allowable flow rate is somewhere in between 2000 and 2500 lpm. The reason for this is that there is a tool in the tool string with this flow rate limitation. With these flow rates, when considering the previously stated hole cleaning flow rate requirements, hole cleaning could become a problem. One way to mitigate this could be to install a flow diverter at the top of the liner. This is not an option for the well in question, however, and falls into the category of modifications which may be made in the future.

While the 7” steerable liner drilling system is not the main focus of this thesis, it is, however, worth noting that the 4 ½” drillpipe used for this system could give quite high flow rate requirements if used inside 13 3/8” casing without a 9 5/8” liner outside. Given that the 7” system already has ECD related challenges due to the large outer diameter of the running tool, this might be a concern since a flow rate of up to 4000 lpm as required in this scenario would probably generate unacceptable ECD values. If used inside a 9 5/8” casing, however, the recommended flow rate becomes 1891 lpm, and might be more feasible.

7.2 Design Constraints for the Steerable Liner Drilling System

One of the major design constraints of the steerable liner drilling system initially appeared to be the fatigue performance of the liner connections. The results of this thesis seem to indicate, however, that this may not be the case. There is of course a fair amount of uncertainty related to these calculations. First of all because it may be difficult to predict what exact loading scenarios the liner will be exposed to downhole, and also because there are varying views with regards to what loads should be taken into account when finding the stress the connection is exposed to. Furthermore, the actual S/N curves for the liner connection in the SLD system could not be used, and the results are consequently not very relevant to the actual operation, even if the theory behind the calculations remains the same.

One design constraint seems to be the quite high torque values the system will be exposed to, partially because of the increased weight of the string due to the liner. This, however, is consistent with the results of similar investigations into casing and liner drilling [31, 42]. There is quite a bit of uncertainty related to the torque values, however. The manually calculated values are obviously uncertain because they are based on a theory, and this theory may in time turn out to be somewhat inaccurate. The simulation results may also be somewhat inaccurate because the simulation program used to calculate the torque does not yet support the system, and therefore may not be able to calculate correctly.

The same uncertainties come into play with regards to the drag calculations. There is, however, more resemblance between the WellPlan simulations and manual calculations for the drag values, which may indicate a higher degree of reliability, although this is not certain. There are also conflicting views related to the theory used to perform the manual drag calculations.

Both torque and drag considerations are, however, seen to have a great impact on what equipment may be used with the steerable liner drilling system.

With regards to ECD calculations, the manual calculations appear to be more conservative than the simulation software. While the resulting ECD is fairly large, it does not seem to become a problem for the operation with regards to pore and fracture pressure limitation. The simulation software has also been known to underestimate the ECD in the past, and the fact that it gives lower values than the manual calculations is therefore to be expected. It was also interesting to see that the Drilling Data Handbook formula for pressure drop in turbulence gave a slightly higher value than the frictional pressure drop formula found in the compendium by Time [11]. However, as the limited amount of field data available seemed to correspond better to the results based on the Drilling Data Handbook, this formula was used to calculate the ECD.

When it comes to hole cleaning, it becomes more complicated, however. This is because it is difficult to know exactly which assumptions the simulation software makes when it tries to evaluate whether or not the hole cleaning will be sufficient. There is of course also the question of what exactly is defined by the simulation software as good hole cleaning. The manual calculations, based on best practice, seem to indicate that it should be possible to achieve sufficient hole cleaning in most cases for the 9 5/8" SLD system. It may become more challenging, however, for the 7" system under certain circumstances.

7.3 Alternative Solutions and the Road Ahead

Future technological developments within drilling and well technology will have to deal with a variety of challenges. The most notable of these may very well be drilling in deep water and drilling in severely depleted reservoirs with unstable formations. The steerable liner drilling system is a system which addresses several of these concerns. The SLD system as of today, however, still has a lot of room for improvement.

One potential further development of the steerable liner drilling system is the addition of an expandable liner, instead of a conventional one. One of the challenges related to this option, is that expandables are, as of today, still not widely used in the industry. There is also a limited amount of experience to draw on. Furthermore, the expandable liner would have to be tested thoroughly, in order to ensure that it could withstand the loads experienced during drilling, while still being able to maintain pressure integrity after being expanded to its final size.

Combining liner drilling and expandable tubulars could offer significant cost savings, and enable monobore wells to be drilled. This is advantageous for several reasons. First of all, it decreases the pressure drop in the production tubing since the inner diameter of the tubing does not change. It also enables larger tubing sizes further down into the well, since an additional casing string does not mean a loss of diameter. Being able to do this effectively would require the development of a liner hanger compatible with liner drilling and expandables, in addition to the already mentioned challenges. Similarly, drilling with screens or slotted liners would also be beneficial, albeit for slightly different reasons than the expandable liner.

Yet another potential future addition to the steerable liner drilling system may be a liner hanger. One example of this is found in the literature where ConocoPhillips reported qualifying such an expandable hanger for casing drilling operations on the Eldfisk field [29]. It would be even more beneficial if it was possible to incorporate a resettable liner hanger in the SLD system, as this would, for instance, allow the liner to be hung off somewhat off the bottom, instead of having it lie on the bottom unsupported if tripping the drillpipe out of the liner to troubleshoot is required.

Another possibility would be to incorporate elements of the ReelWell system into the SLD system. During liner drilling, the annular area in the lower part of the drillstring is quite small, due to the OD of the liner. When the cuttings pass the top of the liner, the OD of the drillstring becomes quite a bit lower. This may lead to difficulties with regards to hole cleaning if the flow rate is not sufficient.

The challenge here is that the flow rate may already be decreased somewhat due to ECD concerns in the narrow annulus between the liner and the borehole. The liner is also rotating slower than a normal drillstring otherwise would have. This is to extend the lifetime of the liner during drilling. The combination of a lower drillstring RPM and a lower flow rate may lead to poorer hole cleaning, since we have less lifting force and less agitation of the drilling cuttings. This may be a concern, since the liner drilling system is meant to be used in deviated holes.

One potential solution to this challenge is to have a separate string along with the drillstring which will be used for mud returns to the surface. This would solve the problem with regards to hole cleaning, but certainly poses other equipment-related and operational challenges. Some of these challenges may be solved as the ReelWell system matures, but this is currently not the case.

A different alternative would be to go from liner drilling and to a kind of casing drilling. This means that longer sections of the well will be drilled with liner/casing as the OD of the string. This would in turn mean a more narrow annular area, and thus a higher flow velocity. A natural concern here is an increase in ECD. One variety of this solution was used by ConocoPhillips on the Eldfisk field in Norway. The operator here drilled a well with Tesco's Casing Drilling system to TD. Upon reaching TD, the casing was converted into a liner, with a liner hanger purpose built for the operation [29]. Tesco has also proposed that its Casing Drilling system be modified for proper adaptation for deepwater use.

Yet another alternative may be to install a flow diverter at the top of the liner. This would divert a certain amount of the flow out into the annulus, and allow less flow down through the liner and bit. This could be beneficial for several reasons. First of all, it could be beneficial because it would allow higher flow rates to be used, without giving excessive ECD in the pilot hole since more of the flow would be diverted. Second, it would give higher flow rates in the section above the liner. This is important because there is a significant increase in the annular area in this section, and this is a challenge with regards to maintaining sufficient annular velocity in order to get proper hole cleaning.

While installing a flow diverter sounds simple in theory, it does also come with its fair share of complications. One such complication is that it would have to be possible to open and close the diverter port remotely, without having to perform some manual intervention. While this may be possible to do, it entails adding complications to an already complicated system. A flow diverter could also pose challenges if it in the future becomes possible to cement the liner in place without having to trip out and change the assembly first. This would again require some sort of opening and closing mechanism to be installed. There are tools currently developed which can probably be used for this purpose with some modifications, but there is still some uncertainty here.

Another aid with regards to hole cleaning might be to allow flow upwards through the liner, in addition to outside of it. This also presents challenges, however.

Deepwater operations is another area where liner drilling may be of use. Since deepwater wells will mainly require subsea completions, drilling with a full string of casing from a mobile drilling unit becomes unnecessary, as well as impractical. Instead of this, a system similar to the casing drilling system is used which is in fact quite similar to the SLD system. The purpose of this is to ensure that the top of the casing/liner is at the wellhead when the section in question has been drilled to TD. Otherwise, excess casing would have to be tripped to the surface after reaching TD. The remaining drillpipe will of course have to be tripped to the surface, but tripping drillpipe in this manner, while still time consuming, is faster than it would be with casing.

Changes may also in the future be made to the hole opening solution of the SLD system. The current design with a reamer might for instance be replaced by an under-reamer, which can be run on the drillpipe along with the rest of the BHA. The reason for not using an under-reamer at this point is that they are not regarded as reliable enough due to the large hole size increase required. This may change in the future, however, and may make the SLD system even more robust.

Another challenge for the SLD system is cementing. In its current design, it is not possible to cement the liner at TD without tripping out first, since there is no float in the liner. One solution to this might be to install some sort of one-way valve or flapper in the liner, which would act as a float. This might make it possible to save time when cementing the liner in place, which would further add to the potential time savings of the steerable liner drilling system. Making such a flapper or valve is not entirely straight-forward, however, since it has to be robust enough to tolerate drilling loads, and must also be reliable enough to be used along with the rest of the system.

8 Conclusion

Although the simulations and manual calculations differ somewhat with regards to the exact tensile loads the system will experience, with 193 tonnes and 255 tonnes respectively, it still seems fair to say that the loading on the drillpipe will be quite high. Therefore, it is recommended to use S-135 grade drillpipe for the liner drilling operation in question, regardless of the choice between 6 5/8” and 5 ½” size. While there are other pipe grades which will be usable as new, they are either too weak, or provide a very low safety factor after having been worn down to premium or class 2. The relatively high torque values, especially those from the manual calculations, also support the use of a high grade drillpipe. This does, however, assume that the tabulated torsional limit values in the Drilling Data Handbook are the actual values, and that there are no unpublished maximum torque values held by the manufacturers.

The conventional 12 ¼” drilling system was found to have a maximum hoisting load of 172 tonnes using simulations and 173 tonnes using manual calculations. Interestingly, the simulations and manual calculations seem to correspond fairly well here. The tensile loads seen in the conventional system are therefore slightly lower than the ones seen in the 1000 m SLD system with 6 5/8” drillpipe. The conventional system uses 5 ½” drillpipe, and this may also be part of the explanation for this. The loads seen in the steerable liner drilling system are, higher and thus impose stricter requirements on the pipe which may be used.

Similarly, the torque values calculated for the liner indicate that standard VAM TOP connections may be too weak in torsion compared to the loads the system will be exposed to during drilling. The difference between simulations and manually calculated values is even greater here, ranging up to 70% more torque from the manual calculations. Even so, the torque at the top of the liner is calculated to be 50 kNm manually and 36 kNm simulated. These values are both somewhat higher than the maximum make-up torque of the connections, and if this is to be used as the design limit, then a different connection must be used.

It should also be mentioned that the maximum torque values listed publicly by the manufacturers may not be the actual torque limits. These are often figures which the manufacturers keep confidential. Therefore, whether or not conventional VAM TOP C-95 53,5 lbs/ft connections would be too weak in torsion for this operation is not certain, but the torque values are very likely to exceed the connection’s maximum torque capacity. Therefore, the possibility of using VAM HTF, or similar connections with a high torque tolerance, should seriously be considered. This would significantly increase the operating window for the steerable liner drilling system, and also provide much higher safety factors with regards to torque.

While the drillpipe will also be exposed to high torque values, this does not pose as great a challenge as it does for the liner connections, however. This is because while drillpipe is, and historically has been, exposed to torque ever since rotary drilling begun, casing and liner drilling is a fairly recent technology on a large scale. Therefore, liner connections which can endure the torque loads it will be exposed to in a drilling environment are not as common. Here as well, the torque calculated using the manual analytical method is far higher than the one found using the WellPlan simulation software. The torque at the top is manually found to be 98,5 kNm for the 6 5/8” 1000 m SLD system, while the simulation indicates 69 kNm. This compares to 91,2 kNm and 52 kNm calculated for the conventional 12 ¼" drilling assembly. While most weld-on tool joints will not be able to withstand the loads seen at the top of the drillstring calculated manually, the availability of high torque drillpipe connections is likely to be better than for liner connections.

With regards to hole cleaning, it is almost always desirable, as long as the formation can handle it, to have as high flow rates as possible. This will ensure a high annular velocity, and that cutting beds do not form and accumulate over time in deviated sections of the well. This does, however, not agree with the desire to have the lowest possible ECD, since the ECD increases along with the flow rate. Based on the hole cleaning calculations performed manually in this thesis, it is also apparent that the flow rate required in order for the SLD system with 5 ½" drillpipe to have sufficient hole cleaning is approximately 3700 lpm, the same as its conventional alternative, while the requirement for the 6 5/8" drillpipe system is 3300 lpm. This translates into ECD values of 1,72 and 1,67 respectively. In other words, if the recommended flow rates are used in the two different systems, the ECD will be somewhat higher for the 5 ½" drillpipe system than the 6 5/8" one. With this in mind, choosing 6 5/8" drillpipe above the liner would be recommended, as the minimum hole cleaning flow rate would be lower, along with a lower ECD if hole cleaning flow rates are used.

If the flow rates are kept the same, the 5 ½" system will obviously give a lower ECD value, but hole cleaning may suffer as a result. The difference is not as large as might be expected, because the largest quantity of the frictional pressure loss occurs at the liner, as a result of the fairly high liner outer diameter and its centralizers. The HRD setting sleeve/running tool and the reamer unit are also major contributors. The running tool, while an important contributor to the pressure loss for the 9 5/8" system, has an even greater impact in the 7" SLD system. This is because the outer diameter of the setting sleeve is larger relative to the hole size, as compared to the 9 5/8" system. This was not explored further, as it was not within the scope of this thesis.

The pilot test of the 9 5/8" steerable liner drilling system is planned to be run on the Brage field during the summer of 2009. While the exact details of this well are still being decided on, it appears as though the flow rate for this well may be limited to around 2000 to 2500 lpm, as mentioned in section 7.1. This will be close to the absolute minimum recommended flow rate for the 6 5/8" drillpipe, and based on both simulations and calculations, hole cleaning may become a challenge for this well. The ECD, however, especially at these flow rates, does not become large enough, reaching only 1,55 s.g. at 2500 lpm, to be a threat with regards to the fracture pressure of the formation, which appears to be around 1,8 s.g. The ECD for liner drilling will still be higher than for conventional drilling.

Based on the pilot test, several answers will probably be provided, with regards to both torque and drag values. Another subject of interest which will also be illuminated further in this test will be the smear effect. The smear effect, while often advertised as a major benefit of casing and liner drilling, has yet to be verified for the steerable liner drilling system, since trials on the BETA field were inconclusive. If proven, the smear effect would provide substantial advantages with regards to hole stability, trouble time, and other such factors, and would therefore be of great value to liner drilling operations. It may also allow for a decrease in the mud weight, which will be a further advantage if the drilling window is narrow. As of right now, however, the smear effect has not been proven sufficiently beyond reasonable doubt, and it can therefore not at the moment be counted on to be an advantage during liner drilling operations.

Liner connection fatigue is another issue which this thesis discusses. The actual value of the fatigue calculations is very limited, however, since the actual S/N curves for the liner connections may not be disclosed or used in this thesis. Connection fatigue is nevertheless a parameter which should be investigated when planning liner drilling operations. Close cooperation with the connection manufacturer will be important in this case, as well as planning the wellpath carefully, in order to avoid doglegs which will hamper the longevity of the casing connections. The advantage of the steerable liner drilling system in this respect is that it rotates the casing at only 30 RPM, while the BHA is rotated at 120-180 RPM. This will help preserve the connections for a longer time period, as they will not cycle as frequently.

Liquid friction is also investigated in this thesis. Although it is a force to be considered, its magnitude does not indicate that it would alter the design requirements for the steerable liner drilling system.

Although several aspects of steerable liner drilling have been examined, there are also aspects which are outside the scope of this thesis. One of these topics, which has not been examined, but is nevertheless important to investigate, is buckling analysis. This becomes important as the string gets heavier and the well longer. Another such topic is cementing, which will also be a challenge for the SDL system. Similarly, the well barrier situation, both when drilling with the system, and when the well is completed and producing, is also outside the scope of this thesis. It is nevertheless a very important topic for liner drilling operations and its usability as a whole.

Steerable liner drilling, if it is proven to be successful in the upcoming pilot tests, is a very exciting prospect for the future. In addition to providing benefits by itself to fields with depleted zones, unstable formations, and deepwater drilling, it also has the potential to be combined with expandables, managed pressure drilling, and the ReelWell system, among others. This means that the potential applications of steerable liner drilling are many, and it could therefore have a strong influence on how drilling operations and systems will evolve further.

References

1. Aadnøy, B.S., *Mechanics of Drilling*. 2006: Shaker Verlag. 196.
2. Metals, A.S.f., *Metals Handbook*. 8th ed. Vol. 9. 1974: Metals Park, Ohio.
3. Haagensen, P.J., *General Introduction to Fatigue Behaviour*, ed. NTNU. 1998: European Steel Design Education Programme.
4. Sches, C., E. Desdoit, and J. Massaglia. *Fatigue Resistant Threaded and Coupled Connectors for Deepwater Riser Systems: Design and Performance Evaluation by Analysis and Full Scale Tests*. in *ASME 27th International Conference on Offshore Mechanics and Arctic Engineering*. 2008. Estoril, Portugal.
5. Lu, Q., et al., *Connection Performance Evaluation for Casing-Drilling Application.* SPE Drilling and Completion, 2008(June 2008): p. 6.
6. Sches, C., et al. *Fatigue Resistant Threaded and Coupled Connectors: The New Standard for Deep Water Riser Applications*. in *International Conference on Offshore Mechanics and Arctic Engineering*. 2007. San Diego, California, USA.
7. Boresi, A.P. and R.J. Schmidt, *Advanced Mechanics of Materials*. Sixth ed. 2003: John Wiley & Sons Inc. 681.
8. Skaugen, E., *Appendix: Analytical model - StatoilHydro BETA Liner Drilling*. 2008, The University of Stavanger. p. 21.
9. Gabolde, G. and J.-P. Nguyen, *Drilling Data Handbook*. 7th ed. 1999: Institut Francais du Pétrole Publications.
10. Diaz, H., et al., *Modeling of ECD in Casing Drilling Operations and Comparison with Experimental and Field Data [SPE 87149]*, in *IADC/SPE Drilling Conference*. 2004: Dallas, Texas USA.
11. Time, R.W., *Two-Phase Flow in Pipelines: Course Compendium*. 2007: The University of Stavanger. 172.
12. Britannica, E. *"Eddy" - Encyclopedia Online Britannica*. 2009 [cited 2009 7th of May]; Available from: http://www.britannica.com/EBchecked/topic/178908/eddy.
13. Adari, R.B., et al. *Selecting drilling fluid properties and flow rates for effective hole cleaning in high-angle and horizontal wells [SPE 63050]*. 2000. Dallas, TX, USA: Soc Pet Eng (SPE).
14. Thorkildsen, J.G., *The Impact of, and Problems associated with, Deviated Wells*, in *Department of Petroleum Engineering*. 2007, University of Stavanger. p. 62.
15. Santarelli, F., *Reducing Downhole Drilling NPT with Liner Drilling?* 2008, Internal Report.
16. StatoilHydro, *Quick Reference Guide: Best Practice - Drilling Operations*. Second ed. 2008: StatoilHydro.
17. WorldOil, *Casing While Drilling: Handbook*. First ed, ed. J.D. Woods. 2003: Gulf Publishing Company. 46.
18. Fontenot, K., et al. *Casing Drilling Activity Expands in South Texas [SPE 79862]*. in *SPE/IADC Drilling Conference*. 2003. Amsterdam, the Netherlands.
19. Billa, R., et al. *Reducing Well Cost Utilizing Liner-Drilling Operations in South Texas [SPE 99110]*. 2006. Richardson, TX 75083-3836, United States: Society of Petroleum Engineers (SPE).
20. Sinor, L.A., et al. *Rotary Liner Drilling for Depleted Reservoirs [SPE 39399]*. 1998. Richardson, TX, USA: Soc Pet Eng (SPE).
21. Vogt, C., et al. *Drilling Liner Technology for Depleted Reservoir [SPE 36827]*. 1996. Richardson, TX, USA: Society of Petroleum Engineers (SPE).

22. Bourassa, K., et al. *A Case History of Casing Directional Drilling in the Norwegian Sector of the North Sea [SPE 112560]*. 2008. Richardson, TX 75083-3836, United States: Society of Petroleum Engineers (SPE).
23. Steppe Iii, R.J., L. Clark, and R. Johns. *Casing Drilling vs. Liner Drilling: Critical Analysis of an Operation in the Gulf of Mexico [SPE 96810]*. 2005. Richardson, TX 75083-3836, United States: Society of Petroleum Engineers (SPE).
24. Eidem, M., *Liner vs Casing Drilling*. 2007, Internal Presentation.
25. Eidem, M., *Drilling with Steerable 9 5/8" & 7" Liner*. 2008, Internal Presentation for D&W North.
26. Warren, T.M., *Drilling with Casing: What it Can and Can't Do for an Asset*. 2006, SPE Distinguished Lecturer Series.
27. Smith, K. *Close Tolerance Liner Drilling and Liner Requirements for Deepwater Applications*. in *Casing while Drilling Technical Conference*. 2004.
28. Strickler, R., et al., *Casing Directional Drilling with a Rotary Steerable System [SPE 92195]*. JPT, Journal of Petroleum Technology, 2005. **57**(11): p. 52-54.
29. Bourassa, K., et al. *Development, Testing, and Field Deployment of a Hydraulically Expanded Solid Liner Hanger in a Casing Directionally Drilled Well in Norway [SPE 112561]*. 2008. Richardson, TX 75083-3836, United States: Society of Petroleum Engineers (SPE).
30. Bourassa, K. and R. Watts. *Casing Directional Drilling (CDD) Experience: Eldfisk Bravo Offshore Norway*. in *WorldOil Casing While Drilling and Liner Drilling Technical Conference and Master Class*. 2007. Houston, Texas USA.
31. Mota, J., et al. *Rotary Liner Drilling Application in Deepwater Gulf of Mexico [SPE 99065]*. 2006. Richardson, TX 75083-3836, United States: Society of Petroleum Engineers (SPE).
32. Gordon, D., et al., *Underbalanced Drilling With Casing Evolution in the South Texas Vicksburg [SPE 84173]*. SPE Drilling and Completion, 2005. **20**(2): p. 86-93.
33. Warren, T.M., R. Tessari, and B. Houtchens, *Casing Drilling with Retrievable Drilling Assemblies [OTC 16564]*, in *Offshore Technology Conference*. 2004: Houston, Texas, USA.
34. Fontenot, K., R. Strickler, and P. Molina, *Improved Wellbore Stability Achieved with Casing Drilling Operations through Drilling Fluids "Smear Effect" [WOCWD-0431-04]*, in *World Oil 2004 Casing While Drilling Technical Conference*. 2004: Houston, Texas USA. p. 7.
35. Jevne, M., *Rotary Steerable Liner Drilling*, in *Department of Petroleum Engineering and Applied Geophysics*. 2007, NTNU: Trondheim. p. 105.
36. Eidem, M., *Steerable 9 5/8" & 7" Drilling Liner (SDL) - Info & Status*. 2008, Internal Presentation for Brage D&W.
37. Treviranus, J., *9 5/8" System Update Meeting*. 2007, Internal Presentation, 08.11.2007.
38. StatoilHydro, B.H.I., *Pictures from BETA Test Facility*. 2008.
39. Eidem, M., *Steerable Liner Drilling on Brage A-13A "Fensfjord"*, in *R&D Increased Oil Recovery Summit*. 2009: IB Centre, StatoilHydro Forus.
40. USA, V. *VAM HTF Description*. 2009 [cited 2009 25.05]; Available from: http://www.vamservices.com/images/flash/vamhtf/index.html.
41. Prideco, G. *H-Series Hi Torque Connection*. 2009 [cited 2009 04.06.2009]; Available from: http://www.grantprideco.com/drilling/products/drillpipe/hitorque.asp.
42. Lindvik, T.B., *Casing Directional Drilling with emphasis on Torque and Drag*, in *Department of Petroleum Engineering*. 2007, University of Stavanger. p. 280.

Appendix

Please note that not all of the simulation results are included in this appendix. The reason for this is that it would require an excessively long appendix. Instead, all the input data for the simulations have been listed, along with one example showing some of the results generated for one of the simulation cases.

For the manual calculations, most of these were done using spreadsheets. Examples have been included, in order to show how the calculations were performed for both torque, drag, and ECD. Due to space considerations, not all have been shown, however.

Appendix A: Simulation Input and Results

Simulation of the 6 5/8” DP 1000 m SLD System:

28.05.2009

TORQUE DRAG NORMAL ANALYSIS SUMMARY REPORT

Case Name :	SLD TDA Base Case	Date :	28.05.2009	Time :	16:42:19
Description :					
Company Name :	STATOILHYDRO SANDBOX	Project Name :	SDL test AIR		
Wellbore Name :	Wellbore #1	Project Description :			

CUSTOMER INFORMATION

Representative : Company : STATOILHYDRO SANDBOX Address :

WELL INFORMATION

Lease Name : Well Number : UWI Type : UWI :
Legal Description :

GENERAL/OFFSHORE CASE INFORMATION

Hole Depth :	3 944,00 m	Hole Depth (TVD) :	2 114,87 m	Well Type :	Platform	Reference Point :	Default Datum (copy) (copy)
Air Gap :	0,00 m	Water Depth :	30,48 m	Date :		Phase:	PROTOTYPE
Datum Description :	Mean Sea Level			Job Type / Description :			

OPERATING PARAMETERS

Cased Hole Friction :	HOLE SECTION DEFINED	**Analysis Options**	
Open Hole Friction :	HOLE SECTION DEFINED	Bending Stress Magnification :	ON
Measured Depth of Bit :	3 944,00 m	Sheave Friction Calculations :	OFF
Hoisting Equipment Weight :	15,00 tonne	Side Force Calculations :	Soft String
		Viscous Torque and Drag :	OFF

ADDITIONAL DATA

	Use	WOB /Overpull (tonne)	Torque at Bit (N-m)
Rotating on Bottom	Yes	10,00	10 000,0
Slide Drilling	No		
Back Reaming	No		
Rotating off Bottom	Yes		
	Use	**Speed (m/min)**	**RPM (rpm)**
Tripping In	Yes	18,29	0
Tripping Out	Yes	18,29	0

FLUID RHEOLOGY

FLUID: Fluid #1

Rheology Model : Bingham Plastic
Cement : No Spacer : No Foamed : No
Base Type : Oil Base Fluid : ESCAID110
Oil Water Ratio : 80,00 % / 20,00 % Salt : 10,00 % Reference : 21,11 °C Average Solids Gravity : 2,000 sg

Rheology Data

Temperature : 50,00 °C Pressure : 1,013 bar Base Density : 1,400 sg Ref. Fluid Properties : Yes
Plastic Viscosity : 20,00 mPa*s Yield Point : 5,000 Pa

DRILLSTRING

Type	Length (m)	Depth (m)	Body OD (in)	Body ID (in)	Stabilizer / Tool Joint Average Joint (m)	Stabilizer / Tool Joint Length (m)	Stabilizer / Tool Joint OD (in)	Stabilizer / Tool Joint ID (in)	Weight (ppf)	MTL	Grade	Class
Drill Pipe	2 923,910	2 923,91	6,625	5,901	9,14	0,482	8,000	4,250	31,54	CS_API 5D/7	S	P
Unknown	3,200	2 927,11	11,875	2,500					100,00	CS_API 5CT [XH]	13CR L-80 (1) [XH]	
Unknown	970,290	3 897,40	9,625	4,670					82,17	CS_API 5CT [XH]	13CR L-80 (1) [XH]	

28.05.2009

TORQUE DRAG NORMAL ANALYSIS SUMMARY REPORT

Case Name :	SLD TDA Base Case	Date :	28.05.2009
Description :		Time :	16:42:19
Company Name :	STATOILHYDRO SANDBOX	Project Name :	SDL test AIR
Wellbore Name :	Wellbore #1	Project Description :	

DRILLSTRING

Type	Length (m)	Depth (m)	Body OD (in)	Body ID (in)	Stabilizer / Tool Joint Average Joint (m)	Length (m)	OD (in)	ID (in)	Weight (ppf)	MTL	Grade	Class
Unknown	4,900	3 902,30	9,625	2,500					118,80	CS_API 5CT [XH]	13CR L-80 (1) [XH]	
Unknown	10,400	3 912,70	9,625	2,000					112,32	CS_API 5CT [XH]	13CR L-80 (1) [XH]	
Positive Displacement Motor	11,200	3 923,90	9,625	2,000					108,00	4145H MOD [SH]	4145H MOD [SH]	
Unknown	3,200	3 927,10	9,625	1,800					172,56	CS_API 5CT [XH]	13CR L-80 (1) [XH]	
Unknown	0,600	3 927,70	12,000	2,000					169,30	CS_API 5CT [XH]	13CR L-80 (1) [XH]	
MWD Tool	2,160	3 929,86	7,024	1,744					111,55	SS07 [SH]	SS07 [SH]	
MWD Tool	5,500	3 935,36	5,200	2,500					114,23	SS07 [SH]	SS07 [SH]	
Steerable Stabilizer	6,100	3 941,46	6,750	2,300		0,460	6,752		80,00	4145H MOD [SH]	4145H MOD [SH]	
Steerable Motor	2,200	3 943,66	6,760	1,500					130,00	ALLOY 25 (2) [SH]	ALLOY 25 (2) [SH]	
Polycrystalline Diamond Bit	0,340	3 944,00	8,500						60,48			

DRILLSTRING NOZZLES

Type	Component	Nozzles (32nd")	Percent Diverted Flow (%)	TFA (in²)
BIT	Polycrystalline Diamond Bit			0,591

28.05.2009

TORQUE DRAG NORMAL ANALYSIS SUMMARY REPORT

Case Name :	SLD TDA Base Case	Date :	28.05.2009
Description :		Time :	16:42:19
Company Name :	STATOILHYDRO SANDBOX	Project Name :	SDL test AIR
Wellbore Name :	Wellbore #1	Project Description :	

MECHANICAL LIMITATIONS

Overpull Margin During a Tripping Out Operation	100,97 tonne	using	90,00 % of yield
Minimum Weight on Bit to Sinusoidal Buckle during a rotating on bottom operation	41,77 tonne	at	2 531,01 m
Minimum Weight on Bit to Helical Buckle During a rotating on bottom operation	52,70 tonne	at	2 531,01 m

Explanation of buckling and stress codes

Buckling: ~ = No Buckling, S = Sinusoidal, H = Helical, L = Lockup Stress, T = Torque F = Fatigue, X = Exceeds 90,00% of yield, Y = Yield Reached

Load Condition	STF	B	Torque at the Rotary Table (N-m)	Total Windup with Bit Torque (revs)	Total Windup without Bit Torque (revs)	Measured Weight (tonne)	Total Stretch (m)	Axial Stress = 0 Distance from Surface (m)	Axial Stress = 0 Distance from Bit (m)	Neutral Point Distance from (m)	Neutral Point Distance from Bit (m)
TRIPPING OUT	~~~	~	0,0	0,0	0,0	191,71	2,46	2 923,91	1 020,09	3 944,00	0,00
ROTATING ON BOTTOM	~T~	~	68 981,1	10,2	8,2	83,72	0,69	2 923,91	1 020,09	2 774,07	1 169,93
TRIPPING IN	~~~	~	0,0	0,0	0,0	50,69	-0,03	2 567,87	1 376,13	3 944,00	0,00
ROTATING OFF BOTTOM	~~~	~	63 819,6	8,4	8,4	93,72	0,99	2 923,91	1 020,09	3 944,00	0,00

Example Results from the Simulation of the 6 5/8" DP 1000 m SLD System:

STATOILHYDRO SANDBOX

Well:Well #1
Wellbore:Wellbore #1
Design:Design #1
Case:SLD Hydraulics Base Case

Hydraulics Pressure: Pump Rate Fixed - ECD vs. Depth

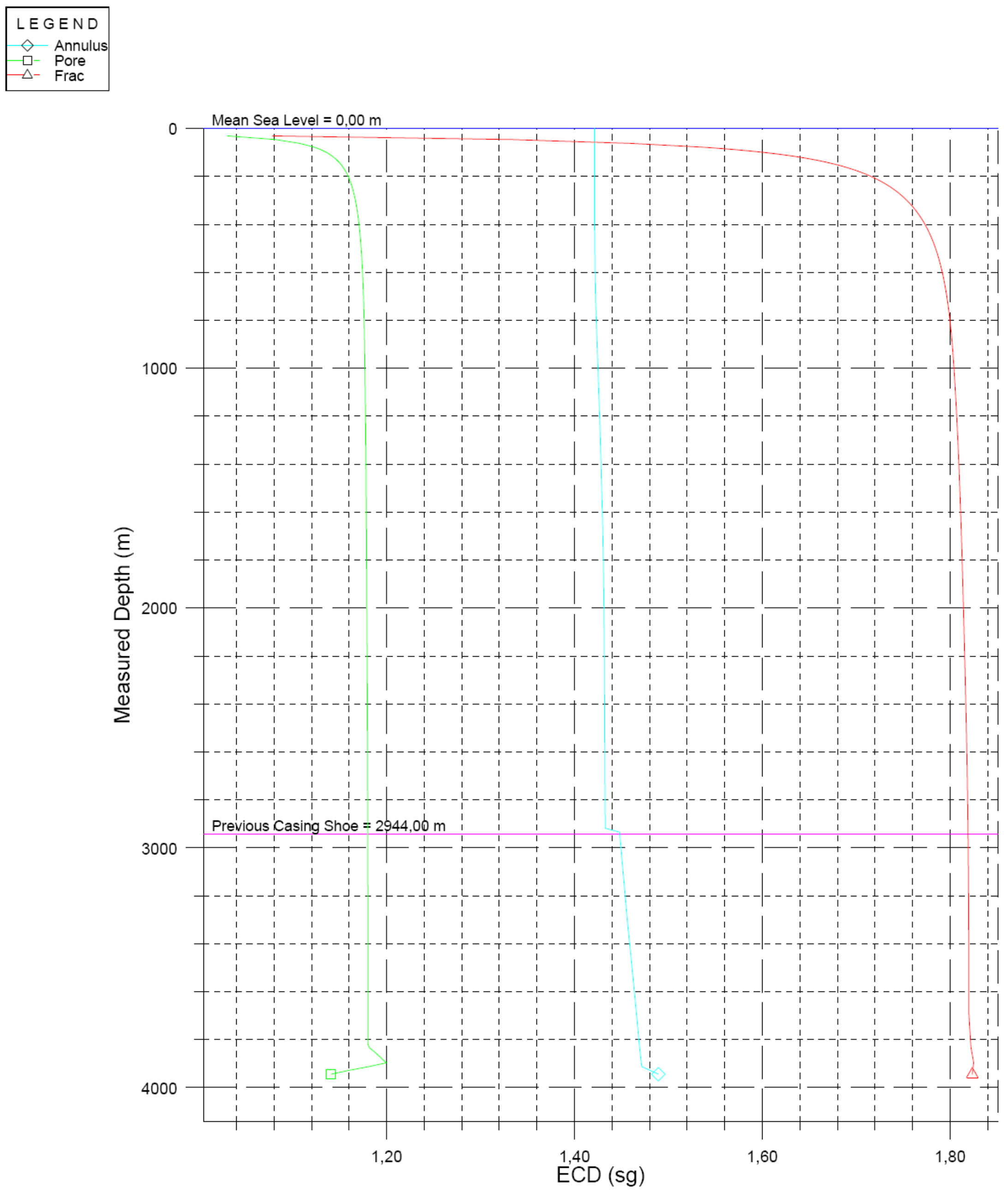

Friday, April 03, 2009 Tab1

STATOILHYDRO SANDBOX

Well:Well #1
Wellbore:Wellbore #1
Design:Design #1
Case:SLD Hydraulics Base Case

Hydraulics Cuttings Transport Operational

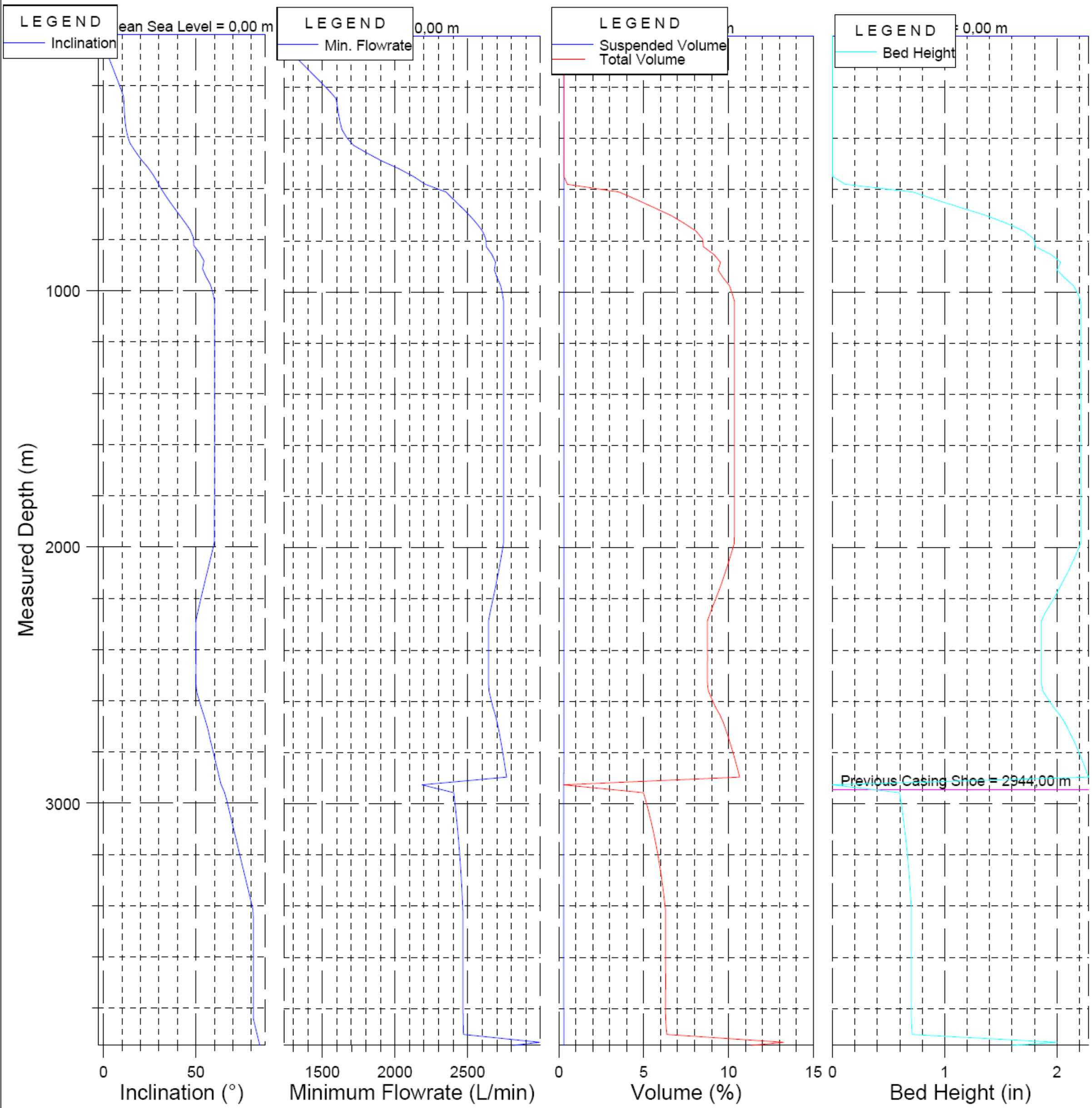

Rate of Penetration: 10,00 m/hr

Pump Rate: 2200,0 L/min

Friday, April 03, 2009 Tab1

STATOILHYDRO SANDBOX

Well:Well #1
Wellbore:Wellbore #1
Design:Design #1
Case:SLD TDA Base Case

Torque Drag Hook Load Chart

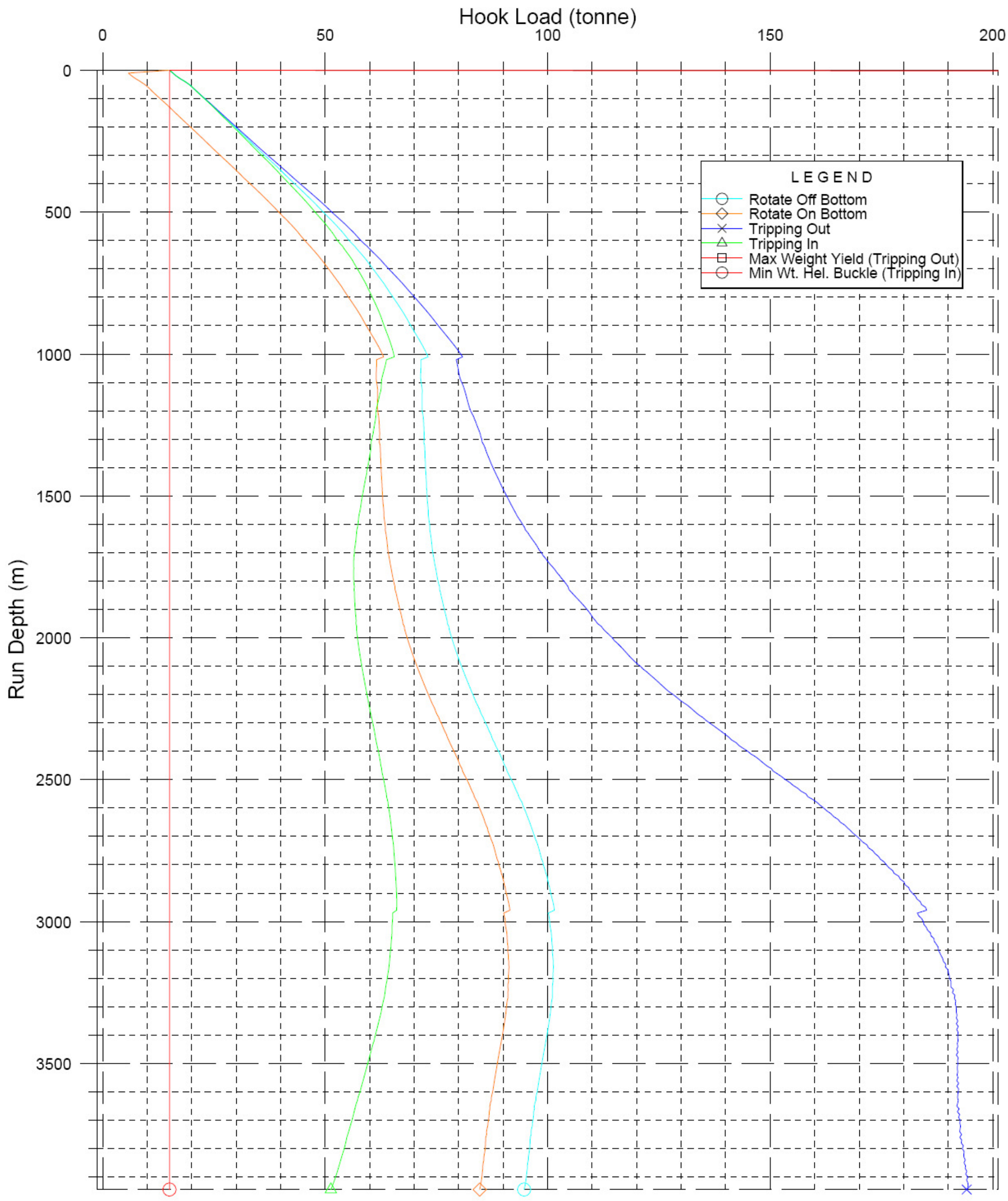

Friday, April 03, 2009 Tab1

STATOILHYDRO SANDBOX

Well:Well #1
Wellbore:Wellbore #1
Design:Design #1
Case:SLD TDA Base Case

Torque Drag Torque Point Chart

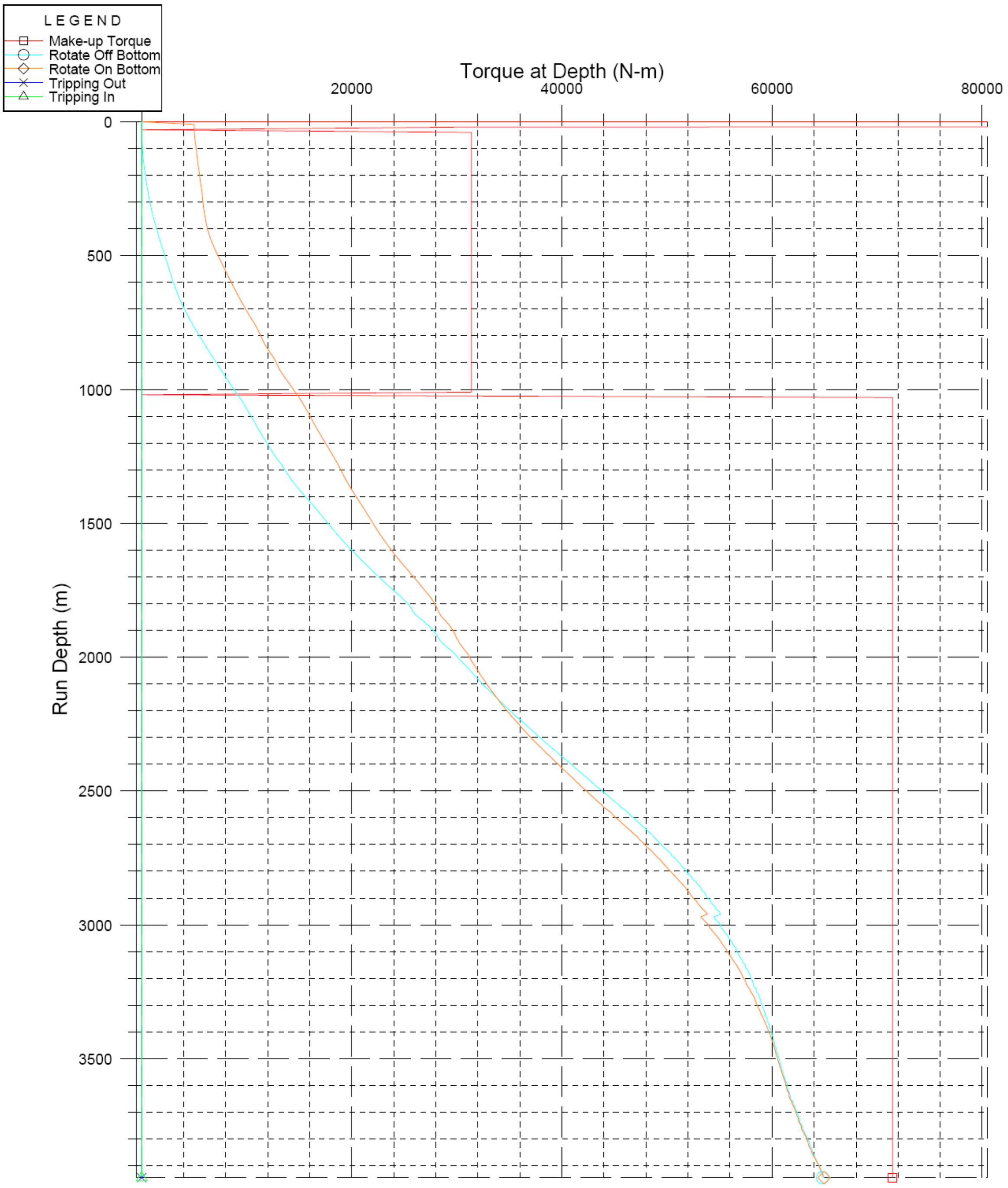

Friday, April 03, 2009 Tab1

Simulation of the 5 ½" DP 1000 m SLD System

28.05.2009

TORQUE DRAG NORMAL ANALYSIS SUMMARY REPORT

Case Name :	SLD TDA Base Case	Date :	28.05.2009	Time :	16:43:30
Description :					
Company Name :	STATOILHYDRO SANDBOX	Project Name :	SDL test AIR		
Wellbore Name :	Wellbore #1	Project Description :			

CUSTOMER INFORMATION

Representative :		Company :	STATOILHYDRO SANDBOX	Address :	

WELL INFORMATION

Lease Name :		Well Number :		UWI Type :		UWI :	
Legal Description :							

GENERAL/OFFSHORE CASE INFORMATION

Hole Depth :	3 944,00 m	Hole Depth (TVD) :	2 114,87 m	Well Type :	Platform	Reference Point :	Default Datum (copy) (copy)
Air Gap :	0,00 m	Water Depth :	30,48 m	Date :		Phase:	PROTOTYPE
Datum Description :	Mean Sea Level			Job Type / Description :			

OPERATING PARAMETERS

Cased Hole Friction :	HOLE SECTION DEFINED	**Analysis Options**	
Open Hole Friction :	HOLE SECTION DEFINED	Bending Stress Magnification :	ON
Measured Depth of Bit :	3 944,00 m	Sheave Friction Calculations :	OFF
Hoisting Equipment Weight :	15,00 tonne	Side Force Calculations :	Soft String
		Viscous Torque and Drag :	OFF

ADDITIONAL DATA

	Use	WOB /Overpull (tonne)	Torque at Bit (N-m)
Rotating on Bottom	Yes	10,00	10 000,0
Slide Drilling	No		
Back Reaming	No		
Rotating off Bottom	Yes		
	Use	**Speed (m/min)**	**RPM (rpm)**
Tripping In	Yes	18,29	0
Tripping Out	Yes	18,29	0

FLUID RHEOLOGY

FLUID: Fluid #1

Rheology Model :	Bingham Plastic						
Cement :	No			Spacer :	No	Foamed :	No
Base Type :	Oil			Base Fluid :	ESCAID110		
Oil Water Ratio :	80,00 % / 20,00 %	Salt :	10,00 %	Reference :	21,11 °C	Average Solids Gravity :	2,000 sg

Rheology Data

Temperature :	50,00 °C	Pressure :	1,013 bar	Base Density :	1,400 sg	Ref. Fluid Properties :	Yes
Plastic Viscosity :	20,00 mPa*s	Yield Point :	5,000 Pa				

DRILLSTRING

Type	Length (m)	Depth (m)	Body OD (in)	Body ID (in)	Stabilizer / Tool Joint Average Joint (m)	Stabilizer / Tool Joint Length (m)	Stabilizer / Tool Joint OD (in)	Stabilizer / Tool Joint ID (in)	Weight (ppf)	MTL	Grade	Class
Drill Pipe	2 923,910	2 923,91	5,500	4,670	9,14	0,457	7,500	3,000	28,87	CS_API 5D/7	S	1
Unknown	3,200	2 927,11	11,875	2,500					100,00	CS_API 5CT [XH]	13CR L-80 (1) [XH]	
Unknown	970,290	3 897,40	9,625	4,670					82,17	CS_API 5CT [XH]	13CR L-80 (1) [XH]	

28.05.2009

TORQUE DRAG NORMAL ANALYSIS SUMMARY REPORT

Case Name :	SLD TDA Base Case	Date :	28.05.2009	Time :	16:43:30
Description :					
Company Name :	STATOILHYDRO SANDBOX	Project Name :	SDL test AIR		
Wellbore Name :	Wellbore #1	Project Description :			

DRILLSTRING

Type	Length (m)	Depth (m)	Body OD (in)	Body ID (in)	Stabilizer / Tool Joint Average Joint (m)	Length (m)	OD (in)	ID (in)	Weight (ppf)	MTL	Grade	Class
Unknown	4,900	3 902,30	9,625	2,500					118,80	CS_API 5CT [XH]	13CR L-80 (1) [XH]	
Unknown	10,400	3 912,70	9,625	2,000					112,32	CS_API 5CT [XH]	13CR L-80 (1) [XH]	
Positive Displacement Motor	11,200	3 923,90	9,625	2,000					108,00	4145H MOD [SH]	4145H MOD [SH]	
Unknown	3,200	3 927,10	9,625	1,800					172,56	CS_API 5CT [XH]	13CR L-80 (1) [XH]	
Unknown	0,600	3 927,70	12,000	2,000					169,30	CS_API 5CT [XH]	13CR L-80 (1) [XH]	
MWD Tool	2,160	3 929,86	7,024	1,744					111,55	SS07 [SH]	SS07 [SH]	
MWD Tool	5,500	3 935,36	5,200	2,500					114,23	SS07 [SH]	SS07 [SH]	
Steerable Stabilizer	6,100	3 941,46	6,750	2,300		0,460	6,752		80,00	4145H MOD [SH]	4145H MOD [SH]	
Steerable Motor	2,200	3 943,66	6,760	1,500					130,00	ALLOY 25 (2) [SH]	ALLOY 25 (2) [SH]	
Polycrystalline Diamond Bit	0,340	3 944,00	8,500						60,48			

DRILLSTRING NOZZLES

Type	Component	Nozzles (32nd")	Percent Diverted Flow (%)	TFA (in²)
BIT	Polycrystalline Diamond Bit			0,591

28.05.2009

TORQUE DRAG NORMAL ANALYSIS SUMMARY REPORT

Case Name :	SLD TDA Base Case	Date :	28.05.2009	Time :	16:43:30
Description :					
Company Name :	STATOILHYDRO SANDBOX	Project Name :	SDL test AIR		
Wellbore Name :	Wellbore #1	Project Description :			

MECHANICAL LIMITATIONS

Overpull Margin During a Tripping Out Operation	160,92 tonne	using	90,00 % of yield
Minimum Weight on Bit to Sinusoidal Buckle during a rotating on bottom operation	31,61 tonne	at	2 923,91 m
Minimum Weight on Bit to Helical Buckle During a rotating on bottom operation	41,23 tonne	at	2 531,01 m

Explanation of buckling and stress codes

Buckling: ~ = No Buckling, S = Sinusoidal, H = Helical, L = Lockup Stress, T = Torque F = Fatigue, X = Exceeds 90,00% of yield, Y = Yield Reached

Load Condition	STF	B	Torque at the Rotary Table (N-m)	Total Windup with Bit Torque (revs)	Total Windup without Bit Torque (revs)	Measured Weight (tonne)	Total Stretch (m)	Axial Stress = 0 Distance from Surface (m)	Axial Stress = 0 Distance from Bit (m)	Neutral Point Distance from (m)	Neutral Point Distance from Bit (m)
TRIPPING OUT	~~~	~	0,0	0,0	0,0	181,70	2,42	2 923,91	1 020,09	3 944,00	0,00
ROTATING ON BOTTOM	~T~	~	64 314,1	15,7	12,5	77,96	0,57	2 869,13	1 074,87	2 763,04	1 180,96
TRIPPING IN	~~~	~	0,0	0,0	0,0	46,77	-0,17	2 172,39	1 771,61	3 944,00	0,00
ROTATING OFF BOTTOM	~~~	~	58 792,9	12,8	12,8	87,96	0,90	2 923,91	1 020,09	3 944,00	0,00

Simulation of the 6 5/8" DP 600 m SLD System

28.05.2009

TORQUE DRAG NORMAL ANALYSIS SUMMARY REPORT

Case Name :	600 m SLD TDA	Date :	28.05.2009	Time :	16:31:42
Description :					
Company Name :	STATOILHYDRO SANDBOX	Project Name :	SDL test AIR		
Wellbore Name :	Wellbore #1	Project Description :			

CUSTOMER INFORMATION

Representative :	Company : STATOILHYDRO SANDBOX	Address :

WELL INFORMATION

Lease Name :	Well Number :	UWI Type :	UWI :
Legal Description :			

GENERAL/OFFSHORE CASE INFORMATION

Hole Depth :	3 944,00 m	Hole Depth (TVD) :	2 114,87 m	Well Type :	Platform	Reference Point :	Default Datum (copy) (copy)
Air Gap :	0,00 m	Water Depth :	30,48 m	Date :		Phase:	PROTOTYPE
Datum Description :	Mean Sea Level			Job Type / Description :			

OPERATING PARAMETERS

Cased Hole Friction :	HOLE SECTION DEFINED	**Analysis Options**	
Open Hole Friction :	HOLE SECTION DEFINED	Bending Stress Magnification :	ON
Measured Depth of Bit :	3 944,00 m	Sheave Friction Calculations :	OFF
Hoisting Equipment Weight :	15,00 tonne	Side Force Calculations :	Soft String
		Viscous Torque and Drag :	OFF

ADDITIONAL DATA

	Use	WOB /Overpull (tonne)	Torque at Bit (N-m)
Rotating on Bottom	Yes	10,00	5 000,0
Slide Drilling	No		
Back Reaming	No		
Rotating off Bottom	Yes		
	Use	**Speed (m/min)**	**RPM (rpm)**
Tripping In	Yes	18,00	0
Tripping Out	Yes	18,29	0

FLUID RHEOLOGY

FLUID: Fluid #1

Rheology Model :	Bingham Plastic						
Cement :	No	Spacer :	No	Foamed :	No		
Base Type :	Oil	Base Fluid :	ESCAID110				
Oil Water Ratio :	80,00 % / 20,00 %	Salt :	10,00 %	Reference :	21,11 °C	Average Solids Gravity :	2,000 sg

Rheology Data

Temperature :	50,00 °C	Pressure :	1,013 bar	Base Density :	1,400 sg	Ref. Fluid Properties :	Yes
Plastic Viscosity :	20,00 mPa*s	Yield Point :	5,000 Pa				

DRILLSTRING

Type	Length (m)	Depth (m)	Body OD (in)	Body ID (in)	Stabilizer / Tool Joint Average Joint (m)	Stabilizer / Tool Joint Length (m)	Stabilizer / Tool Joint OD (in)	Stabilizer / Tool Joint ID (in)	Weight (ppf)	MTL	Grade	Class
Drill Pipe	3 323,910	3 323,91	6,625	5,901	9,14	0,482	8,000	4,250	31,54	CS_API 5D/7	S	P
Unknown	3,200	3 327,11	11,875	2,500					100,00	CS_API 5CT [XH]	13CR L-80 (1) [XH]	
Unknown	570,290	3 897,40	9,625	4,670					82,17	CS_API 5CT [XH]	13CR L-80 (1) [XH]	

28.05.2009

TORQUE DRAG NORMAL ANALYSIS SUMMARY REPORT

Case Name :	600 m SLD TDA	Date :	28.05.2009	Time :	16:31:42
Description :					
Company Name :	STATOILHYDRO SANDBOX	Project Name :	SDL test AIR		
Wellbore Name :	Wellbore #1	Project Description :			

DRILLSTRING

Type	Length (m)	Depth (m)	Body OD (in)	Body ID (in)	Stabilizer / Tool Joint Average Joint (m)	Stabilizer / Tool Joint Length (m)	Stabilizer / Tool Joint OD (in)	Stabilizer / Tool Joint ID (in)	Weight (ppf)	MTL	Grade	Class
Unknown	4,900	3 902,30	9,625	2,500					118,80	CS_API 5CT [XH]	13CR L-80 (1) [XH]	
Unknown	10,400	3 912,70	9,625	2,000					112,32	CS_API 5CT [XH]	13CR L-80 (1) [XH]	
Positive Displacement Motor	11,200	3 923,90	9,625	2,000					108,00	4145H MOD [SH]	4145H MOD [SH]	
Unknown	3,200	3 927,10	9,625	1,800					172,56	CS_API 5CT [XH]	13CR L-80 (1) [XH]	
Unknown	0,600	3 927,70	12,000	2,000					169,30	CS_API 5CT [XH]	13CR L-80 (1) [XH]	
MWD Tool	2,160	3 929,86	7,024	1,744					111,55	SS07 [SH]	SS07 [SH]	
MWD Tool	5,500	3 935,36	5,200	2,500					114,23	SS07 [SH]	SS07 [SH]	
Steerable Stabilizer	6,100	3 941,46	6,500	2,300		0,460	6,750		80,00	4145H MOD [SH]	4145H MOD [SH]	
Steerable Motor	2,200	3 943,66	6,750	1,500					130,00	ALLOY 25 (2) [SH]	ALLOY 25 (2) [SH]	
Polycrystalline Diamond Bit	0,340	3 944,00	8,500						60,48			

DRILLSTRING NOZZLES

Type	Component	Nozzles (32nd")	Percent Diverted Flow (%)	TFA (in^2)
BIT	Polycrystalline Diamond Bit			0,591

HOLE SECTION

Type	Section Depth (m)	Section Length (m)	Shoe Depth (m)	Tapered	Hole ID (in)	Drift (in)	Effective Hole Diameter (in)	Coefficient of Friction	Linear Capacity (L/m)	Volume Excess (%)
Casing	2 944,00	2 944,000	2 944,00		12,347	12,250	12,347	0,25	77,28	
Open Hole	3 944,00	1 000,000			12,250		12,250	0,30	76,04	0,00

Well bore friction factors not used (calibrated)

MECHANICAL LIMITATIONS

Overpull Margin During a Tripping Out Operation	117,00 tonne	using	90,00 % of yield
Minimum Weight on Bit to Sinusoidal Buckle during a rotating on bottom operation	35,35 tonne	at	3 278,25 m
Minimum Weight on Bit to Helical Buckle During a rotating on bottom operation	47,41 tonne	at	2 529,46 m

Explanation of buckling and stress codes

Buckling: ~ = No Buckling, S = Sinusoidal, H = Helical, L = Lockup Stress, T = Torque F = Fatigue, X = Exceeds 90,00% of yield, Y = Yield Reached

Load Condition	STF	B	Torque at the Rotary Table (N-m)	Total Windup with Bit Torque (revs)	Total Windup without Bit Torque (revs)	Measured Weight (tonne)	Total Stretch (m)	Axial Stress = 0 Distance from Surface (m)	Axial Stress = 0 Distance from Bit (m)	Neutral Point Distance from (m)	Neutral Point Distance from Bit (m)
TRIPPING OUT	~~~	~	0,0	0,0	0,0	175,74	2,20	3 323,91	620,09	3 944,00	0,00
ROTATING ON BOTTOM	~~~	~	56 432,4	8,7	7,6	78,39	0,50	3 000,23	943,77	2 533,14	1 410,86

28.05.2009

TORQUE DRAG NORMAL ANALYSIS SUMMARY REPORT

Case Name :	600 m SLD TDA	Date :	28.05.2009	Time :	16:31:42
Description :					
Company Name :	STATOILHYDRO SANDBOX	Project Name :	SDL test AIR		
Wellbore Name :	Wellbore #1	Project Description :			

Explanation of buckling and stress codes

Buckling: ~ = No Buckling, S = Sinusoidal, H = Helical, L = Lockup Stress, T = Torque F = Fatigue, X = Exceeds 90,00% of yield, Y = Yield Reached

Load Condition	STF	B	Torque at the Rotary Table (N-m)	Total Windup with Bit Torque (revs)	Total Windup without Bit Torque (revs)	Measured Weight (tonne)	Total Stretch (m)	Axial Stress = 0 Distance from Surface (m)	Axial Stress = 0 Distance from Bit (m)	Neutral Point Distance from (m)	Neutral Point Distance from Bit (m)
TRIPPING IN	~~~	~	0,0	0,0	0,0	48,39	-0,15	2 435,33	1 508,67	3 944,00	0,00
ROTATING OFF BOTTOM	~~~	~	56 150,8	7,7	7,7	88,39	0,84	3 323,91	620,09	3 944,00	0,00

Simulation of the 6 5/8" DP 300 m SLD System

28.05.2009

TORQUE DRAG NORMAL ANALYSIS SUMMARY REPORT

Case Name :	300 m SLD TDA	Date :	28.05.2009	Time :	16:33:32
Description :					
Company Name :	STATOILHYDRO SANDBOX	Project Name :	SDL test AIR		
Wellbore Name :	Wellbore #1	Project Description :			

CUSTOMER INFORMATION

Representative : Company : STATOILHYDRO SANDBOX Address :

WELL INFORMATION

Lease Name : Well Number : UWI Type : UWI :
Legal Description :

GENERAL/OFFSHORE CASE INFORMATION

Hole Depth :	3 944,00 m	Hole Depth (TVD) :	2 114,87 m	Well Type :	Platform	Reference Point :	Default Datum (copy) (copy)
Air Gap :	0,00 m	Water Depth :	30,48 m	Date :		Phase:	PROTOTYPE
Datum Description :	Mean Sea Level			Job Type / Description :			

OPERATING PARAMETERS

Cased Hole Friction :	HOLE SECTION DEFINED	**Analysis Options**	
Open Hole Friction :	HOLE SECTION DEFINED	Bending Stress Magnification :	ON
Measured Depth of Bit :	3 944,00 m	Sheave Friction Calculations :	OFF
Hoisting Equipment Weight :	15,00 tonne	Side Force Calculations :	Soft String
		Viscous Torque and Drag :	OFF

ADDITIONAL DATA

	Use	WOB /Overpull (tonne)	Torque at Bit (N-m)
Rotating on Bottom	Yes	10,00	5 000,0
Slide Drilling	No		
Back Reaming	No		
Rotating off Bottom	Yes		
	Use	**Speed (m/min)**	**RPM (rpm)**
Tripping In	Yes	18,00	0
Tripping Out	Yes	18,29	0

FLUID RHEOLOGY

FLUID: Fluid #1

Rheology Model : Bingham Plastic
Cement : No Spacer : No Foamed : No
Base Type : Oil Base Fluid : ESCAID110
Oil Water Ratio : 80,00 % / 20,00 % Salt : 10,00 % Reference : 21,11 °C Average Solids Gravity : 2,000 sg

Rheology Data

Temperature : 50,00 °C Pressure : 1,013 bar Base Density : 1,400 sg Ref. Fluid Properties : Yes
Plastic Viscosity : 20,00 mPa*s Yield Point : 5,000 Pa

DRILLSTRING

Type	Length (m)	Depth (m)	Body OD (in)	Body ID (in)	Stabilizer / Tool Joint Average Joint (m)	Stabilizer / Tool Joint Length (m)	Stabilizer / Tool Joint OD (in)	Stabilizer / Tool Joint ID (in)	Weight (ppf)	MTL	Grade	Class
Drill Pipe	3 623,910	3 623,91	6,625	5,901	9,14	0,482	8,000	4,250	31,54	CS_API 5D/7	S	P
Unknown	3,200	3 627,11	11,875	2,500					100,00	CS_API 5CT [XH]	13CR L-80 (1) [XH]	
Unknown	270,290	3 897,40	9,625	4,670					82,17	CS_API 5CT [XH]	13CR L-80 (1) [XH]	

28.05.2009

TORQUE DRAG NORMAL ANALYSIS SUMMARY REPORT

Case Name :	300 m SLD TDA	Date :	28.05.2009	Time :	16:33:32
Description :					
Company Name :	STATOILHYDRO SANDBOX	Project Name :	SDL test AIR		
Wellbore Name :	Wellbore #1	Project Description :			

DRILLSTRING

Type	Length (m)	Depth (m)	Body		Stabilizer / Tool Joint				Weight (ppf)	MTL	Grade	Class
			OD (in)	ID (in)	Average Joint (m)	Length (m)	OD (in)	ID (in)				
Unknown	4,900	3 902,30	9,625	2,500					118,80	CS_API 5CT [XH]	13CR L-80 (1) [XH]	
Unknown	10,400	3 912,70	9,625	2,000					112,32	CS_API 5CT [XH]	13CR L-80 (1) [XH]	
Positive Displacement Motor	11,200	3 923,90	9,625	2,000					108,00	4145H MOD [SH]	4145H MOD [SH]	
Unknown	3,200	3 927,10	9,625	1,800					172,56	CS_API 5CT [XH]	13CR L-80 (1) [XH]	
Unknown	0,600	3 927,70	12,000	2,000					169,30	CS_API 5CT [XH]	13CR L-80 (1) [XH]	
MWD Tool	2,160	3 929,86	7,024	1,744					111,55	SS07 [SH]	SS07 [SH]	
MWD Tool	5,500	3 935,36	5,200	2,500					114,23	SS07 [SH]	SS07 [SH]	
Steerable Stabilizer	6,100	3 941,46	6,500	2,300		0,460	6,750		80,00	4145H MOD [SH]	4145H MOD [SH]	
Steerable Motor	2,200	3 943,66	6,750	1,500					130,00	ALLOY 25 (2) [SH]	ALLOY 25 (2) [SH]	
Polycrystalline Diamond Bit	0,340	3 944,00	8,500						60,48			

DRILLSTRING NOZZLES

Type	Component	Nozzles (32nd")	Percent Diverted Flow (%)	TFA (in²)
BIT	Polycrystalline Diamond Bit			0,591

HOLE SECTION

Type	Section Depth (m)	Section Length (m)	Shoe Depth (m)	Tapered	Hole ID (in)	Drift (in)	Effective Hole Diameter (in)	Coefficient of Friction	Linear Capacity (L/m)	Volume Excess (%)
Casing	2 944,00	2 944,000	2 944,00		12,347	12,250	12,347	0,25	77,28	
Open Hole	3 944,00	1 000,000			12,250		12,250	0,30	76,04	0,00

Well bore friction factors not used (calibrated)

MECHANICAL LIMITATIONS

Overpull Margin During a Tripping Out Operation	123,19 tonne	using	90,00 % of yield
Minimum Weight on Bit to Sinusoidal Buckle during a rotating on bottom operation	25,07 tonne	at	3 623,91 m
Minimum Weight on Bit to Helical Buckle During a rotating on bottom operation	37,62 tonne	at	3 623,91 m

Explanation of buckling and stress codes

Buckling: ~ = No Buckling, S = Sinusoidal, H = Helical, L = Lockup Stress, T = Torque F = Fatigue, X = Exceeds 90,00% of yield, Y = Yield Reached

Load Condition	STF	B	Torque at the Rotary Table (N-m)	Total Windup with Bit Torque (revs)	Total Windup without Bit Torque (revs)	Measured Weight (tonne)	Total Stretch (m)	Axial Stress = 0 Distance from Surface (m)	Axial Stress = 0 Distance from Bit (m)	Neutral Point Distance from (m)	Neutral Point Distance from Bit (m)
TRIPPING OUT	~~~	~	0,0	0,0	0,0	169,39	2,07	3 623,91	320,09	3 944,00	0,00
ROTATING ON BOTTOM	~~~	~	51 904,2	8,1	6,9	77,60	0,44	2 922,80	1 021,20	2 500,39	1 443,61

28.05.2009

TORQUE DRAG NORMAL ANALYSIS SUMMARY REPORT

Case Name :	300 m SLD TDA	Date :	28.05.2009	Time :	16:33:32
Description :					
Company Name :	STATOILHYDRO SANDBOX	Project Name :	SDL test AIR		
Wellbore Name :	Wellbore #1	Project Description :			

Explanation of buckling and stress codes

Buckling: ~ = No Buckling, S = Sinusoidal, H = Helical, L = Lockup Stress, T = Torque F = Fatigue, X = Exceeds 90,00% of yield, Y = Yield Reached

Load Condition	STF	B	Torque at the Rotary Table (N-m)	Total Windup with Bit Torque (revs)	Total Windup without Bit Torque (revs)	Measured Weight (tonne)	Total Stretch (m)	Axial Stress = 0 Distance from Surface (m)	Axial Stress = 0 Distance from Bit (m)	Neutral Point Distance from (m)	Neutral Point Distance from Bit (m)
TRIPPING IN	~~~	~	0,0	0,0	0,0	50,60	-0,11	2 506,49	1 437,51	3 944,00	0,00
ROTATING OFF BOTTOM	~~~	~	51 609,6	7,0	7,0	87,60	0,80	3 623,91	320,09	3 944,00	0,00

Simulation of the Conventional 12 ¼" Drilling System

28.05.2009

TORQUE DRAG NORMAL ANALYSIS SUMMARY REPORT

Case Name :	Conventional TDA	Date :	28.05.2009	Time :	16:25:10
Description :					
Company Name :	STATOILHYDRO SANDBOX	Project Name :	SDL test AIR		
Wellbore Name :	Wellbore #1	Project Description :			

CUSTOMER INFORMATION

Representative : Company : STATOILHYDRO SANDBOX Address :

WELL INFORMATION

Lease Name : Well Number : UWI Type : UWI :
Legal Description :

GENERAL/OFFSHORE CASE INFORMATION

Hole Depth :	3 944,00 m	Hole Depth (TVD) :	2 114,87 m	Well Type :	Platform	Reference Point :	Default Datum (copy) (copy)
Air Gap :	0,00 m	Water Depth :	30,48 m	Date :		Phase:	PROTOTYPE
Datum Description :	Mean Sea Level			Job Type / Description :			

OPERATING PARAMETERS

Cased Hole Friction :	HOLE SECTION DEFINED	**Analysis Options**	
Open Hole Friction :	HOLE SECTION DEFINED	Bending Stress Magnification :	ON
Measured Depth of Bit :	3 944,00 m	Sheave Friction Calculations :	OFF
Hoisting Equipment Weight :	15,00 tonne	Side Force Calculations :	Soft String
		Viscous Torque and Drag :	OFF

ADDITIONAL DATA

	Use	WOB /Overpull (tonne)	Torque at Bit (N-m)
Rotating on Bottom	Yes	12,00	10 000,0
Slide Drilling	No		
Back Reaming	No		
Rotating off Bottom	Yes		
	Use	Speed (m/min)	RPM (rpm)
Tripping In	Yes	18,29	0
Tripping Out	Yes	18,29	0

FLUID RHEOLOGY

FLUID: Fluid #1

Rheology Model : Bingham Plastic

Cement :	No	Spacer :	No	Foamed :	No
Base Type :	Oil	Base Fluid :	ESCAID110		
Oil Water Ratio :	80,00 % / 20,00 % Salt : 10,00 %	Reference :	21,11 °C	Average Solids Gravity :	2,000 sg

Rheology Data

Temperature :	50,00 °C	Pressure :	1,013 bar	Base Density :	1,400 sg	Ref. Fluid Properties :	Yes
Plastic Viscosity :	20,00 mPa*s	Yield Point :	5,000 Pa				

DRILLSTRING

Type	Length (m)	Depth (m)	Body OD (in)	Body ID (in)	Stabilizer / Tool Joint Average Joint (m)	Stabilizer / Tool Joint Length (m)	Stabilizer / Tool Joint OD (in)	Stabilizer / Tool Joint ID (in)	Weight (ppf)	MTL	Grade	Class
Drill Pipe	3 782,670	3 782,67	5,500	4,670	9,14	0,457	7,031	3,000	28,87	CS_API 5D/7	S	P
Heavy Weight Drill Pipe	83,740	3 866,41	5,500	3,375	9,14	1,219	7,250	3,313	60,10	CS_1340 MOD	1340 MOD	
Cross Over	1,120	3 867,53	8,000	2,800					147,00	CS_API 5D/7	4145H MOD	

28.05.2009

TORQUE DRAG NORMAL ANALYSIS SUMMARY REPORT

Case Name :	Conventional TDA	Date :	28.05.2009	Time :	16:25:10
Description :					
Company Name :	STATOILHYDRO SANDBOX	Project Name :	SDL test AIR		
Wellbore Name :	Wellbore #1	Project Description :			

DRILLSTRING

Type	Length (m)	Depth (m)	Body OD (in)	Body ID (in)	Stabilizer / Tool Joint Average Joint (m)	Stabilizer / Tool Joint Length (m)	Stabilizer / Tool Joint OD (in)	Stabilizer / Tool Joint ID (in)	Weight (ppf)	MTL	Grade	Class
Drill Collar	27,660	3 895,19	8,000	2,810					157,37	CS_API 5D/7	4145H MOD (2)	
Mechanical Jar	9,300	3 904,49	8,000	2,810					138,40	15-15LC MOD (1) [SH]	15-15LC MOD (1) [SH]	
Drill Collar	9,190	3 913,68	8,000	2,810					157,37	CS_API 5D/7	4145H MOD (2)	
Integral Blade Stabilizer	2,340	3 916,02	8,062	2,875		0,305	8,453		93,72	CS_API 5D/7	4145H MOD	
Drill Collar	3,060	3 919,08	8,062	2,875					154,33	CS_API 5D/7	4145H MOD (2)	
Cross Over	2,390	3 921,47	8,250	2,875					147,00	CS_API 5D/7	4145H MOD	
MWD Tool	3,100	3 924,57	8,062	2,375					141,11	15-15LC MOD (1) [SH]	15-15LC MOD (1) [SH]	
Integral Blade Stabilizer	1,200	3 925,77	8,062	2,375		0,305	12,203		169,06	CS_API 5D/7	4145H MOD	
Logging While Drilling	7,720	3 933,49	8,000	2,375					141,11	15-15LC MOD (1) [SH]	15-15LC MOD (1) [SH]	
Non-Mag Crossover Sub	0,570	3 934,06	8,000	2,375					147,00	SS_15-15LC	15-15LC MOD (2)	
Non-Mag Crossover Sub	2,790	3 936,85	8,000	2,375					147,00	SS_15-15LC	15-15LC MOD (2)	
Near Bit Stabilizer	0,810	3 937,66	8,000	2,375		0,305	12,203		154,38	CS_API 5D/7	4145H MOD	
MWD Tool	5,800	3 943,46	9,625	2,375					95,96	15-15LC MOD (1) [SH]	15-15LC MOD (1) [SH]	
Polycrystalline Diamond Bit	0,540	3 944,00	12,250						462,31			

DRILLSTRING NOZZLES

Type	Component	Nozzles (32nd")		Percent Diverted Flow (%)	TFA (in²)
BIT	Polycrystalline Diamond Bit	2 X 16	4 X 20		1,620

HOLE SECTION

Type	Section Depth (m)	Section Length (m)	Shoe Depth (m)	Tapered	Hole ID (in)	Drift (in)	Effective Hole Diameter (in)	Coefficient of Friction	Linear Capacity (L/m)	Volume Excess (%)
Casing	2 944,00	2 944,000	2 944,00		12,347	12,250	12,347		77,28	
Open Hole	3 944,00	1 000,000			12,250		12,294	0,30	76,59	0,93

Well bore friction factors not used (calibrated)

28.05.2009

TORQUE DRAG NORMAL ANALYSIS SUMMARY REPORT

Case Name :	Conventional TDA	Date :	28.05.2009	Time :	16:25:10
Description :					
Company Name :	STATOILHYDRO SANDBOX	Project Name :	SDL test AIR		
Wellbore Name :	Wellbore #1	Project Description :			

Explanation of buckling and stress codes

Buckling: ~ = No Buckling, S = Sinusoidal, H = Helical, L = Lockup Stress, T = Torque F = Fatigue, X = Exceeds 90,00% of yield, Y = Yield Reached

Load Condition	STF	B	Torque at the Rotary Table (N-m)	Total Windup with Bit Torque (revs)	Total Windup without Bit Torque (revs)	Measured Weight (tonne)	Total Stretch (m)	Axial Stress = 0 Distance from Surface (m)	Axial Stress = 0 Distance from Bit (m)	Neutral Point Distance from (m)	Neutral Point Distance from Bit (m)
TRIPPING OUT	~~~	~	0,0	0,0	0,0	103,10	1,35	3 583,40	360,60	3 944,00	0,00
ROTATING ON BOTTOM	~~~	~	24 053,7	9,5	5,3	78,08	0,37	2 462,07	1 481,93	2 745,78	1 198,22
TRIPPING IN	~~~	~	0,0	0,0	0,0	74,92	0,28	2 352,18	1 591,82	3 944,00	0,00
ROTATING OFF BOTTOM	~~~	~	12 932,0	5,0	5,0	90,08	0,86	2 938,17	1 005,83	3 944,00	0,00

Appendix B: Manual Calculation Examples

Example of the manual calculations for contact friction: (6 5/8" drillpipe and 1000 m liner))

Section 10	Build-up section	
Top Length	3840 mMD	2102 mTVD
Bottom Length	3944 mMD	2114 mTVD
Top Inclination	81 °	1.41 rad
Bottom Inclination	84 °	1.47 rad
Top Azimuth	85 °	1.48 rad
Bottom Azimuth	85 °	1.48 rad
Average DLS	.87 °/30 m	
Radius	1986 m	
Friction Factor	0.3	
Section length	104 mMD	12 mTVD
Average weight	117.5 kg/m	
WOB	10000 N	
TOB	10000 Nm	
Total weight	-5.3 N	
Force at top, hoist	61853.4 N	
Force at top, lower	60905. N	

Section 9	Straight Inclined	
Top Length	3420 mMD	2036 mTVD
Bottom Length	3840 mMD	2102 mTVD
Top Inclination	81 °	1.41 rad
Bottom Inclination	81 °	1.41 rad
Top Azimuth	85 °	1.48 rad
Bottom Azimuth	85 °	1.48 rad
Average DLS	. °/30 m	
Radius	#DIV/0!	
Friction Factor	0.3	
Section length	420 mMD	66 mTVD
Average weight	100.47 kg/m	
Total weight	64761.8 N	
Force at top, hoist	249276.2 N	
Force at top, lower	3001.667155	

Section 8	Build-up	
Top Length	2550 mMD	1686 mTVD
Bottom Length	3420 mMD	2036 mTVD
Top Inclination	50 °	.87 rad
Bottom Inclination	81 °	1.41 rad
Top Azimuth	85 °	1.48 rad
Bottom Azimuth	85 °	1.48 rad
Average DLS	1.07 °/30 m	
Radius	1608 m	
Friction Factor	0.28	
Section length	870 mMD	350 mTVD
Average weight	73.95 kg/m	
Total weight	318870. N	
Force at top, hoist	734711.3 N	
Force at top, lower	392312.7 N	

Section 7	Straight Inclined	
Top Length	2280 mMD	1512 mTVD
Bottom Length	2550 mMD	1686 mTVD
Top Inclination	50 °	.87 rad
Bottom Inclination	50 °	.87 rad
Top Azimuth	85 °	1.48 rad
Bottom Azimuth	85 °	1.48 rad
Average DLS	. °/30 m	
Radius	#DIV/0!	
Friction Factor	0.25	
Section length	270 mMD	174 mTVD
Average weight	38.57 kg/m	
Total weight	384529.3 N	
Force at top, hoist	819934.3 N	
Force at top, lower	438410.2438	

Section 6	Drop-off	
Top Length	1980 mMD	1340 mTVD
Bottom Length	2280 mMD	1512 mTVD
Top Inclination	60 °	1.05 rad
Bottom Inclination	50 °	.87 rad
Top Azimuth	85 °	1.48 rad
Bottom Azimuth	85 °	1.48 rad
Average DLS	1. °/30 m	
Radius	1719 m	
Friction Factor	0.25	
Section length	300 mMD	172 mTVD
Average weight	38.57 kg/m	
Total weight	449549.2 N	
Force at top, hoist	951772.6 N	
Force at top, lower	505979.2 N	

Section 5	Straight Inclined	
Top Length	1950 mMD	1325 mTVD
Bottom Length	1980 mMD	1340 mTVD
Top Inclination	60 °	1.05 rad
Bottom Inclination	60 °	1.05 rad
Top Azimuth	85 °	1.48 rad
Bottom Azimuth	85 °	1.48 rad
Average DLS	. °/30 m	
Radius	#DIV/0!	
Friction Factor	0.25	
Section length	30 mMD	15 mTVD
Average weight	38.57 kg/m	
Total weight	455224.2 N	
Force at top, hoist	959904.9 N	
Force at top, lower	509196.7835	

Section 4	Left-side Bend	
Top Length	1050 mMD	875 mTVD
Bottom Length	1950 mMD	1325 mTVD
Top Inclination	60 °	1.05 rad
Bottom Inclination	60 °	1.05 rad
Top Azimuth	201 °	3.51 rad
Bottom Azimuth	85 °	1.48 rad
Average DLS	3.87 °/30 m	
Radius	444 m	
Friction Factor	0.25	
Section length	900 mMD	450 mTVD
Average weight	38.57 kg/m	
Total weight	625503.2 N	
Force at top, hoist	1600091. N	
Force at top, lower	284011.7486	

Section 3	Straight Inclined	
Top Length	1030 mMD	865 mTVD
Bottom Length	1050 mMD	875 mTVD
Top Inclination	60 °	1.05 rad
Bottom Inclination	60 °	1.05 rad
Top Azimuth	201 °	3.51 rad
Bottom Azimuth	201 °	3.51 rad
Average DLS	. °/30 m	
Radius	#DIV/0!	
Friction Factor	0.25	
Section length	20 mMD	10 mTVD
Average weight	38.57 kg/m	
Total weight	629309.3 N	
Force at top, hoist	1605545.1 N	
Force at top, lower	286169.7058	

Section 2	Build-up	
Top Length	36 mMD	36 mTVD
Bottom Length	1030 mMD	865 mTVD
Top Inclination	°	. rad
Bottom Inclination	60 °	1.05 rad
Top Azimuth	201 °	3.51 rad
Bottom Azimuth	201 °	3.51 rad
Average DLS	1.81 °/30 m	
Radius	949 m	
Friction Factor	0.25	
Section length	994 mMD	829 mTVD
Average weight	38.57 kg/m	
Total weight	943062.6 N	
Force at top, hoist	2490113.4 N	
Force at top, lower	601343.6 N	

Section 1	Straight Vertical	
Top Length	mMD	mTVD
Bottom Length	36 mMD	36 mTVD
Top Inclination	°	. rad
Bottom Inclination	°	. rad
Top Azimuth	201 °	3.51 rad
Bottom Azimuth	201 °	3.51 rad
Average DLS	. °/30 m	
Radius	#DIV/0!	
Friction Factor	0.25	
Section length	36 mMD	36 mTVD
Average weight	38.57 kg/m	
Total weight	**956656.1 N**	
Force at top, hoist	2503706.8 N	
	2504 kN	
	255 tonnes	
Force at top, lower	614937. N	
	615 kN	
	62.685 tonnes	

Example of the manual calculations for torque – Liner: (6 5/8" drillpipe and 1000 m liner)

Mud Density	1.4 s.g.	Flow rate	2000 l/min	.03333 m^3/s	Mass flow rate	46.667 kg/s	
Buyoancy factor	0.821656051	Nozzle area	.591 in^2	.00038129 m^2	Nozzle Force	4079.72 N	4.08 kN
		Nozzle velocity	87.423 m/s				

Section 10	Build-up section	
Top Length	3840 mMD	2102 mTVD
Bottom Length	3944 mMD	2114 mTVD
Top Inclination	81 °	1.41 rad
Bottom Inclination	84 °	1.47 rad
Top Azimuth	85 °	1.48 rad
Bottom Azimuth	85 °	1.48 rad
Average DLS	.87 °/30 m	
Radius	1986 m	
Friction Factor	0.3	
Section length	104 mMD	12 mTVD
Average weight	65.4 kg/m	
WOB	N	
TOB	Nm	
Total weight	7834.1 N	
Force at top, hoist	28774.5 N	
Force at top, lower	28334.7 N	
Static torque	7285.2 Nm	

Section 9	Straight Inclined	
Top Length	3420 mMD	2036 mTVD
Bottom Length	3840 mMD	2102 mTVD
Top Inclination	81 °	1.41 rad
Bottom Inclination	81 °	1.41 rad
Top Azimuth	85 °	1.48 rad
Bottom Azimuth	85 °	1.48 rad
Average DLS	. °/30 m	
Radius	#DIV/0!	
Friction Factor	0.3	
Section length	420 mMD	66 mTVD
Average weight	65.4 kg/m	
Total weight	49994.4 N	
Force at top, hoist	150777.7 N	
Force at top, lower	-9357.584179	
Static torque	17045.6 Nm	

Section 8	Build-up	
Top Length	2944 mMD	1899 mTVD
Bottom Length	3420 mMD	2036 mTVD
Top Inclination	66 °	1.15 rad
Bottom Inclination	81 °	1.41 rad
Top Azimuth	85 °	1.48 rad
Bottom Azimuth	85 °	1.48 rad
Average DLS	.95 °/30 m	
Radius	1818 m	
Friction Factor	0.30	
Section length	476 mMD	137 mTVD
Average weight	65.4 kg/m	
Total weight	137664.2 N	
Force at top, hoist	343732.7 N	
Force at top, lower	158511.4 N	
Static torque	50003.1 Nm	

Static torque	**50. kNm**

Example of the manual calculations for torque – Drillpipe: (6 5/8" drillpipe and 1000 m liner)

Mud Density	1.4 s.g.		Flow rate	2000 l/min	.03333 m^3/s	Mass flow rate	46.667 kg/s	
Buyoancy factor	0.821656051		Nozzle area	.591 in^2	.00038129 m^2	Nozzle Force	4079.72 N	4.08 kN
			Nozzle velocity	87.423 m/s				

NO TORQUE INCREASE HERE AS THE LINER ROTATES WITH THE SAME RPM AS THE DRILLSTRING.

Section 10	Build-up section	
Top Length	3912 mMD	2112 mTVD
Bottom Length	3944 mMD	2114 mTVD
Top Inclination	84 °	1.46 rad
Bottom Inclination	84 °	1.47 rad
Top Azimuth	85 °	1.48 rad
Bottom Azimuth	85 °	1.48 rad
Average DLS	.47 °/30 m	
Radius	3667 m	
Friction Factor	0.3	
Section length	32 mMD	2 mTVD
Average weight	35.28 kg/m	
WOB	N	
TOB	Nm	
Total weight	-3387.6 N	
Force at top, hoist	4513.9 N	
Force at top, lower	4502.2 N	
Static torque	692.1 Nm	

Section 9	Straight Inclined	
Top Length	3420 mMD	2036 mTVD
Bottom Length	3840 mMD	2102 mTVD
Top Inclination	81 °	1.41 rad
Bottom Inclination	81 °	1.41 rad
Top Azimuth	85 °	1.48 rad
Bottom Azimuth	85 °	1.48 rad
Average DLS	. °/30 m	
Radius	#DIV/0!	
Friction Factor	0.3	
Section length	420 mMD	66 mTVD
Average weight	35.28 kg/m	
Total weight	19352.2 N	
Force at top, hoist	70318.3 N	
Force at top, lower	-15827.76103	
Static torque	692.1 Nm	

Section 8	Build-up	
Top Length	2550 mMD	1686 mTVD
Bottom Length	2944 mMD	1898 mTVD
Top Inclination	65 °	1.13 rad
Bottom Inclination	81 °	1.41 rad
Top Azimuth	85 °	1.48 rad
Bottom Azimuth	85 °	1.48 rad
Average DLS	1.26 °/30 m	
Radius	1368 m	
Friction Factor	0.25	
Section length	394 mMD	212 mTVD
Average weight	38.57 kg/m	
Total weight	99637.8 N	
Force at top, hoist	157782.2 N	
Force at top, lower	61112.8 N	
Static torque	9204.5 Nm	

Section 7	Straight Inclined	
Top Length	2280 mMD	1512 mTVD
Bottom Length	2550 mMD	1686 mTVD
Top Inclination	50 °	.87 rad
Bottom Inclination	50 °	.87 rad
Top Azimuth	85 °	1.48 rad
Bottom Azimuth	85 °	1.48 rad
Average DLS	. °/30 m	
Radius	#DIV/0!	
Friction Factor	0.25	
Section length	270 mMD	174 mTVD
Average weight	38.57 kg/m	
Total weight	165297.1 N	
Force at top, hoist	243005.2 N	
Force at top, lower	107210.3313	
Static torque	10850.5 Nm	

Section 6	Drop-off	
Top Length	1980 mMD	1340 mTVD
Bottom Length	2280 mMD	1512 mTVD
Top Inclination	60 °	1.05 rad
Bottom Inclination	50 °	.87 rad
Top Azimuth	85 °	1.48 rad
Bottom Azimuth	85 °	1.48 rad
Average DLS	1. °/30 m	
Radius	1719 m	
Friction Factor	0.25	
Section length	300 mMD	172 mTVD
Average weight	38.57 kg/m	
Total weight	230317. N	
Force at top, hoist	349113. N	
Force at top, lower	188919.8 N	
Static torque	20062.6 Nm	

Section 5	Straight Inclined	
Top Length	1950 mMD	1325 mTVD
Bottom Length	1980 mMD	1340 mTVD
Top Inclination	60 °	1.05 rad
Bottom Inclination	60 °	1.05 rad
Top Azimuth	85 °	1.48 rad
Bottom Azimuth	85 °	1.48 rad
Average DLS	. °/30 m	
Radius	#DIV/0!	
Friction Factor	0.25	
Section length	30 mMD	15 mTVD
Average weight	38.57 kg/m	
Total weight	235991.9 N	
Force at top, hoist	357245.3 N	
Force at top, lower	192137.4504	
Static torque	20269.4 Nm	

Section 4	Left-side Bend	
Top Length	1050 mMD	875 mTVD
Bottom Length	1950 mMD	1325 mTVD
Top Inclination	60 °	1.05 rad
Bottom Inclination	60 °	1.05 rad
Top Azimuth	201 °	3.51 rad
Bottom Azimuth	85 °	1.48 rad
Average DLS	3.87 °/30 m	
Radius	444 m	
Friction Factor	0.25	
Section length	900 mMD	450 mTVD
Average weight	38.57 kg/m	
Total weight	406271. N	
Force at top, hoist	612483.8 N	
Force at top, lower	55132.92141	
Static torque	25358.4 Nm	

Section 3	Straight Inclined	
Top Length	1030 mMD	865 mTVD
Bottom Length	1050 mMD	875 mTVD
Top Inclination	60 °	1.05 rad
Bottom Inclination	60 °	1.05 rad
Top Azimuth	201 °	3.51 rad
Bottom Azimuth	201 °	3.51 rad
Average DLS	. °/30 m	
Radius	#DIV/0!	
Friction Factor	0.25	
Section length	20 mMD	10 mTVD
Average weight	38.57 kg/m	
Total weight	410077. N	
Force at top, hoist	617937.8 N	
Force at top, lower	57290.87868	
Static torque	25497.1 Nm	

Section 2	Build-up	
Top Length	36 mMD	36 mTVD
Bottom Length	1030 mMD	865 mTVD
Top Inclination	°	. rad
Bottom Inclination	60 °	1.05 rad
Top Azimuth	201 °	3.51 rad
Bottom Azimuth	201 °	3.51 rad
Average DLS	1.81 °/30 m	
Radius	949 m	
Friction Factor	0.25	
Section length	994 mMD	829 mTVD
Average weight	38.57 kg/m	
Total weight	723830.4 N	
Force at top, hoist	1206949. N	
Force at top, lower	372464.8 N	
Static torque	48527.5 Nm	

Section 1	Straight Vertical	
Top Length	mMD	mTVD
Bottom Length	36 mMD	36 mTVD
Top Inclination	°	. rad
Bottom Inclination	°	. rad
Top Azimuth	201 °	3.51 rad
Bottom Azimuth	201 °	3.51 rad
Average DLS	. °/30 m	
Radius	#DIV/0!	
Friction Factor	0.25	
Section length	36 mMD	36 mTVD
Average weight	38.57 kg/m	
Static torque	**48.5 kNm**	

Example of the combined torque load on liner and drillpipe: (6 5/8" drillpipe and 1000 m liner)

Depth [mMD]	Torque [Nm]
3944	0
3912	2933.7
3840	7977.3
3420	17737.7
2944	50695.2
2550	59207.6
2280	60853.6
1980	70065.7
1950	70272.5
1050	75361.5
1030	75500.2
36	98530.6
0	98530.6

Example of the manual calculations for pressure drop: (6 5/8” drillpipe and 1000 m liner – 2000 lpm))

Section 1 - Mud motor + Stabilizer		Section 2 - OnTrak		Section 3 - CoPilot	
Density	1.4 s.g.	Density	1.4 s.g.	Density	1.4 s.g.
Annulus OD	8.5 inches	Annulus OD	8.5 inches	Annulus OD	8.5 inches
Annulus ID/Pipe OD	6.75 inches	Annulus ID/Pipe OD	5.2 inches	Annulus ID/Pipe OD	7.02 inches
Length	8.3 m	Length	5.5 m	Length	2.16 m
Q, flowrate	2000 l/min	Q, flowrate	2000 l/min	Q, flowrate	2000 l/min
Dynamic Viscosity	20 cP	Dynamic Viscosity	20 cP	Dynamic Viscosity	20 cP
Pressure Loss	33.857 kPa	Pressure Loss	4.058 kPa	Pressure Loss	14.222 kPa
Section 4 -Reamer Unit		**Section 5 - 9 5/8" Liner**		**Liner Stabilizers**	
Density	1.4 s.g.	Density	1.4 s.g.	Density	1.4 s.g.
Annulus OD	12.25 inches	Annulus OD	12.25 inches	Annulus OD	12.25 inches
Annulus ID/Pipe OD	12. inches	Annulus ID/Pipe OD	9.63 inches	Annulus ID/Pipe OD	11. inches
Length	.6 m	Length	917. m	Length	83. m
Q, flowrate	2000 l/min	Q, flowrate	2000 l/min	Q, flowrate	2000 l/min
Dynamic Viscosity	20 cP	Dynamic Viscosity	20 cP	Dynamic Viscosity	20 cP
Pressure Loss	364.265 kPa	Pressure Loss	578.952 kPa	Pressure Loss	434.865 kPa
Section 6 - HRD Setting Sleeve		**Section 7 - 6 5/8" Drillpipe**			
Density	1.4 s.g.	Density	1.4 s.g.		
Annulus OD	12.25 inches	Annulus OD	12.25 inches		
Annulus ID/Pipe OD	11.88 inches	Annulus ID/Pipe OD	6.63 inches		
Length	3.2 m	Length	2923. m		
Q, flowrate	2000 l/min	Q, flowrate	2000 l/min		
Dynamic Viscosity	20 cP	Dynamic Viscosity	20 cP		
Pressure Loss	581.009 kPa	Pressure Loss	244.586 kPa		

Total length:	3942.76 mMD		
Pressure Loss w/o stabilizers	1820.949 kPa	18.21 bar	
Pressure Loss w/stabilizers	2255.813 kPa	22.56 bar	
TVD @TD	2115 mTVD		
Hydrostatic pressure @TD	290.47 bar		
Including Loss w/o stabilizers	308.68 bar		
Including Loss w/stabilizers	313.03 bar		
ECD w/o stab	1.49 s.g.	Increase	.088 s.g.
ECD w/stab	1.51 s.g.	Increase	.109 s.g.

Appendix D: Well Path Information

Modified Brage Wellpath

MD (m)	INC (°)	AZ (°)	TVD (m)	DLS (°/30m)
0	0	0	0	0
35.93	0	0	35.93	0
196.8	8.5	201	196.21	1.585
199.5	8.5	201	198.88	0
209.91	9.11	201	209.17	1.758
219.86	9.8	201	218.98	2.08
229.92	10.4	201	228.89	1.789
239.86	10.75	201	238.66	1.056
249.89	10.91	201	248.51	0.479
259.92	11.05	201	258.36	0.419
269.86	11.07	201	268.11	0.06
279.9	11.09	201	277.96	0.06
299.92	11.27	201	297.6	0.27
309.97	11.35	201	307.46	0.239
319.92	11.43	201	317.21	0.241
329.98	11.58	201	327.07	0.447
339.94	11.68	201	336.83	0.301
349.99	11.76	201	346.67	0.239
359.96	11.9	201	356.43	0.421
369.92	12.16	201	366.17	0.783
379.98	12.56	201	375.99	1.193
389.94	12.9	201	385.71	1.024
400	13.08	201	395.51	0.537
409.96	13.41	201	405.21	0.994
419.93	13.93	201	414.89	1.565
430	14.7	201	424.65	2.294
439.98	15.63	201	434.28	2.796
450.05	16.57	201	443.96	2.8
460.06	17.53	201	453.53	2.877
470	18.6	201	462.98	3.229
479.99	19.62	201	472.42	3.063
490.07	20.5	201	481.89	2.619
500.02	21.5	201	491.17	3.015
510.01	22.76	201	500.43	3.784
520.07	24.1	201	509.66	3.996
530.06	25.21	201	518.74	3.333
540.04	26.15	201	527.73	2.826
560.08	27.89	201	545.58	2.605
570.05	28.69	201	554.36	2.407
580.03	29.46	201	563.09	2.315
590.01	30.24	201	571.74	2.345
600.06	31.06	201	580.39	2.448
610.02	31.9	201	588.88	2.53
620.06	32.83	201	597.36	2.779

630.1	33.73	201	605.75	2.689
640.05	34.57	201	613.99	2.533
650.09	35.44	201	622.21	2.6
660.04	36.55	201	630.26	3.347
680.06	38.41	201	646.15	2.787
690.1	39.54	201	653.95	3.376
700.06	40.71	201	661.57	3.524
710.01	41.82	201	669.05	3.347
720.05	42.76	201	676.48	2.809
729.98	43.62	201	683.72	2.598
740.01	44.55	201	690.92	2.782
750.01	45.65	201	697.98	3.3
759.96	46.62	201	704.87	2.925
770	47.35	201	711.72	2.181
779.93	48.16	201	718.4	2.447
789.93	48.58	201	725.04	1.26
799.94	48.41	201	731.68	0.509
809.89	48.24	201	738.29	0.513
819.97	48.59	201	744.98	1.042
830.01	49.36	201	751.57	2.301
840.03	50.44	201	758.03	3.234
849.97	51.68	201	764.27	3.742
859.98	52.75	201	770.41	3.207
869.99	53.71	201	776.4	2.877
879.94	54.24	201	782.25	1.598
889.86	54.45	201	788.03	0.635
899.88	54.21	201	793.88	0.719
909.89	53.56	201	799.78	1.948
919.96	53.42	201	805.77	0.417
940.16	54.86	201	817.6	2.139
950.13	55.91	201	823.26	3.159
960.09	56.94	201	828.77	3.102
970.09	57.64	201	834.17	2.1
980.1	57.93	201	839.51	0.869
990.06	58.24	201	844.78	0.934
1000.1	58.71	201	850.03	1.404
1010.11	59.24	201	855.19	1.588
1020.04	59.52	201	860.24	0.846
1029.96	60	201	865.24	1.452
1040.03	60	201	870.27	0
1050.08	60	201	875.3	0
1060.09	60	200	880.3	2.595
1070.04	60	199	885.28	2.611
1080.08	60	198	890.3	2.588
1090.11	60	197	895.31	2.59
1100	60	196	900.26	2.627
1110	60	195	905.26	2.598
1120	60	194	910.26	2.598
1130	60	193	915.26	2.598
1140	60	192	920.26	2.598
1170	60	187	935.27	4.33

1200	60	183	950.27	3.464
1230	60	178	965.28	4.33
1260	60	173	980.29	4.33
1290	60	170	995.29	2.598
1320	60	166	1010.29	3.464
1350	60	162	1025.3	3.464
1380	60	158	1040.3	3.464
1410	60	154	1055.31	3.464
1440	60	150	1070.31	3.464
1470	60	145.5	1085.32	3.897
1500	60	141	1100.32	3.897
1530	60	137	1115.33	3.464
1560	60	133	1130.33	3.464
1590	60	130	1145.33	2.598
1620	60	127	1160.34	2.598
1650	60	123	1175.34	3.464
1680	60	120	1190.34	2.598
1710	60	118	1205.35	1.732
1740	60	115	1220.35	2.598
1770	60	110	1235.36	4.33
1800	60	105	1250.36	4.33
1830	60	100	1265.37	4.33
1860	60	96	1280.37	3.464
1890	60	92	1295.38	3.464
1916.21	60	89	1308.49	2.974
1920	60	88.5	1310.38	3.428
1950	60	85	1325.38	3.031
1980	60	85	1340.38	0
2010	59	85	1355.61	1
2040	58	85	1371.29	1
2070	57	85	1387.4	1
2100	56	85	1403.96	1
2130	55	85	1420.95	1
2160	54	85	1438.37	1
2190	53	85	1456.22	1
2220	52	85	1474.48	1
2250	51	85	1493.16	1
2280	50	85	1512.24	1
2310	50	85	1531.52	0
2340	50	85	1550.81	0
2370	50	85	1570.09	0
2400	50	85	1589.37	0
2430	50	85	1608.66	0
2460	50	85	1627.94	0
2490	50	85	1647.22	0
2520	50	85	1666.51	0
2550	50	85	1685.79	0
2580	51	85	1704.87	1
2605.39	52	85	1720.68	1.182
2610	52	85	1723.52	0
2640	53.5	85	1741.68	1.5

2670	55	85	1759.2	1.5
2700	56	85	1776.19	1
2730	57	85	1792.75	1
2760	58	85	1808.87	1
2790	59	85	1824.55	1
2820	60	85	1839.77	1
2850	61	85	1854.54	1
2880	62	85	1868.86	1
2910	63	85	1882.71	1
2940	64	85	1896.1	1
2947.77	65	85	1899.44	3.861
2970	66	85	1908.66	1.35
3000	67	85	1920.62	1
3030	68	85	1932.1	1
3060	69	85	1943.1	1
3090	70	85	1953.6	1
3120	71	85	1963.62	1
3150	72	85	1973.14	1
3180	73	85	1982.16	1
3210	74	85	1990.68	1
3240	75	85	1998.7	1
3270	76	85	2006.21	1
3300	77	85	2013.21	1
3327.72	78	85	2019.21	1.082
3330	78	85	2019.68	0
3360	79	85	2025.67	1
3390	80	85	2031.13	1
3420	81	85	2036.08	1
3450	81	85	2040.78	0
3480	81	85	2045.47	0
3510	81	85	2050.16	0
3540	81	85	2054.86	0
3570	81	85	2059.55	0
3600	81	85	2064.24	0
3622.98	81	85	2067.84	0
3630	81	85	2068.93	0
3660	81	85	2073.63	0
3688.92	81	85	2078.15	0
3690	81	85	2078.32	0
3720	81	85	2083.01	0
3750	81	85	2087.71	0
3780	81	85	2092.4	0
3810	81	85	2097.09	0
3840	81	85	2101.79	0
3870	82	85	2106.22	1
3900	83	85	2110.14	1
3930	84	85	2113.53	1
3960	85	85	2116.41	1
3990	86	85	2118.76	1
4020	87	85	2120.59	1
4023.85	87	85	2120.79	0

4050	88	85	2121.93	1.147
4080	89	85	2122.72	1
4110	90	85	2122.98	1
4140	90	85	2122.98	0
4170	90	85	2122.98	0
4200	90	85	2122.98	0
4230	90	85	2122.98	0
4260	90	85	2122.98	0
4290	90	85	2122.98	0
4320	90	85	2122.98	0
4350	90	85	2122.98	0
4380	90	85	2122.98	0
4410	90	85	2122.98	0
4440	90	85	2122.98	0
4470	90	85	2122.98	0
4500	90	85	2122.98	0
4530	90	85	2122.98	0
4560	90	85	2122.98	0
4590	90	85	2122.98	0
4620	90	85	2122.98	0
4650	90	85	2122.98	0
4680	90	85	2122.98	0
4710	90	85	2122.98	0
4740	90	85	2122.98	0
4770	90	85	2122.98	0
4800	90	85	2122.98	0
4830	90	85	2122.98	0
4860	90	85	2122.98	0
4876.38	90	85	2122.98	0